University of Alberta
Printing Department

Digitized by the Internet Archive
in 2019 with funding from
University of Alberta Libraries

https://archive.org/details/Smithers1965

Thesis
1965
#77

TELLURIUM ISOTOPE FRACTIONATION IN NATURE AND IN THE LABORATORY

by

Ronald M. Smithers

A THESIS
SUBMITTED TO THE FACULTY OF GRADUATE STUDIES
IN PARTIAL FULFILMENT OF THE REQUIREMENTS FOR THE DEGREE
OF MASTER OF SCIENCE

DEPARTMENT OF PHYSICS
EDMONTON, ALBERTA
APRIL, 1965

ABSTRACT

It is well known that natural and laboratory processes can alter isotopic abundances. This thesis is an initial study to find the extent to which tellurium isotope ratios may be altered.

In the introduction, a brief review of historical isotope studies is given and some of the natural mechanisms which alter isotope abundances summarized. Isotope fractionation studies of sulphur and selenium are reviewed more extensively because tellurium is similar to sulphur and selenium.

The vibrational frequencies are computed for isotopic compounds of tellurium. From these, vibrational partition function ratios are calculated and these ratios are in turn used to calculate equilibrium constants for various Te^{130} - Te^{122} exchange reactions at different temperatures. Providing that the exchange can be effected, variations in the Te^{130}/Te^{122} ratio in equilibrium isotope reactions of up to 2.6% at 20°C are predicted. Calculations are also made of kinetic isotope effects predicting values as high as 1.0175 for the ratio of isotopic rate constants.

Experimental verification of some of the theoretical predictions was obtained. In the chemical reduction of potassium tellurite at room temperature, the $Te^{122}O_3^=$ ion was found to be reduced 1.0071 ± 0.0003 times faster than the reduction rate of $Te^{130}O_3^=$. In a microbiological reduction of tellurite ion, the $Te^{122}O_3^=$ ion was found to be reduced 1.0060 ± 0.0005 times faster than the reduction rate of $Te^{130}O_3^=$.

On the bases of the theoretical predictions, the effects noted in both reduction studies are related to tellurium oxygen bond breakage.

Of four natural samples, three were identical in their Te^{122}/Te^{130} ratio; whereas, the fourth was enriched by 0.4 percent in the lighter isotope.

ACKNOWLEDGEMENTS

The author wishes to express his sincere thanks to his supervisor, Dr. H. R. Krouse, for suggesting this project and for his inspiration, guidance, and assistance in the course of this investigation. The assistance of various members of the Department of Computing Science; the technical services of P. Alexander, glassblower; and assistance of R. McCready of the Department of Microbiology in obtaining bacterial cultures and medium are also greatly appreciated.

Finally, I wish to acknowledge the assistance of my wife, Marilyn, and Mrs. P. Babet in the preparation of the manuscript.

TABLE OF CONTENTS

INTRODUCTION Page 1

A. Equilibrium Isotope Effects 3
B. Kinetic Isotope Effects 4
C. Mechanisms of Isotope Fractionation in Nature 6
1. Physical processes 6
a. Diffusion 6
b. Isotopic vapour pressures 7
c. Miscellaneous 9
2. Chemical processes 9
a. Equilibrium isotopic exchange 9
b. Kinetic isotope effects 13
3. Biological processes 13
D. The Group VIA Elements 15
1. General chemistry 15
2. Isotope fractionation studies 18
a. Sulphur 18
b. Selenium 26
3. Tellurium 28
a. History and occurrence 28
b. Uses 30
c. Physical properties 30
d. Chemical properties 34
e. Absolute abundances of the isotopes of tellurium 35
E. Advantages of looking at sulphur, selenium, and tellurium isotopes simultaneously in natural deposits 37

THEORY 41

A. Theory of Equilibrium Isotope Effects 42

B. Evaluation of Partition Function Ratios 45
C. Kinetic Isotope Effects 49
D. Isotope Fractionation During First Order Competing Reactions 56

THEORETICAL CALCULATIONS 59
A. Calculation of Equilibrium Exchange Constants 59
B. Calculation of Ratios of Isotopic Rate Constants 64

EXPERIMENTAL 68
A. Extraction of Tellurium from Natural Samples 69
B. Chemical Reduction of K_2TeO_3 71
C. Reduction of K_2TeO_3 by Scopulariopsis brevicaulis 73
1. Reduction of K_2TeO_3 on liquid medium 75
2. Extraction of elemental tellurium reduced from K_2TeO_3 in the biological investigation 76
D. Preparation of TeF_6 77
E. Mass Spectrometric Analysis 80

RESULTS AND DISCUSSION 85
A. Chemical Reduction of Potassium Tellurite 85
B. Microbiological Reduction Study 88
C. Natural Isotopic Abundance Studies 91

BIBLIOGRAPHY 93

APPENDIX I
CALCULATIONS OF ISOTOPIC VIBRATIONAL FREQUENCY SHIFTS FOR TELLURIUM - CONTAINING MOLECULES A1
A. Diatomic Molecules A1
B. Polyatomic Molecules A5
TeF_6 A7

$TeBr_4$ A14
SCTe A18
H_2Te A22
$TeO_3^=$ A30

APPENDIX II

IBM 7040 COMPUTER PROGRAMS FOR CALCULATION OF ISOTOPIC VIBRATIONAL FREQUENCIES AND PARTITION FUNCTION RATIOS A36

A. Calculation of Isotopic Vibrational Frequencies and Partition Function Ratios for Diatomic Species A37

B. Computation of Isotopic Vibrational Frequencies for XY_6 Molecules A40

C. Computation of Isotopic Vibrational Frequencies for XY_4 Molecules A43

D. Computation of Vibrational Frequencies for XYZ Molecules A46

E. Computation of Force Constants for Non-linear XY_2 Molecules A49

F. Computation of Isotopic Vibrational Frequencies and Partition Function Ratios for Non-linear XY_2 Molecules A55

G. Computation of Force Constants, Apex Angle, Isotopic Vibrational Frequencies, and Partition Function Ratios for Pyramidal XY_3 Molecules A58

H. Computation of Partition Function Ratios for General Molecules A63

LIST OF TABLES

		Page
I.	Occurrence of Tellurium	31
II.	Absolute Abundances of the Isotopes of Tellurium	38
III.	Q_2'/Q_1' for Te-containing Molecules	61
IV.	Equilibrium Constants for $Te^{130} \rightleftharpoons Te^{122}$ Exchange Reactions	62
V.	Minimum Values of k_{130}/k_{122}	65
VI.	Summary of the Calculated Ratios of Rate Constants for the Reduction of K_2TeO_3	67
VII.	Ion Species Resulting from the Ionization of TeF_6	84
VIII.	Te^{130}/Te^{122} Fractionation Study	86
IX.	Calculation of Vibrational Frequency Shifts for Te^{130} and Te^{122}-containing Molecules	A6

LIST OF FIGURES

		Page
Figure 1.	O^{18} Growth Rings in the Jurassic Belemnite	12
Figure 2.	The Distribution of S^{34} in Nature	20
Figure 3.	The Biological Sulphur Cycle	22
Figure 4.	Variations in the Se^{82}/Se^{76} Ratio Found For Natural Samples	27
Figure 5.	Fluorine Line	78
Figure 6.	Typical Tellurium Spectra	82
Figure 7.	Te^{122}/Te^{130} Fractionation Study	87
Figure 8.	Variation of Isotopic Composition of Product with Percent Reaction	89
Figure 9.	Normal Vibrations of an Octahedral XY_6 Molecule	A 8
Figure 10.	Normal Vibrations of a Tetrahedral XY_4 Molecule	A15
Figure 11.	Relationship Between Force Constants for H_2Te	A26
Figure 12.	Normal Vibrations of a Pyramidal XY_3 Molecule	A32

INTRODUCTION

The concept of isotopes, new and revolutionary in 1910, is today basic to our understanding of the structure of matter.

The first direct evidence of the existence of isotopes came from studies of radioactive elements and their decay products. Soon the chemists investigating the decay products found pairs of radioactive elements which were inseparable and appeared to be identical in their chemical properties. Soddy (100) in 1910 suggested that such substances differing in their physical properties but having the same chemical properties be called "isotopes". He suggested that the existence of isotopes was a general phenomenon and that we could also expect the stable elements to be mixtures of these inseparable species, or isotopes.

J. J. Thomson in 1912 (128) using his positive ray apparatus, showed that neon was indeed a mixture of at least two kinds of atoms having atomic weights of 20 and 22 since the positive ion beam formed from neon was resolved into two beams. This was the first evidence for the existence of isotopes among the stable elements.

Aston (2) and Dempster (25), subsequently examined the isotopes of many other elements. During the two decades to follow, practically all the elements had been investigated. Today, the known stable elements consist of mixtures of from one to ten isotopes and these total to about 300 different stable isotopes in addition to the radioactive species. The radioactive disintegration studies suggested that isotopic abundances of an element in a deposit could be altered by radioactive decay. Richards (90) found that lead associated with thorium ores had a higher atomic weight than that associated with uranium ores. This was reasonable since Th^{232} decay terminates in Pb^{208}; whereas U^{238} decays finally to Pb^{206}. By knowing the amount of radioactively produced lead present relative to the amount of undecayed parent, the age of lead deposits can be determined.

Similarly, Aldrich and Nier (1) observed that the amount of Ar^{40} associated with K^{40} was up to three times the concentration of Ar^{40} in atmospheric argon. The amount of Ar^{40} produced by the radioactive decay of K^{40} has been used to date the time of formation of potassium minerals. Many other radioactive isotopes have been used for dating purposes.

However, despite all the information about isotopes that had been discovered prior to 1930, it was believed that isotopes were identical in their chemical properties and that the stable isotopes of the elements were of constant abundance in nature. But soon after the discovery of deuterium, the heavy isotope of hydrogen, by Urey, Brickwedde, and Murphy (112) in 1932, it was shown by theory and experiment that the isotopes of the light elements did differ in their chemical properties and that the separation of these isotopes by chemical means was possible.

A. Equilibrium Isotope Effects

In 1933 Urey and Rittenberg (114) calculated the equilibrium constants for the reaction

$$H_2(g) + D_2(g) \rightleftharpoons 2HD(g)$$

at different temperatures. They found these to differ from unity which indicated that the isotopes of hydrogen were different chemically. The reaction was carried out in the laboratory at various temperatures by Rittenberg, Bleakney, and Urey (91) and the equilibrium constants determined. These were found to be close to those calculated theoretically. This was the beginning of many

isotope fractionation investigations which compared experimental results with theoretical calculations.

Urey and Greiff (116) calculated the equilibrium constants for some of the light elements such as lithium, boron, carbon, nitrogen, chlorine, and bromine. Their results indicated equilibrium fractionations varying from 1% to 10% and experimental confirmations of some of these were soon obtained. For example, Weber et al (127) found CO_2 in equilibrium with water to be enriched in O^{18} by 4.6% at $0^{\circ}C$ as compared with 4.4% predicted by theory. Other equilibrium isotope effects and data are summarized by Urey (118). Many isotope exchange reactions involving the isotopes of the light elements have been studied in recent years and the agreement between theory and experiment has been excellent. To date, (with the exception of this thesis) selenium is the heaviest element for which exchange reactions have been investigated (60).

B. Kinetic Isotope Effects

In 1932 when Urey and Washburn (113) were doing their experiments with deuterium and protium, they discovered that partially electrolyzed water was enriched in deuterium, protium having been evolved faster than

deuterium at the cathode. Two years later, Bach, Bonhoeffer, and Fajans (5) showed that H_2 reacted over three times faster than D_2 with bromine. The same year Farkas and Farkas (37) reported similar results in the photochemical reactions of H_2 and D_2 with chlorine. Urey and Teal (117) and Eidinoff (31) have reviewed the extensive work done on the relative reaction rates of H_2 and D_2 - containing compounds.

Kinetic isotope effects were similarly found for other lighter elements. In 1949 Lindsay, McElheran, and Thode (65) and Bigeleisen and Friedman (12) reported carbon isotope effects in the decomposition of oxalic acid and the decarboxylation of malonic acid. These results were reported on further by Lindsay, Bourns, and Thode (63,64) in 1951 and 1952 and were in excellent agreement with theory.

To date, much literature is available on the mathematical calculation of isotopic rate constants. In 1935 Eyring (36) set forth the theory of absolute rates from which the ratio of rate constants for reactions of isotopic molecules can be calculated, and this has been revised by Bigeleisen (11) to an expression which is more convenient to use. Several authors (23, 92, 106) have written reviews on kinetic isotope effects.

C. Mechanisms of Isotope Fractionation in Nature

Natural isotope fractionation mechanisms can be subdivided into physical, chemical, and biological processes.

1. Physical processes of natural isotope fractionation

a. Diffusion: The mass dependence of diffusion in the solid, liquid, or gaseous state can lead to isotopic fractionation and this is one of the principles used in commercial isotope separation. Studies of natural diffusion phenomena for many isotopes have been reported. An interesting example is the studies of nitrogen isotopes by Hoering (53). He discovered that nitrogen contaminants in natural gas were enriched in N^{14} over the nitrogen found in the associated crude oil. He suggested that migration of the oil and gas through porous deposits was responsible. Migration by molecular flow in which the mean free path of the gas is greater than the pore dimensions results in flow rates of the isotopic molecules which are inversely proportional to the square root of the masses. This postulate was later verified by a laboratory diffusion experiment and he was able to produce to some degree the fractionation found in nature.

With lighter isotopes and low temperature conditions, the isotopic alteration can be quite high. This is exemplified by a recent lithium diffusion experiment in titanium dioxide by Johnson and Krouse (55). Lithium was allowed to diffuse to a depth of 1.7 mm at room temperature and the innermost lithium was found to be 7 percent enriched in Li^6 in comparison to the undiffused lithium showing that the Li^6 diffuses quite noticeably faster than the Li^7.

b. Isotopic vapour pressures: Friedman (39) suggested that the different vapour pressures of the isotopic compounds might influence the natural abundance of each isotope. He showed that there was a gradual depletion of the deuterium content in rainfall samples progressing from the Pacific Coast of North America inland over the Rocky Mountains. He found further that ocean waters near the equator were found to be enriched in deuterium in comparison to ocean waters polewards. Both these phenomena are caused by the preferential evaporation of H_2O over HDO. In the rainfall study, the HDO condenses faster enriching the coastal regions in HDO while the remaining vapour enriched in H_2O moves further inland.

The oxygen isotopes of the earth's water bodies behave similarly. Epstein (34) reported that the O^{18} content of the ice is very low in the Arctic regions relative to ocean waters and that the actual value in the ice cap varies in a cyclic fashion with depth. This cyclic phenomenon which is due to seasonal changes may be explained by thinking of the atmosphere between the equator and the poles as a distillation column. Water is evaporated from the oceans at the equator, rises upward at the equator, and spreads out toward the poles. In the distillation of the water, the simple process separation factor α is given by the ratio of vapour pressures of the two isotopic water species as

$$\alpha = \frac{PH_2O^{16}}{PH_2O^{18}} = \begin{matrix} 1.008 \text{ at } 25^\circ C \\ 1.011 \text{ at } 0^\circ C \end{matrix}$$

Since H_2O^{16} has the higher vapour pressure, the O^{18} is favoured in the liquid and will be depleted in the vapour. As rain falls in the different latitudes, the vapour spreading out towards the poles becomes more and more depleted in the heavy isotope. We therefore have a multistage process. The extent of the isotope fractionation which in this case is the depletion of O^{18} in snow fall-

ing on the Greenland ice caps will depend on the number of stages in the process and on the difference in temperature between the equator and the poles. Thus, the depletion of O^{18} in the snow and ice in the Arctic will, in general, be higher in winter than summer. Seasonal fluctuations in the O^{18} content with depths have shown up in the layers of ice in the Greenland glacier. From such studies, estimates of the age of glaciers can be determined by simply counting O^{18} concentration rings. Such fractionations caused by differences in vapour pressure are termed "Rayleigh" fractionations.

c. Miscellaneous: It is expected that differences in the isotopic solubilities, melting and sublimation points might be other mechanisms of natural isotope fractionation. Very little work to date has been reported on these physical processes.

2. Chemical processes

a. Equilibrium isotopic exchange: Friedman suggested further that equilibrium isotope exchange reactions would produce fractionation of isotopes in natural processes. For example, a study of fumaroles in Yellowstone Park showed the deuterium content to be depleted by as much as 45%. He suggested that this might

be the result of the equilibrium exchange reaction

$$H_2 + HDO \underset{}{\overset{K}{\rightleftharpoons}} HD + H_2O$$

The equilibrium constant for exchange reactions is dependent upon temperature, and if this hypothesis is the only contributing factor, theoretical considerations, based on the observed deuterium depletions, place the temperatures of these fumaroles above 400°C.

In the exchange of the oxygen isotopes between carbonate and water, the heavy isotope O^{18} is favored in the carbonate over that of that water. This reaction can be written in the form

$$1/3\ CO_3^{16=} + H_2O^{18} \underset{}{\overset{K}{\rightleftharpoons}} 1/3\ CO_3^{18=} + H_2O^{16}$$

The equilibrium constant has been determined by Clayton (20) to be 1.0301 at 25°C. meaning that at 25°C. limestone and calcium carbonate material will be enriched in O^{18} over that of sea water by about 3%. The exact extent of this enrichment will depend on the temperature of the water at the time of deposition. The reaction has been studied in detail by Urey (119) and he suggested that it might be used in the determination of temperatures and that the accurate measurement of the O^{18} content of

suitable marine carbonate sediments would indicate the temperature of the seas at the time of deposition.

According to Clayton the temperature T is given by the equation:

$$\ln K = 2725\ T^{-2}$$

As a direct result of this temperature dependence, the concept of the O^{18} or paleo-temperature scale was formulated.

Studies were carried out by Urey et al (120), Epstein et al (32), and McCrea (73) using well preserved samples of belemnites from the U. S., Sweden, Denmark, England, France, Holland, and Germany and these showed that the temperatures which were determined seemed reasonable.

A fascinating study was made by Epstein (33) of the O^{18} content in the carbonate shells generated by marine animals. The subject of investigation was a Jurassic belemnite, an extinct animal which flourished about 120 million years ago. Successive growth rings of the shells showed a cyclic variation in the heavy oxygen (O^{18}) content which were associated with seasonal variations in temperatures. Figure 1 shows these seasonal vibrations in temperature as indicated by the O^{18} content of the

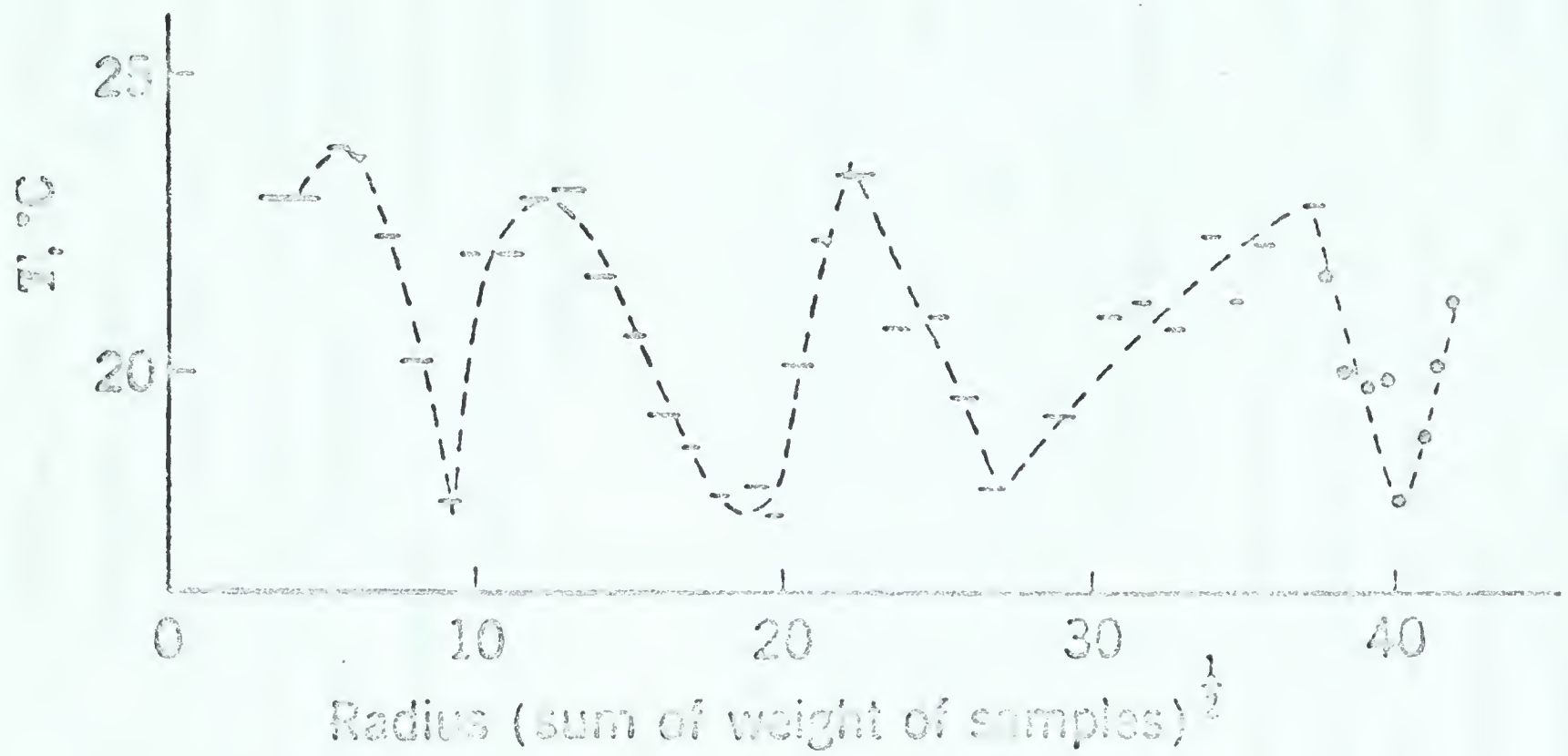

Fig. 1.--O^{18} growth rings in the Jurassic belemnite.

Taken from Thode (108)

growth rings of the belemnite. Such an oxygen isotope study, therefore, not only gives us information about climatic conditions in various parts of the world millions of years ago, but tells us something about the lives and habits of animals that now are extinct.

b. Kinetic isotope effects: Due to the difficulty in observing purely chemical kinetic isotope effects in nature, very little has been reported in the literature. Numerous reports have been given for kinetic isotope fractionation in biochemical processes and will be discussed later in connection with sulphur isotope fractionation.

3. Biological processes

Biological and microbiological isotope fractionations are perhaps due to both physical and chemical processes. Because of the complexity of the mechanisms, there is insufficient data to verify whether isotopes are fractionated in such processes as enzyme complexing and diffusion through biological membranes. Significant isotope fractionations have been realized with carbon, nitrogen, oxygen, and sulphur in biochemical processes and the results in many instances are consistent with similar inorganic chemical processes.

Nier and Gulbransen (83) and two years later, Nier and Murphy (84) found that in general, limestones were enriched and plants depleted in the heavier carbon isotope. They reported variations up to 5% in the C^{12}/C^{13} abundances. Many workers have since re-affirmed these results and can be found in the literature (6,22,38,62, 71,80,86,97,107,110,130,133,134,135). One of the many interesting results of these investigations was that both land and marine plants tend to concentrate C^{12}, although the latter do this to a lesser degree. This phenomenon may be attributed to differences in the cellular structures of the two types of plants, assuming that the concentration of the C^{12} is due to kinetic and/or equilibrium isotope effects in the photosynthesis of atmospheric CO_2.

Much investigation of the isotope fractionation due to bacteria has been carried out. The most fruitful of these investigations have been carried out with sulphur, and this will be discussed in more detail later.

D. The Group VIA Elements

1. General chemistry (47), (96)

The group VI A elements include oxygen, sulphur, selenium, tellurium, and polonium and are characterized by 6 valence electrons. They differ in nuclear charge, in size, and in the number of inner electron "shells". Little is known about polonium since work on it has been retarded because of its high radioactivity. It occurs naturally in uranium minerals such as pitchblende but only to the extent of 5×10^{-9} per cent of the mineral. Thus its occurrence is so small that its significance in stable isotope fractionation processes is negligible.

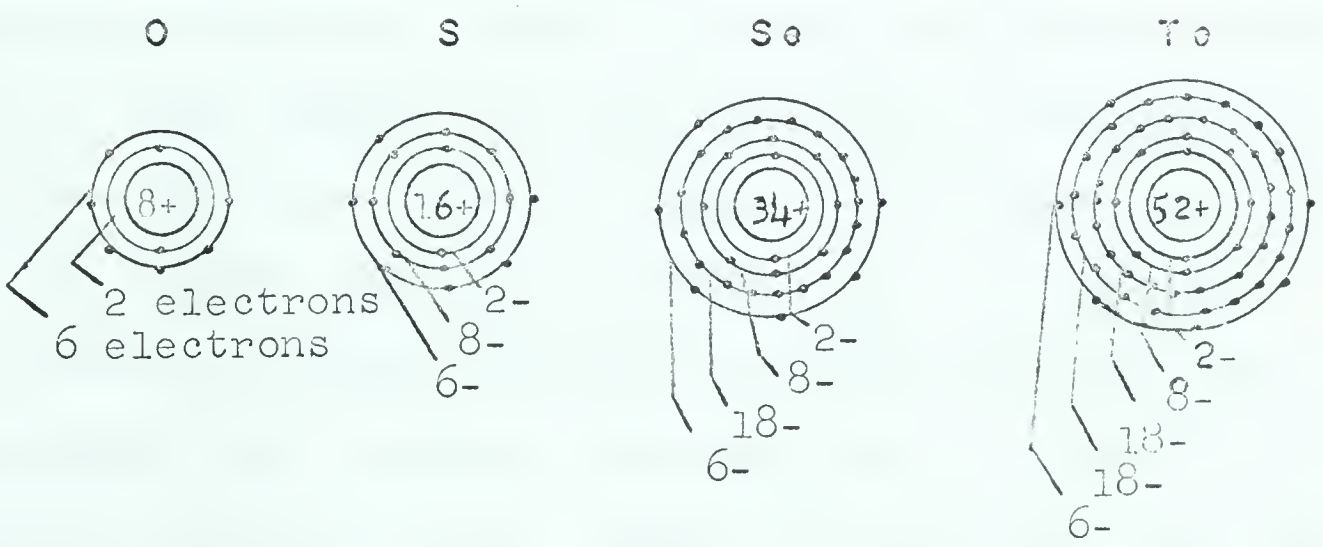

The Group VIA Elements

The firmness with which the outer electrons are held increases with increasing nuclear charge, but is diminished as the distance from the nucleus and the number of inner electron shells increases. Since the two latter effects predominate, it may be predicted that the electrons are most tightly held by the oxygen atom and most easily lost (or shared) by the tellurium atom. This assumption accounts for and is in accord with the systematic variation in physical and chemical properties which these elements show.

The elements of the group readily form compounds or ions by sharing or adding 2 electrons, provided by atoms of other elements, to complete the octet of the inert-gas structure thereby acquiring an oxidation state of -2. This tendency is most prominent in the case of the smallest atom, that of oxygen, and least in the case of the largest atom, that of tellurium. In addition, the atoms of sulphur, selenium, and tellurium may lose (or share) their valence electrons so as to acquire oxidation states up to +6. Oxygen does not show this tendency, because its electrons are so tightly bound that no other element, with the possible exception of fluorine, is able to remove them. The change in oxidation state

of an element during a chemical reaction is one of the factors which determines the extent to which isotope abundances may be altered in the laboratory or by natural processes.

All of the elements of the group show allotropy. Just as oxygen can exist as diatomic O_2 and triatomic O_3, the other elements can be obtained in more than one form, the forms differing either in the number of atoms per molecule, or in the arrangement of molecules in the solid. There is, going from sulphur to tellurium, an increasing disposition toward formation of long chains of atoms held together by covalent bonds. In general, the larger the atom, the less the tendency to form multiple bonds and the greater the tendency of each atom to be bound to more than one atom. Oxygen stands alone from the group in being a diatomic gas at room temperature.

As would be expected because of the increasing number of electronic shells, the ionic radii increases from 1.40Å for oxygen, 1.84Å for sulphur, 1.98Å for selenium, to 2.4Å for tellurium (47). Also of interest, the oxidation potential for each of these elements is as follows: oxygen, -1.23 volts; sulphur, -0.14 volts; selenium, +0.40 volts; and tellurium, +0.72 volts (96).

Thus, there is a much greater tendency for oxygen to form H_2O than for tellurium to form H_2Te. Unlike H_2O and H_2S, H_2Se and H_2Te are better reducing agents than hydrogen.

From the foregoing discussion, it is readily seen why the properties of sulphur, selenium, and tellurium vary from the decidedly non-metallic nature of sulphur to the mildly metallic character of tellurium. For example, the free element sulphur is a non-conductor of electricity, selenium is a poor conductor (but its conductivity increases proportionately to its illumination), and tellurium is somewhat better than selenium.

2. Isotope fractionation studies

In considering isotope fractionation in the chemical group VIA, oxygen has received extensive study and some examples have been previously cited. It would seem, however, that tellurium isotopes should resemble sulphur and selenium in their behavior because of the similarities of their valence states. Therefore, some of the significant findings of sulphur and selenium isotope fractionation studies are reviewed here.

a. Sulphur: Extensive studies of the variations in the isotopic abundances of sulphur have been

carried out. It was clear that differences in the chemical properties of the sulphur isotopes did exist and that isotope fractionation could be expected in natural processes.

For example, calculations of the isotope exchange constant for the reaction

$$S^{32}O_4^{=} + H_2S^{34} \underset{}{\overset{K}{\rightleftharpoons}} S^{34}O_4^{=} + H_2S^{32}$$

gives K at 25°C to be 1.071, thus favoring the enrichment of S^{34} in the sulphate by about seven percent (111). It was therefore suspected that a trend toward this favoured distribution existed in nature with sulphates enriched and sulphides depleted in the heavy isotope of sulphur, S^{34}.

The initial data published by Thode, Macnamara, and Collins (104) showed that the S^{32}/S^{34} ratio in terrestial samples varied by as much as 5%. As predicted, sulphates were generally found to be enriched in S^{34} while sulphides were depleted in the heavier isotope. Figure 2 shows the general distribution of sulphur isotopes in nature. The sulphur isotope distribution data are expressed in terms of δS^{34} °/oo defined as follows:

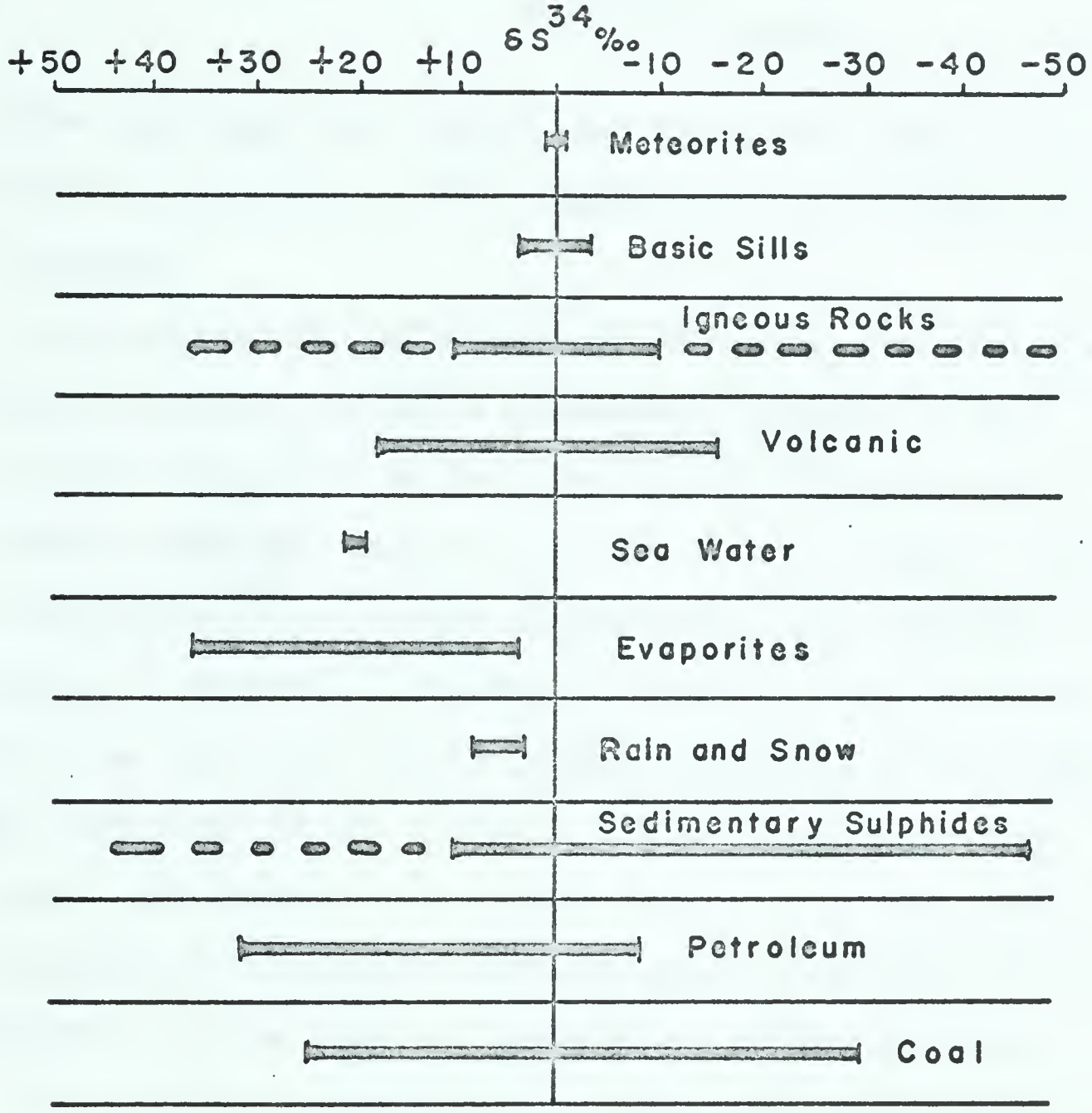

FIG. 2 THE DISTRIBUTION OF S^{34} IN NATURE

Taken from Thode (108)

$$\delta S^{34}\ {}^{o}/_{oo} = \frac{(S^{34}/S^{32})_{sample} - (S^{34}/S^{32})_{standard}}{(S^{34}/S^{32})_{standard}}$$

Positive and negative δ-values mean that the samples are enriched or depleted in S^{34} respectively with respect to the standard.

It was reported by Macnamara and Thode (68) that the sulphur in meteorites had a remarkably constant S^{32}/S^{34} ratio which was close to the average S^{32}/S^{34} ratio for terrestial samples. These facts led them to believe that the meteoritic S^{32}/S^{34} ratio represented the primordial abundance of terrestial sulphur before any fractionation occurred or the ratio of the sulphur isotopes in the earth at the time that it was formed. It is clear that since the earth was formed, the sulphur in the crust has been fractionated in biological and geological processes due to differences in the chemical properties of the isotopes.

The exchange cited does not take place under normal conditions (124) and all efforts to establish it under laboratory conditions for a reasonable length of time failed. Therefore, Tudge and Thode (111) suggested that the following biological sulphur cycle might well provide the mechanism for this fractionation in nature (Fig. 3).

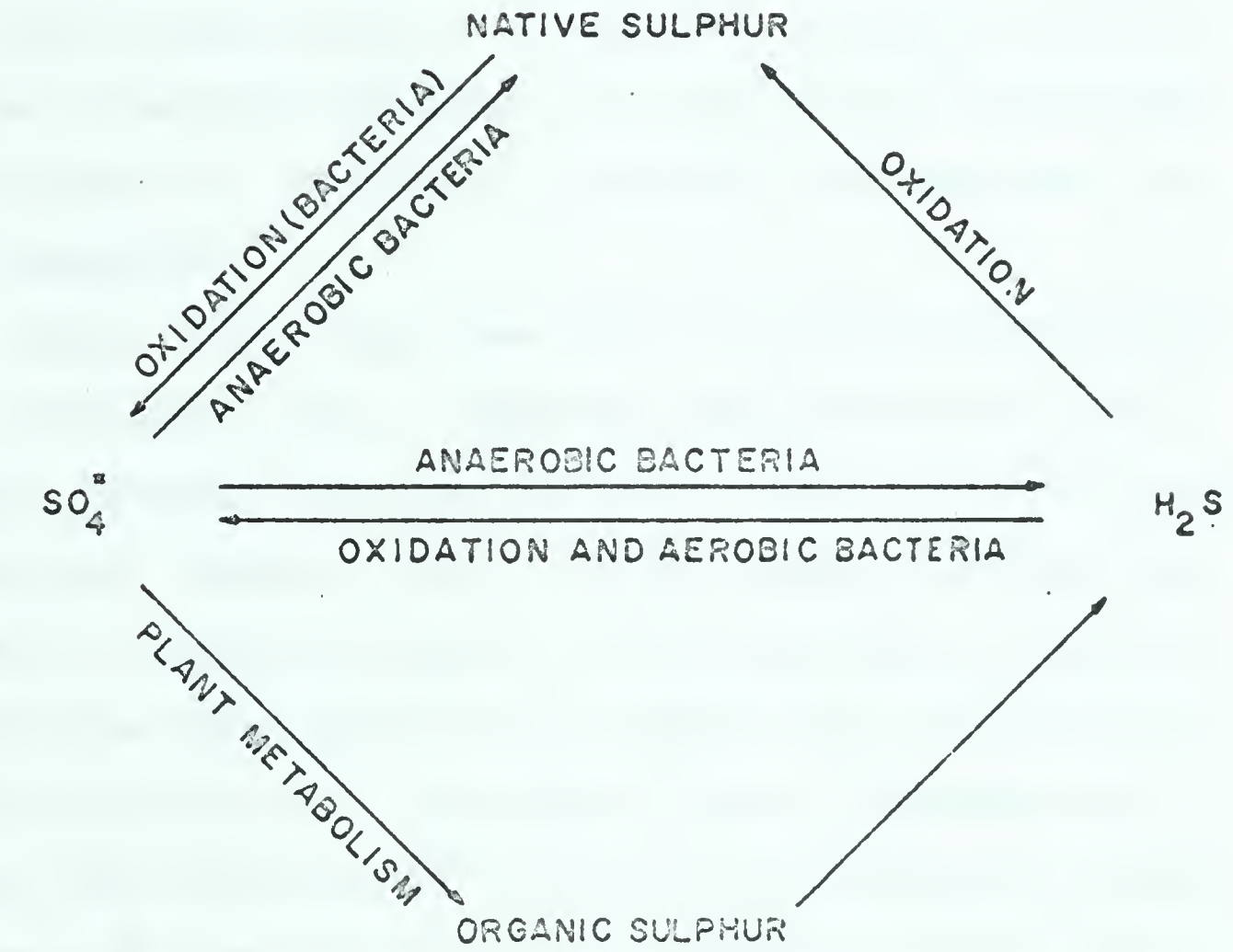

FIG. 3 THE BIOLOGICAL SULPHUR CYCLE IN NATURE
Taken from Thode (108)

According to Thode (108) the bacterial reduction process is found to be a unidirectional, not an equilibrium process, and isotope fractionation occurs because the light-isotope containing compounds react faster than the species containing the heavier isotope. Thode goes on to say that in particular, the bacterial reduction of sulphate is largely responsible for the isotopic variations which occur in the oceans, evaporites, and materials in the sediments.

Many studies have been made of isotope fractionation in the sulphur cycle. Anaerobic reducing and photosynthetic hydrogen sulphide oxidizing bacteria abound in the Cyrenacian lakes of Africa. These produce a sedimentary layer of elemental sulphur (15) and analysis of samples from these lakes gave direct evidence for the fractionation of sulphur in the sulphur cycle. Macnamara and Thode (69) found the S^{34} content of the elemental sulphur to be 3.2% less than that of the soluble sulphate from the same lake.

Further evidence is provided in the salt domes of Louisiana and Texas (107) where elemental sulphur was depleted by about 4% and sulphide by about 5% in S^{34} relative to the associated gypsum. Two possibilities

exist for the formation of this sulphur by reduction of the sulphate: - either the high temperature reduction of the sulphate by organic matter (oil fields associated with the salt domes), or by the bacterial reduction of the sulphate with petroleum providing a source of carbon and free energy for life. The first of these mechanisms, however, seems incapable of causing the large fractionation observed; whereas, the latter is quite capable of doing so, as shown by the Cyrenacian Lake study. Miller (78) added further evidence to the "bacterial reduction" postulate by isolating anaerobic sulphate-reducing bacteria in these deposits. Thus the production of carbon dioxide by these sulphate-reducing bacteria alters the calcium sulphate to a porous calcitic limestone with elemental sulphur embedded in it and this accounts for the type of deposit that is present in these salt domes today.

The hypothesis that sulphate-reducing bacteria were responsible for the sulphur isotope fractionation has been substantiated by laboratory experiments. Thode, Kleerekoper, and McElheran (105) showed that Desulphovibrio desulfuricans while reducing sulphate, produced H_2S which was 1% richer in S^{32} than the nutrient. In subsequent studies, Harrison and Thode (44) found that this fraction-

ation varied with reaction conditions and that the maximum enrichment was 2.5% at 25°C. Kaplan and Rittenberg (57) in 1964 reported enrichments as high as 4.6%. They showed also that other micro-organisms such as S. cerevisiae were capable of carrying out fractionation of oxidized sulphur compounds in reduction experiments with equal or greater efficiency.

McElheran in 1951 (74) was unable to find any fractionation in the oxidation of sulphur to sulphate by Thiobacillus but in 1964 Kaplan and Rittenberg (57) reported an enrichment of 1.8% of S^{32} in oxidizing H_2S to $SO_4^{=}$ by chemosynthetic oxidation and an enrichment of 1.0% in photosynthetic oxidation. Nakai and Jensen (96) published results in 1964 for the bacterial reduction and oxidation of sulphur using marine mud cultures. Values for the ratio of the isotopic (S^{32} and S^{34}) rate constants of about 1.020 were found for the reduction experiments, and values ranged from 1.0003 to 1.0017 for the oxidation experiment. Fractionation factors between sulphate and sulphide in bottom sediments vary between 1.03 and 1.04 for sea samples and 1.005 to 1.009 for fresh water samples, indicating that the sulphate produced becomes more enriched in S^{32} than does sulphur or sulphide.

b. Selenium: An investigation into the isotopic fractionation of selenium was conducted by Krouse and Thode (60). They reported Se^{82}/Se^{76} ratios as found in figure 4. The Se^{82}/Se^{76} ratio varied 1.5% in the samples examined. The distribution bears some similarity to that of the sulphur isotopes. Samples of plant materials and soil showed the largest variation in isotope ratios; whereas, selenides from massive sulphide ores showed little or no variation with respect to meteoritic selenium.

They further reported that $Se^{76}O_3^=$ was reduced 1.5% faster than $Se^{82}O_3^=$ to elemental selenium. This result is in agreement with a simple theoretical calculation. This compares to a 2.3% kinetic isotope effect in the chemical reduction of $S^{32}O_4^=$ and $S^{34}O_4^=$ reported by Harrison and Thode (44).

Further investigation into the isotope fractionation of selenium has been carried out by Rees (89). Among other experiments, he carried out investigations into the kinetic isotope effects in the reduction of Se^{IV} to Se^{o}, and into the isotope exchange reaction between Se^{IV} and Se^{VI}. He reported a kinetic isotope effect varying from 1.6% at 40°C to 2.0% at 24°C for a 20% reduction of sodium selenite,

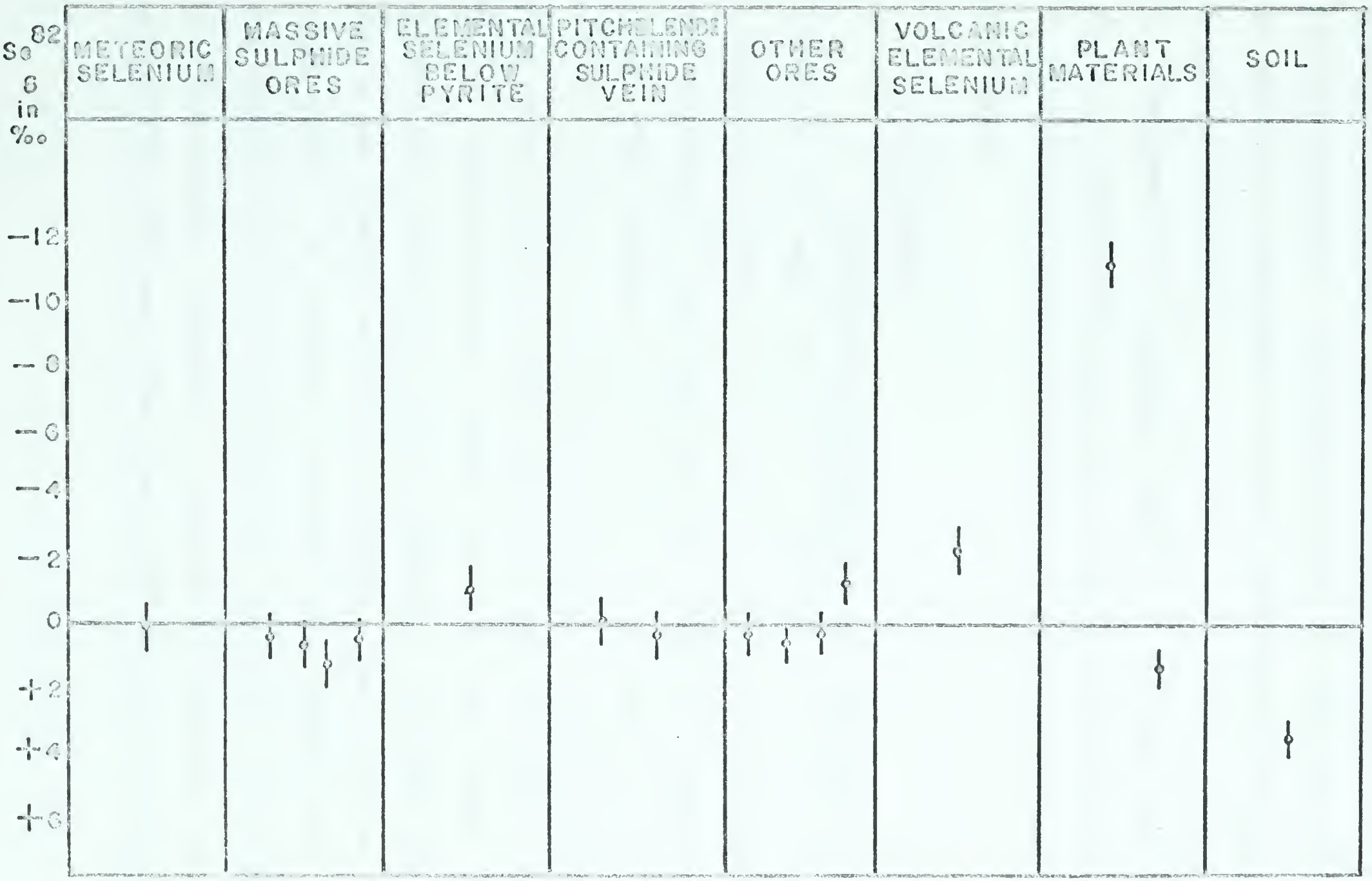

FIG. 4 VARIATIONS IN THE Se^{82} / Se^{76} RATIO FOUND FOR NATURAL SAMPLES

and phase fractionations of 2.7% and 4.2% respectively for 59 - and 146 - day equilibrations of Se^{VI} and Se^{IV}. In each case, the higher valence states were enriched in the heavier Se^{82}.

Because of the numerous reports of isotopic fractionation of sulphur and selenium, a similar fractionation of tellurium isotopes by natural processes is strongly predicted.

3. Tellurium

a. History and occurrence - The discovery of tellurium was made late in the eighteenth century (76). A peculiar mineral known as white gold-ore or grey gold-ore occurring in the sandstone near Zalathna, Transylvania, was considered by chemists and mineralogists as a kind of alloy of antimony and bismuth. Various forms were given a host of names but not until 1782 that F.J. Müller von Reichenstein showed that there was neither any bismuth nor antimony in the new mineral, and suspected that a new element had been discoverd. Then sometime after 1789, M. H. Klaproth extracted the unknown metal and observed some of its properties from which concluded that the mineral contained a peculiar and distinct metal essentially different from every other metallic substance

hitherto known. It was he who named it tellurium after the earth (Latin - tellus).

Tellurium occurs in only a few places and in small quantities; it is less abundantly distributed than any other element in the sulphur family. According to the data of spectrographic analysis, it is absent in the spectra of the sun and the stars, however, it could be explained by the low sensitivity of the spectrographic method with respect to these elements (98). According to F. W. Clarke and H. S. Washington (19), the igneous rocks on the earth's crust contain 8×10^{-2} percent sulphur, $n \times 10^{-8}$ percent selenium, and $n \times 10^{-9}$ percent tellurium; or tellurium is about as abundant as gold. It occurs combined with gold, silver, bismuth, and many other metals. The chief tellurium minerals are the tellurides, but some tellurites and tellurates exist in natural form. These are listed in Table I. Tellurium has not been detected in soils (123). It is found in many volcanic areas and has been found in "minute" amounts in some meteorites (29). It is obtained principally as a by-product of the refining of other minerals with which it combines.

b. Uses - To cite some uses, it is used in coloring glass, preparation of organic dye-stuffs, manufacture of high resistance alloys, staining silver, as a delicate test of sterilization in bacteriology, identification of presence of diphtheria and other germs, in motor fuels as an anti-knock constituent, insecticides, germicides, fungicides and wood preservatives, and in the manufacture of extremely hard alloys having very great tensile strength. Its main use in recent years is in the semiconductor field where it has found use as an intrinsic photoconductive detector (77) and also in rectifiers (96).

c. Physical properties - Tellurium exists primarily as "metallic" tellurium which is the most stable allotrope. This form is grey black in color with a metallic luster and of hexagonal crystal structure. In 1913 Cohen and Kröner (21) claimed that tellurium existed in two dynamic allotropes, and according to Mellor (76) tellurium is obtained in the amorphous form as a black powder when tellurium is precipitated from an acid solution. The amorphous form suffers no change upon heating until it is melted (m.p. 452°C) and then it is transformed into the very brittle and easily powdered white-grey crystalline form.

Table I OCCURRENCE OF TELLURIUM (76), (98)

Native Element	Te
Tellurides	
Altaite	PbTe
Arseniotellurite	$Te_2As_2O_7$
Arsenotellurite	$Te_2As_2S_7$
Calaverite	$AuTe_2$
Coloradoite	HgTe
Csiklovaite	Bi_2TeS_2
Frohbergite	$FeTe_2$
Goldfieldite	$Cu_6Sb_2(S,Te)_3$
Goldschmidtite	Au_2AgTe_6
Grünlingite	Bi_4S_3Te
Hedleyite	Bi_7Te_3
Hessite	Ag_2Te
Hydrogen telluride	H_2Te
Josëite	Bi_3TeS
Krennerite	(Au,Ag)Te
Melonite	Ni_2Te_3
Montbrayite	Au_2Te_3
Muthmannite	(Ag, Au)Te
Nagyagite	$Au_2Sb_2Pb_{10}Te_6S_{15}$

Oruetite	$Bi_3Te_3Bi_2S_3$
Petzite	$(Ag,Au)_2Te$
Pilasonite	Bi_3Te_2
Rickardite	Cu_4Te_3
" Stutzite	Ag_4Te
Sylvanite	$AuAgTe_4$
Talapite	$Bi(S,Te)_3Ag_3$
Telluro bismuthite	Bi_2Te_3
Tetradymite	Bi_2Te_2
Vondiestite	$(Ag,Au)_5BiTe_4$
Wehrlite	Bi_7Te_7Ag
Weissite	Cu_2Te

Mixtures

Coolgardite	coloradoite, petzite, calaverite, sylvanite
Henryite	lead telluride and pyrites
Kalgoorlite	coloradoite, petzite, and tellurium
White tellurium (Gelberg, mullerite)	antimonial telluride of gold, silver, and lead

Tellurites

Durdenite	$Fe_2(TeO_3)_3.4H_2O$
Tellurite	TeO_2

Dunhamite	$PbTeO_3$
Emmonsite	$Fe_2(TeO_3)_3 \cdot 2H_2O$
Mackayite	$Fe_2(TeO_3)_3 \cdot nH_2O$

Tellurates

Ferrotellurite	$FeTeO_4$
Magnolite	Hg_2TeO_4
Montanite	$Bi(OH)_2TeO_4$

Textbooks as recently as 1953 claimed a hexagonal lattice and the existence of two polymorphic modifications α and β with a transition point at 354°C. However, Bose (14) in 1941 showed by x-ray diffraction that precipitated tellurium is not amorphous but is hexagonal in a finely divided state, ie. it is the same as metallic tellurium, and Dodwell (27) proved in 1945 that tellurium does not change its structure when heated up to 360°C and consequently does not have any polymorphic varieties. Crystallization of tellurium fused in sodium hydrosulphate and cooled in carbon dioxide results in the formation of a crystalline star resembling that of antimony.

d. Chemical properties - In agreement with the general observation that the basic properties of the natural families of elements increases with atomic weight, tellurium exhibits a greater basicity than selenium and sulphur.

H. Davy (24) was the first to discover hydrogen telluride (H_2Te), which he formed by the electrolysis of water plus acid using a tellurium cathode. H_2Te is also formed by the action of acids on tellurides, but the electrolytic process gives the best yields. It is a colorless gas with a foul smell resembling that of hydrogen sulphide.

Heating of tellurium in the presence of oxygen produces tellurium dioxide, TeO_2. It forms small, colorless, octahedral crystals. The hydrated form of tellurium dioxide is tellurous acid, H_2TeO_3. Tellurium monoxide is formed when tellurium sulphite is heated between 180° and 230°C in vacuo ($TeSO_3 \longrightarrow TeO + SO_2$). It is a brown, porous mass, stable in dry air but decomposes when heated into tellurium and tellurium dioxide. Tellurium trioxide (TeO_3) is formed when telluric acid (H_2TeO_4) is heated above 360°C but below red heat. If the temperature be too high, the trioxide decomposes into the dioxide. TeO_3 is orange-yellow and crystalline in form.

Tellurium combines with the halogens to produce tellurium halides. Of particular interest in this work is the relatively unreactive tellurium hexafluoride (TeF_6) gas and its possible use in mass spectrometric determination of the tellurium isotopes. Both hexa-halides and tetra-halides are possible. In the case of fluorine, TeF_6 is formed at temperatures reaching 200°C in excess fluorine, whereas, TeF_4 is formed at temperatures below 180°C in excess tellurium (56).

e. Absolute abundances of the isotopes of tellurium - The first report of tellurium isotopes came in 1925 when Aston (3) discovered Te^{126},

Te^{128}, and Te^{130} using his mass spectrograph. As to their relative abundance, he only reported that the latter two were of equal intensity and double that of the first. Then in 1931 he reported Te^{125} (4). Bainbridge (7) in 1932 reported isotopes 122, 123, 124, and 127 and Bartlett (8) in 1934 predicted from $\Delta m/\Delta z$ plots that there should be isotopes Te^{118} and Te^{120}. Dempster (26) in 1936 confirmed Bainbridge's and Bartlett's results using his mass spectrometer but that there was no Te^{118} nor Te^{127}. It was not until 1942 when R. Migeotte (77) using a Bainbridge mass spectrograph reported the eight isotopes with percentage abundances. Four years later, Williams and Yuster (132) confirmed these eight isotopes giving relative abundances. White and Cameron two years later reported similar results (131). The latest values of the isotopes and their percentage abundances were given by Hollander et al in 1953 (54). The results of these investigations are summarized in Table II.

As regarding the atomic mass of each of the isotopes, Duckworth et al (28) in 1951 first reported the masses Te^{126}, Te^{128}, and Te^{130} as 125.9427, 127.9471, and 129.9467 respectively and one year later, Halsted (43) gave the atomic masses for all eight isotopes. Up to 1960, these were the accepted values and no new values were found in

the literature. These values are as given below:

Mass Number	Atomic Mass (amu)
120	119.94288
122	121.94193
123	122.94368
124	123.94278
125	124.94460
126	125.94420
128	127.94649
130	129.94853

E. Advantages of looking at sulphur, selenium, and tellurium isotopes simultaneously in natural deposits

One of the reasons for considering tellurium for an isotope fractionation study is to compare its behaviour with results already obtained with sulphur and selenium. As it has already been shown, a considerable number of studies of the S^{32}/S^{34} variations have yielded much information about natural processes. The preliminary study which has been conducted with Se^{76}/Se^{82} also looks promising in that it shows some similarities to the sulphur isotope distribution.

Whereas sulphur exists in nature from the -2 to the +6 valence states, it is very rare that selenium exists in valence states higher than +4, and tellurium rarely exists

Table II

Absolute Abundances of the Isotopes of Tellurium

Worker Year Reference	Aston 1925 (3)	Aston 1931 (4)	Bainbridge 1932 (7)	Bartlett 1934 (8)	Dempster 1936 (26)
Instrument	Mass spectrograph, photometric detection	Mass spectrograph, photometric detection	Mass spectroscope, magnetic scanning, photometric detection	Predicted from $\Delta m/\Delta z$ plots.	Mass spectrometer, electronic detection
Ion source	Te vapour	Te vapour	Te vapour		Spark between tellurium and palladium electrodes
Isotopes reported	Te^{126} Te^{128} Te^{130}	Te^{125}	Te^{122} Te^{123} Te^{124} Te^{127}	Te^{118} Te^{120} Te^{124} Te^{130}	No Te^{118} nor Te^{127} Te^{120}
Mass number	Abundances (per cent)				
120			----		
122			2.9		
123	Te^{128} and		1.6		
124	Te^{130} equal		4.5		
125	intensity and	6.6	6.0		
126	double that	20.9	19.0		
128	of Te^{125}	36.1	32.8		
130		36.4	33.1		

Table II cont'd

Worker Year Reference	Migeotto 1936 (77)	Williams and Yuster 1946 (132)	White and Cameron 1948 (131)	Hollander et al. 1953 (54)
Instrument	Bainbridge mass spectroscope, photometric detection	Nier 60° mass spectrometer, magnetic scanning, electronic detection	60° mass spectrometer, magnetic scanning, electronic detector	
Ion source	Te ions excited by Hg 4359 line	Ionization of TeF_6 gas with 100 volt electrons	Bombarding TeF_6 gas with 30-75 volt electrons	
Isotopes reported	Te^{120} Te^{125} Te^{122} Te^{126} Te^{123} Te^{128} Te^{124} Te^{130}	same	same	same

Mass number	Abundances (%)					
		*Average	TeF_3^+	TeF_5^+		
120	1.5	0.26			0.091	0.089
122	2.9	7.05	6.89	7.14	2.49	2.46
123	1.6	2.47	2.42	2.51	0.89	0.87
124	4.5	13.3	13.2	13.4	4.63	4.61
125	6.0	20.15	19.8	20.5	7.01	6.99
126	19.0	54.2	53.8	54.12	18.72	18.71
128	32.8	92.3	92.0	92.5	31.72	31.79
130	33.1	100	100	100	34.49	34.49

*Relative abundances

in a valence state as high as +4. This results because of the different oxidation potentials for the elements. Further, similar chemical reactions of these elements have different temperature dependences, and because of their different sizes, the three elements behave differently in physical processes such as diffusion.

If all three elements can be simultaneously examined isotopically, it may be possible to separate the various physical, chemical, and biological processes which have occurred in a deposit.

THEORY

An isotope effect, or isotope fractionation, occurs when the relative abundances of the isotopes of an element in some system are altered by physical or chemical means, and is a result of slight differences in the properties of these isotopes. Chemically an effect may occur when two or more molecular species containing the element in question co-exist in chemical equilibrium (equilibrium isotope effect) or when one or more molecular species change their identity in the course of a chemical reaction (kinetic isotope effect).

The principles of isotopic fractionation are now well-known and it is possible to calculate, from a knowledge of the fundamental vibrational frequencies of the compounds, the extent to which the isotopes might be expected to fractionate in a naturally occurring process.

Looking at the members of the group VIA elements, there is a mass difference of two or a percentage mass difference of 13% in the case of the two oxygen isotopes O^{16} and O^{18}; a mass difference of two or a percentage mass difference of 7% in the case of S^{32} and S^{34}; a mass difference of six or percentage mass difference of 8% in the case of Se^{76} and Se^{82}; and a mass difference of eight or percentage mass difference of 7% in the case of Te^{130} and Te^{122}.

Significant isotope effects have been found for the two oxygen, sulphur, and selenium isotopes respectively, and therefore, some fractionation of the tellurium isotopes is expected.

A. Theory of Equilibrium Isotope Effects

Although chemical equilibrium may be considered as that condition of a chemical system where the rate at which a forward reaction is taking place is exactly balanced by the rate of the reverse reaction, the theory of equilibrium isotope effects is best considered in terms of the statistical mechanics of a system of particles in dynamic equilibrium.

Urey and Rittenberg (114), (115), were the first to show by theoretical calculations that marked differences in the equilibrium constants of isotopic exchange reactions should exist. Urey and Grieff (116) applied statistical mechanics to the calculation of equilibrium exchange constants in terms of distribution functions and "summation over states" terms and this was simplified by Urey (118) and Bigeleisen and Mayer (10). Their simplification made it possible to calculate the equilibrium constants of isotopic reactions solely with a knowledge of the vibrational frequencies of the isotopic molecules. It is to be noted,

however, that such a treatment does not consider the time taken to attain equilibrium or whether there in fact exists a mechanism by which equilibrium may be attained.

An isotopic exchange reaction may be written

$$aA_1 + bB_2 \underset{\rightarrow}{\overset{K}{\leftarrow}} aA_2 + bB_1 \qquad (1)$$

where the subscripts 1 and 2 refer to the light and heavy isotopes respectively and A and B are molecules having the element under consideration as a common constituent. From thermodynamics (72), the standard free energy change for the above reaction is given in terms of the equilibrium constant by

$$-RT \ln K = \Delta F^{o} \qquad (2)$$

or

$$-RT \ln K = aF_{A_2} + bF_{B_1} - aF_{A_1} - bF_{B_2} \qquad (3)$$

In terms of the partition function "Q", the free energy can be written as (F = Gibbs free energy)

$$F = E_o + RT \ln N - RT \ln Q \qquad (4)$$

where N is Avagadro's number, E_o is the zero point energy, and Q is the total partition function given by

$$Q = \sum_n g_n e^{-\epsilon_n/kT} \qquad (5)$$

where g_n is the statistical weight factor and the summation extends over all the quantum states of energy ϵ_n. A d-fold degenerate level would count as d states.

If only one molecule is considered in unit volume instead of one mole, N is replaced by unity and the second term of (4) disappears. Substitution of (4) into (3) and simplification gives

$$K = \left\{ \left[\frac{Q_{A_2}}{Q_{A_1}}\right]^a \Big/ \left[\frac{Q_{B_2}}{Q_{B_1}}\right]^b \right\} \exp \left[\frac{aE_{oA_2} + bE_{oB_1} - aE_{oA_1} - bE_{oB_2}}{kT}\right] \qquad (6)$$

Since they are determined by the electrical forces, the potential energy curves have been found to be essentially identical for isotopic molecules. Referring all energies to the minimum of the potential energy curves rather than the zero point energy simplifies (6) to

$$K = \left[\frac{Q_{A_2}}{Q_{A_1}}\right]^a \Big/ \left[\frac{Q_{B_2}}{Q_{B_1}}\right]^b \qquad (7)$$

and the equilibrium constant becomes the ratios of the partition functions for the two isotopically substituted molecules.

B. Evaluation of Partition Function Ratios

The partition function of a molecule depends upon its mass, moments of inertia, fundamental vibrational frequencies, temperature, and nuclear spins of the constituent atoms. It is, however, possible to evaluate partition function ratios for isotopic molecules using only vibrational frequencies.

Following Herzberg (49) considering a volume V,

$$Q = \frac{(2\pi MkT)^{3/2}}{h^3} \cdot V \cdot \frac{kT}{hcB} \prod_i^{3n-5} \frac{e^{-u_i/2}}{1-e^{-u_i}} \frac{1}{\sigma} \prod (2I+1) \prod \frac{(2I+1)}{2}^2 \qquad (8)$$

for diatomic (or linear polyatomic) molecules, and

$$Q = \frac{(2\pi MkT)^{3/2}}{h^3} \cdot V \cdot \left[\frac{\pi}{ABC}\left(\frac{kT}{hc}\right)^3\right]^{1/2} \prod_i^{3n-6} \frac{e^{-u_i/2}}{1-e^{-u_i}} \left[\frac{1}{\sigma} \prod (2I+1) \prod \frac{(2I+1)^2}{2}\right] \qquad (9)$$

for polyatomic molecules, where

n = number of atoms in the molecule

M = total molecular mass

k = Boltzman constant

A,B,C = rotational comstants of the molecules, related to its principal moments of inertia, i.e.,

$$A = \frac{h}{8\pi^2 c I_A}$$

$u_i = \frac{h\nu_i}{kT}$ where ν_i is the i^{th} fundamental frequency of the molecule.

The product $\prod_i$ extends over all i fundamental frequencies of the polyatomic molecule and the bracketed terms are symmetry and nuclear spin factors. The nuclear spin factors cancel out in later expressions and have no effect on the estimation of isotope effects. The symmetry factors are discussed later.

Thus, for two isotopic polyatomic molecules,

$$\frac{Q_2}{Q_1} = \left[\frac{M_2}{M_1}\right]^{3/2} \cdot \left[\frac{I_{A_2} I_{B_2} I_{C_2}}{I_{A_1} I_{B_1} I_{C_1}}\right]^{1/2} \prod_i^{3n-6} \frac{e^{-u_{2i}/2}}{1-e^{-u_{2i}}} \cdot \frac{1-e^{-u_{1i}}}{e^{-u_{1i}/2}} \qquad (10)$$

Urey (118) simplified the two expressions (8) and (9) and defined new partition functions which were the equilibrium constants for exchange reactions between the compound considered and the separated atoms. Both sides of equations (8) and (9) are multiplied by $(M_1/M_2)^{3/2n}$ where M_1 and M_2 are the atomic weights of the isotopic atoms being considered and n is the number of the isotopic atoms exchanged. Further, the right sides of (8) and (9) are multiplied and divided by (u_1/u_2) and $\prod_i (u_{1_i}/u_{2i})$ respectively. According to the Teller-Redlich theorem (70,87),

$$\frac{I_2}{I_1}\left[\frac{M_2}{M_1}\right]^{3/2}\left[\frac{M_1}{M_2}\right]^{3/2n}\left[\frac{u_1}{u_2}\right]=\left[\frac{A_2B_2C_2}{A_1B_1C_1}\right]^{1/2}\left[\frac{M_2}{M_1}\right]^{3/2}\left[\frac{M_1}{M_2}\right]^{3/2n}\prod_i\left[\frac{u_{1_i}}{u_{2_i}}\right] \qquad (11)$$

Carrying out the steps above and using (11), equation (10) becomes

$$\frac{Q_2}{Q_1}=\left[\frac{M_{2_i}}{M_{1_i}}\right]^{3/2}\frac{\sigma_1}{\sigma_2}\cdot\frac{u_2}{u_1}\cdot\frac{e^{-u_2/2}(1-e^{-u_1})}{e^{-u_1/2}(1-e^{-u_2})} \qquad (12)$$

and

$$\frac{Q_2}{Q_1}=\frac{3n-6}{\left|\ i\ \right|}\left[\frac{M_{2_i}}{M_{1_i}}\right]^{3/2}\frac{\sigma_1}{\sigma_2}\frac{3n-6}{\left|\ i\ \right|}\frac{u_{2_i}}{u_{1_i}}\cdot\frac{e^{-u_2/2}(1-e^{-u_1})}{e^{-u_1/2}(1-e^{-u_2})} \qquad (13)$$

for diatomic molecules and polyatomic molecules respectively.

The terms $(M_{2_i}/M_{1_i})^{3/2}$ will not affect the expression for an equilibrium constant since they will appear in both numerator and denominator. Thus the equilibrium constant can be given by

$$K=\left[\frac{Q_2'}{Q_1'}_A\right]^a\Big/\left[\frac{Q_2'}{Q_1'}_B\right]^b \qquad (14)$$

where $\frac{Q_2'}{Q_1'}=\left[\frac{M_1}{M_2}\right]^{3/2n}\cdot\frac{Q_2}{Q_1}$ is the relation between the new partition function ratio and the old ratio. K can now

be calculated with only a knowledge of the vibrational frequencies of the isotopic molecules. These frequencies are obtained either by direct observation or by calculation from observations on a more abundant isotope by means of force equations.

This expression excludes the anharmonic terms in the vibrational energy, and assumes that the rotational partition functions have reached classical values. However, these have been investigated by Urey (118) and Herzberg (49) and the approximation is not greatly in error when considering the ratios of partition functions for isotopic molecules, provided the observed fundamental frequencies are used rather than the zero order frequencies and that the temperature is low enough so that only low lying vibrational states have appreciable populations. The ratio of symmetry numbers will be unity if the molecule under consideration contains only one atom of the element for which an exchange is considered or if the molecule contains more than one such atom but these atoms occupy indistinguishable positions in the molecule and are all exchanged in the reaction.

Thus, we have for diatomic molecules

$$\frac{Q_2'}{Q_1'} = \frac{u_2}{u_1} \cdot \frac{e^{-u_2/2} \cdot (1 - e^{-u_1})}{e^{-u_1/2} \cdot (1 - e^{-u_2})} \qquad (15)$$

and for polyatomic molecules,

$$\frac{Q_2'}{Q_1'} = \prod_{i}^{3n-6} \frac{u_{2i}}{u_{1i}} \cdot \frac{e^{-u_{2i}} \cdot (1 - e^{-u_{1i}})}{e^{-u_{1i}} \cdot (1 - e^{-u_{2i}})} \qquad (16)$$

These expressions have been simplified by Urey (118) and Bigeleisen and Mayer (10) for manual calculations. In the work of this thesis IBM 7040 programs were set up to calculate the exact expressions directly.

C. Kinetic Isotope Effects

The theory of isotope fractionation in kinetic chemical reactions is considered in terms of the theory of absolute reaction rates. This theory was developed by Eyring (36) and Evans and Polanyi (35) from a statistical treatment of reaction rates. Bigeleisen (9) then used their theory and collision theory to develop formulae which predict the kinetic isotope effect.

This theory is developed around two postulates. Firstly, there exists an "activated complex" in chemical equilibrium with the initial state of the reactants and intermediate between this initial state and a final state of the products. Secondly, this "activated complex" decomposes at a definite rate to form the products of the reaction.

From these postulates, the rate constant k can be written (40a) as

$$k = \frac{k'T}{h} \cdot k_T tK$$

where

k' = Boltzman constant

T = absolute temperature

h = Planck's constant

k_T = transmission coefficient

t = quantum mechanical tunnelling correction

K = equilibrium constant for the equilibrium between the reactant and the activated complex

Thus, for isotopic molecules, the ratio of rate constants becomes,

$$\frac{k_1}{k_2} = \frac{k_{T1}}{k_{T2}} \cdot \frac{t_1}{t_2} \cdot \frac{K_1}{K_2}$$

Hirschfelder and Wigner (52) have conducted a theoretical study to show that the transmission coefficients ratio is very nearly unity for systems above room temperature having a distribution in the velocities of the reacting isotopic molecules. Also, t_1 is set equal to t_2, the assumption of which is discussed by Bigeleisen (13). Thus we can write

$$\frac{k_1}{k_2} = \frac{K_1}{K_2}$$

From the previous discussion of equilibrium constants,

$$\frac{K_1}{K_2} = \frac{Q_2'}{Q_1'} \Bigg/ \frac{Q_2^{\ddagger}}{Q_1^{\ddagger}} \qquad (17)$$

where Q_1 and Q_2 refer to partition functions for the reactants, and $Q_1^{\ddagger}$ and $Q_2^{\ddagger}$ refer to partition functions for the activated complexes. The partition function ratios can be set up in the same manner as was done in part A of the theory. For the activated complex, however, we have to consider its nature. According to the theory, one of the vibrational degrees of freedom of the activated complex is non-genuine, corresponding to the cleavage (or formation) of a bond. Thus, supposing that the L^{th} vibrational mode is non-genuine, so that U_L has a pure imaginary value, the vibrational contribution to the partition function of the activated complex will then take the form

$$\prod_i^{3n^{\ddagger}-7} \frac{e^{-U_i/2}}{1-e^{-U_i}}$$

so that

$$\frac{Q_2^{\ddagger}}{Q_1^{\ddagger}} = \frac{3n^{\ddagger}-7}{\left| \quad j \quad \right|} \left[\frac{M_{2j}^{\ddagger}}{M_{1j}^{\ddagger}} \right]^{3/2} \frac{U_{2L}^{\ddagger}}{U_{1L}^{\ddagger}} \left| \quad i \neq L \right| \frac{U_{2i}^{\ddagger}}{U_{1i}^{\ddagger}} \cdot \frac{e^{-U_{2i}^{\ddagger}/2}(1-e^{-U_{1i}^{\ddagger}})}{e^{-U_{1i}^{\ddagger}/2}(1-e^{-U_{2i}^{\ddagger}})}$$

for polyatomic molecules.

Again, the mass ratios will cancel so we can write

$$\frac{Q_2^{\ddagger''}}{Q_1^{\ddagger''}} = \frac{U_{2L}^{\ddagger}}{U_{1L}^{\ddagger}} \frac{3n^{\ddagger}-7}{\left| \quad i \neq L \right|} \frac{U_{2i}^{\ddagger}}{U_{1i}^{\ddagger}} \cdot \frac{e^{-U_{2i}^{\ddagger}}(1-e^{-U_{1i}^{\ddagger}})}{e^{-U_{1i}^{\ddagger}/2}(1-e^{-U_{2i}^{\ddagger}})}$$

now

$$U_L = \frac{hc}{kT} \cdot \omega_L \qquad \omega = \text{frequency}$$

so that

$$\frac{U_{2L}^{\ddagger}}{U_{1L}^{\ddagger}} = \frac{\omega_{2L}^{\ddagger}}{\omega_{1L}^{\ddagger}}$$

Furthermore, this "imaginary" frequency is the stretching frequency of the bond being broken (or formed). Thus, this frequency can be expressed as the square root of the inverse of the effective masses along the co-ordinate of decomposition of the activated complex. Our expression then becomes

$$\frac{Q_2^{\ddagger''}}{Q_1^{\ddagger''}} = \left[\frac{M_2^{\ddagger}}{M_1^{\ddagger}}\right]^{1/2} \prod_{i\neq L}^{3n^{\ddagger}-7} \frac{U_{2i}^{\ddagger}}{U_{1i}^{\ddagger}} \cdot \frac{e^{-U_{2i}^{\ddagger}/2}\,(1 - e^{-U_{1i}^{\ddagger}})}{e^{-U_{1i}^{\ddagger}/2}\,(1 - e^{-U_{2i}^{\ddagger}})}$$

writing this as

$$\frac{Q_2^{\ddagger''}}{Q_1^{\ddagger''}} = \left[\frac{M_2}{M_1}\right]^{1/2} \frac{Q_2^{\ddagger'}}{Q_1^{\ddagger'}}$$

it can be seen that equation (17) can be written as

$$\frac{k_1}{k_2} = \left[\frac{Q_2'}{Q_1'} \Big/ \frac{Q_2^{\ddagger'}}{Q_1^{\ddagger'}}\right] \cdot \left[\frac{M_2^{\ddagger}}{M_1^{\ddagger}}\right]^{1/2} \qquad (18)$$

From equation (18) it can be seen that the light molecule usually has a greater rate constant since the factor $(M_2^{\ddagger}/M_1^{\ddagger})^{1/2}$ is always greater than unity and the reacting molecule is usually more tightly bound than the activated complex. That is

$$\frac{Q_2'}{Q_1'} > \frac{Q_2^{\ddagger'}}{Q_1^{\ddagger'}}$$

Regarding the ratio $(M_2^{\ddagger}/M_1^{\ddagger})$, two different approaches can be made. Wolfsberg (136) gives the following reasoning. Consider a molecule, X-A-B-Y in which the A-B bond is broken. If the A-B bond is strong compared to the X-A, B-Y bonds, then the latter will shorten as the former lengthens and the reduced mass will be closer to $(\frac{AB}{A+B})$. If, however, the A-B bond is the weaker, then the reduced mass will be closer to $(M_{XA}.M_{XB})/(M_{XA} + M_{XB})$ since the mass centres M_{XA} and M_{XB} are being separated.

Since very little is known about the nature of the activated complex, the rate constant cannot be evaluated specifically. However, three different approaches are feasible which follow the formalism of the theory and incorporate the idea that in the transition state, the vibrational frequencies of the activated complex are the same as those of the reactant molecule except for that corresponding to bond cleavage or formation. Approaches I and III give extreme lower and upper limits respectively that might be expected for the ratio of rate constants and approach II gives an intermediate and best description of the physical situation.

I. When the partition function ratio term is very close to unity which occurs when the temperature is high. In the high temperature limit,

$$\frac{k_1}{k_2} = \left[\frac{M_2^{\ddagger}}{M_1^{\ddagger}} \right]^{1/2}$$

The mass ratio can either be the atomic mass ratio or mass fragment ratio.

II. Where the activated complex is identical to the starting material, with the exception that the frequency associated with the breaking bond is missing. In this case,

$$\frac{Q_2'}{Q_1'} \Big/ \frac{Q_2^{\ddagger'}}{Q_1^{\ddagger'}} = \frac{Q(\omega_{2L})}{Q(\omega_{1L})}$$

where this ratio is the same as the partition function ratio for diatomic isotopic molecules with frequencies ω_{2L} and ω_{1L}, ω_L being that frequency in the starting material which is missing in the activated complex. The mass ratio is evaluated as before.

III. Where the activated complex has some structure which is strictly speaking unknown, but for which the value of the partition function ratio lies between that for the starting material (with the omission of a

frequency term) and unity. The extreme case of unity may be approached if in the transition state there is a complexing of the reacting molecule with other material, so that a complicated structure is formed in which not many of the vibrational frequencies are sensitive to isotopic substitution. In this case,

$$\frac{k_1}{k_2} = \frac{Q_2}{Q_1} \cdot \left[\frac{M_2^{\ddagger}}{M_1^{\ddagger}}\right]^{1/2}$$

These three approaches give for a particular model of the activated complex an intermediate (II) as well as extreme (I, and III) estimates for the ratio of rate constants.

D. Isotope fractionation during first order competing reactions

In general, we have the competitive isotopic reactions of the type

$$A_1 + B \xrightarrow{k_1} X_1 + Y$$

$$A_2 + B \xrightarrow{k_2} X_2 + Y$$

where subscripts 1 and 2 refer to the light and heavy isotopic species respectively. The rate constant k

indicates how fast A is converted to X.

The rate of the reaction is given in terms of the rate constant as

$$\text{Rate} = kC_A C_B$$

where k = the rate constant

C_A = concentration of reactant A

C_B = concentration of reactant B

A first order reaction is one where the time dependence of product formation can be written as

$$\frac{dX}{dt} = k(A_0 - X)B$$

where A_0 is the initial concentration of the reactant.

Thus, for the competing reactions mentioned,

$$\frac{dX_1}{dt} = k_1(A_{01} - X_1)B$$

$$\frac{dX_2}{dt} = k_2(A_{02} - X_2)B$$

At $t = 0$, $X_1 = X_2 = 0$, so upon integrating,

$$\frac{k_1}{k_2} = \frac{\log\left[\frac{A_{01}}{A_{01} - X_1}\right]}{\log\left[\frac{A_{02}}{A_{02} - X_2}\right]}$$

If we designate the fraction of molecules which have reacted as

$$f = \frac{X_1 + X_2}{A_{01} + A_{02}} = \frac{X_1(1 + X_2/X_1)}{A_{01}(1 + A_{02}/A_{01})}$$

and the integrated isotopic composition of the product as

$$r = \frac{X_2/X_1}{A_{02}/A_{01}}$$

we can write

$$\frac{k_1}{k_2} = \frac{\log\left[1 - f\,\frac{1 + A_{02}/A_{01}}{1 + X_2/X_1}\right]}{\log\left[1 - rf\,\frac{1 + A_{02}/A_{01}}{1 + X_2/X_1}\right]} \qquad (19)$$

Thus, the ratio of the rate constants for competitive isotopic reactions is obtained from the determination of isotopic ratios in the initial reactant A_{02}/A_{01} and in the product X_2/X_1 after fraction f of the molecules have reacted.

THEORETICAL CALCULATIONS

A. Calculation of equilibrium exchange constants

As was noted, the extent to which one would expect isotopic fractionation to take place in exchange reactions is found from the partition function ratios. Thus, the partition function ratios have been calculated for various molecules containing Te^{130} and Te^{122}.

Appendix I contains calculations of vibrational frequencies for some Te^{130} and Te^{122}-containing compounds for which molecular data such as symmetry type and fundamental vibrational frequencies were available. For the diatomic species, anharmonicity corrections were made. Since Te^{130} is the most abundant isotope, and also since use of this mass number gave results closest to the observed, it was assumed that fundamental frequencies applied to compounds containing this isotope. The frequencies of the Te^{122}-containing molecules were then calculated by means of force field equations from these observed values.

In most cases, sets of equations describing the force fields were accompanied by force constants already calculated. However, in the case of H_2Te and $TeO_3^=$ the force constants had not been previously calculated so

these were calculated by substituting the known fundamental frequencies into a set of force equations describing the molecule.

From the isotopic vibrational frequencies, the partition function ratios at various temperatures were calculated using equations (15) and (16) for diatomic and polyatomic molecules respectively. The equilibrium exchange constants for possible isotopic exchange reactions were then calculated using equation (14). Tables III and IV give the partition function ratios and equilibrium exchange constants respectively. Looking at Table IV, the values in the body of the table are the equilibrium constants for exchange reactions between the compounds listed along the top and the compounds listed down the left-hand column calculated for the temperatures listed in the far right-hand column. A constant greater than unity means that the heavier isotope is concentrated in the compound in the left-hand column.

For example, consider TeF_6 in the left-hand column, and TeO at the top of the table. The value 1.0234 is found at 20°C in the table where the TeO column and TeF_6 row intersect. This is the equilibrium constant for the reaction:

Table III

Q_2'/Q_1' for Te-containing molecules

°C	GeTe	PbTe	SnTe	TeO	SiTe	TeTe	HTe	TeF_6	$TeBr_4$	SCTe	$TeO_3^=$	H_2Te
0	1.00270	1.00205	1.00235	1.00409	1.00278	1.00230	1.00114	1.03067	1.00467	1.00833	1.01398	1.00241
10	1.00252	1.00191	1.00219	1.00386	1.00261	1.00215	1.00110	1.02882	1.00435	1.00779	1.01313	1.00230
20	1.00236	1.00178	1.00205	1.00364	1.00244	1.00201	1.00105	1.02713	1.00406	1.00731	1.01236	1.00220
30	1.00221	1.00167	1.00192	1.00344	1.00230	1.00188	1.00101	1.02559	1.00380	1.00686	1.01165	1.00211
40	1.00208	1.00157	1.00181	1.00326	1.00216	1.00177	1.00097	1.02416	1.00357	1.00646	1.01100	1.00202
50	1.00196	1.00147	1.00170	1.00309	1.00204	1.00166	1.00093	1.02285	1.00335	1.00609	1.01040	1.00193
60	1.00184	1.00139	1.00160	1.00293	1.00193	1.00156	1.00090	1.02164	1.00316	1.00575	1.00985	1.00186
70	1.00174	1.00131	1.00151	1.00279	1.00182	1.00148	1.00086	1.02052	1.00298	1.00544	1.00933	1.00178
80	1.00165	1.00124	1.00143	1.00265	1.00173	1.00140	1.00083	1.01949	1.00281	1.00515	1.00886	1.00172
90	1.00156	1.00117	1.00135	1.00252	1.00164	1.00132	1.00080	1.01853	1.00266	1.00489	1.00842	1.00165
100	1.00148	1.00111	1.00128	1.00241	1.00155	1.00125	1.00077	1.01764	1.00252	1.00464	1.00802	1.00159
200	1.00093	1.00069	1.00080	1.00157	1.00099	1.00078	1.00056	1.01136	1.00157	1.00295	1.00515	1.00113
300	1.00064	1.00047	1.00055	1.00110	1.00068	1.00053	1.00042	1.00790	1.00107	1.00204	1.00358	1.00085
400	1.00046	1.00034	1.00040	1.00081	1.00050	1.00039	1.00033	1.00579	1.00078	1.00149	1.00262	1.00065
500	1.00035	1.00026	1.00030	1.00062	1.00038	1.00029	1.00026	1.00443	1.00059	1.00113	1.00200	1.00052
600	1.00028	1.00020	1.00024	1.00049	1.00030	1.00023	1.00022	1.00349	1.00046	1.00089	1.00158	1.00042
700	1.00022	1.00016	1.00019	1.00040	1.00024	1.00019	1.00018	1.00282	1.00037	1.00072	1.00128	1.00035
800	1.00018	1.00014	1.00016	1.00033	1.00020	1.00015	1.00015	1.00233	1.00031	1.00059	1.00105	1.00029
900	1.00015	1.00011	1.00013	1.00027	1.00017	1.00013	1.00013	1.00195	1.00026	1.00050	1.00088	1.00025
1000	1.00013	1.00010	1.00011	1.00023	1.00014	1.00011	1.00011	1.00165	1.00022	1.00042	1.00075	1.00021

Table IV. Equilibrium Constants for Te^{130} - Te^{122} Exchange Reactions

	$Te^{130}F_6$ / $Te^{122}F_6$	$Te^{130}O_3^{=}$ / $Te^{122}O_3^{=}$	$SCTe^{130}$ / $SCTe^{122}$	$Te^{130}Br_4$ / $Te^{122}Br_4$	$Te^{130}O$ / $Te^{122}O$	$SiTe^{130}$ / $SiTe^{122}$	$GeTe^{130}$ / $GeTe^{122}$	H_2Te^{130} / H_2Te^{122}	$SnTe^{130}$ / $SnTe^{122}$	$Te^{130}Te^{130}$ / $Te^{130}Te^{122}$	$PbTe^{130}$ / $PbTe^{122}$	HTe^{130} / HTe^{122}	T°C
$Te^{130}F_6$ / $Te^{122}F_6$	1.0000	1.0165	1.0222	1.0259	1.0265	1.0298	1.0279	1.0281	1.0283	1.0283	1.0286	1.0294	0
		1.0146	1.0197	1.0230	1.0234	1.0246	1.0247	1.0249	1.0250	1.0251	1.0253	1.0261	20
		1.0123	1.0167	1.0194	1.0197	1.0208	1.0208	1.0209	1.0211	1.0212	1.0213	1.0219	50
		1.0095	1.0129	1.0151	1.0152	1.0161	1.0161	1.0160	1.0163	1.0164	1.0165	1.0169	100
$Te^{130}O_3^{=}$ / $Te^{122}O_3^{=}$		1.0000	1.0056	1.0093	1.0098	1.0112	1.0112	1.0115	1.0116	1.0117	1.0119	1.0128	0
			1.0050	1.0083	1.0087	1.0099	1.0100	1.0101	1.0103	1.0103	1.0106	1.0113	20
			1.0043	1.0070	1.0073	1.0083	1.0084	1.0085	1.0087	1.0087	1.0089	1.0095	50
			1.0034	1.0055	1.0056	1.0065	1.0065	1.0064	1.0067	1.0068	1.0069	1.0072	100
$SCTe^{130}$ / $SCTe^{122}$			1.0000	1.0036	1.0042	1.0055	1.0056	1.0059	1.0060	1.0060	1.0063	1.0072	0
				1.0032	1.0037	1.0049	1.0049	1.0051	1.0052	1.0053	1.0055	1.0063	20
				1.0027	1.0030	1.0040	1.0041	1.0042	1.0044	1.0044	1.0046	1.0052	50
				1.0021	1.0022	1.0031	1.0032	1.0030	1.0034	1.0034	1.0035	1.0039	100
$Te^{130}Br_4$ / $Te^{122}Br_4$				1.0000	1.0006	1.0019	1.0020	1.0023	1.0023	1.0024	1.0026	1.0035	0
					1.0004	1.0016	1.0017	1.0019	1.0020	1.0020	1.0023	1.0030	20
					1.0003	1.0013	1.0014	1.0014	1.0016	1.0017	1.0019	1.0024	50
					1.0001	1.0010	1.0010	1.0009	1.0012	1.0013	1.0014	1.0017	100
$Te^{130}O$ / $Te^{122}O$					1.0000	1.0013	1.0014	1.0017	1.0017	1.0018	1.0020	1.0029	0
						1.0012	1.0013	1.0014	1.0016	1.0016	1.0019	1.0026	20
						1.0010	1.0011	1.0012	1.0014	1.0014	1.0016	1.0022	50
						1.0009	1.0009	1.0008	1.0011	1.0012	1.0013	1.0016	100
$SiTe^{130}$ / $SiTe^{122}$						1.0000	1.0001	1.0004	1.0004	1.0005	1.0007	1.0016	0
							1.0001	1.0002	1.0004	1.0004	1.0007	1.0014	20
							1.0001	1.0001	1.0003	1.0004	1.0006	1.0011	50
							1.0001	1.0000	1.0003	1.0003	1.0004	1.0008	100

Table IV Cont'd

	$\frac{GeTe^{130}}{GeTe^{122}}$	$\frac{H_2Te^{130}}{H_2Te^{122}}$	$\frac{SnTe^{130}}{SnTe^{122}}$	$\frac{Te^{130}Te^{130}}{Te^{130}Te^{122}}$	$\frac{PbTe^{130}}{PbTe^{122}}$	$\frac{HTe^{130}}{HTe^{122}}$	T°C
$\frac{GeTe^{130}}{GeTe^{122}}$	1.0000	1.0003	1.0005	1.0004	1.0006	1.0016	0
		1.0002	1.0003	1.0003	1.0006	1.0013	20
		1.0000	1.0003	1.0003	1.0005	1.0010	50
		1.0000	1.0002	1.0002	1.0004	1.0007	100
$\frac{H_2Te^{130}}{H_2Te^{122}}$		1.0000	1.0001	1.0004	1.0004	1.0013	0
			1.0001	1.0002	1.0004	1.0011	20
			1.0002	1.0003	1.0005	1.0010	50
			1.0003	1.0003	1.0005	1.0003	100
$\frac{SnTe^{130}}{SnTe^{122}}$			1.0000	1.0000	1.0003	1.0012	0
				1.0000	1.0003	1.0010	20
				1.0000	1.0002	1.0008	50
				1.0000	1.0002	1.0005	100
$\frac{Te^{130}Te^{130}}{Te^{130}Te^{122}}$				1.0000	1.0002	1.0012	0
					1.0002	1.0010	20
					1.0002	1.0007	50
					1.0001	1.0005	100
$\frac{PbTe^{130}}{PbTe^{122}}$					1.0000	1.0009	0
						1.0007	20
						1.0005	50
						1.0003	100
$\frac{HTe^{130}}{HTe^{122}}$						1.0000	

$$Te^{130}O + Te^{122}F_6 \rightleftarrows^{K} Te^{122}O + Te^{130}F_6$$

This means that provided the reaction is possible, a 2.3% tellurium isotope effect is predicted and the TeF_6 species will be enriched by 2.3% in the heavier isotope.

B. Calculation of ratios of isotopic rate constants

As mentioned in the theory, intermediate values as well as upper and lower extremes could be determined for the ratio of kinetic rate constants. The lower limit reached at high temperatures is where

$$\frac{k_1}{k_2} = \left[\frac{M_2^{\ddagger}}{M_1^{\ddagger}} \right]^{1/2}$$

and $(M_2^{\ddagger}/M_1^{\ddagger})^{1/2}$ represents the effective mass of the complex along the reaction co-ordinate. If this is simply the reduced mass of the atoms whose bond is directly involved in the reaction, $M_2^{\ddagger}$ and $M_1^{\ddagger}$ are the isotopic reduced masses of the molecules. Table V gives the minimum value of the rate constant ratio to be expected in a kinetic isotope reaction in which the bond is broken between the diatomic molecules listed. These are temperature independent.

Minimum Value of k_{130}/k_{122}						
GeTe	PbTe	SnTe	TeO	SiTe	TeTe	HTe
1.012	1.020	1.016	1.004	1.006	1.016	1.000

Table V

Considering now the reduction of potassium tellurite, and suppose the rate determining step is the cleavage of a Te - O bond:

I. The high temperature limit for k_1/k_2 is the mass term 1.004 if atom fragments are considered or 1.002 if mass fragments in the "di-fragmental molecule" TeO_2 - O are used.

II. The intermediate value and closest to the physical situation is $\left[\frac{Q_2'}{Q_1'} \Big/ \frac{Q_2^{\ddagger}}{Q_1^{\ddagger}}\right] \cdot \left[\frac{M_2^{\ddagger}}{M_1^{\ddagger}}\right]^{1/2}$ where $Q_2^{\ddagger\prime} \Big/ Q_1^{\ddagger\prime}$ is simply that for $TeO_3^{=}$ with the frequency contribution of the Te - O bond omitted. This mode is most probably one component of the doubly degenerate E type asymmetric stretching vibration ω_3.

$$\frac{Q_2'}{Q_1^{\ddagger}} \Big/ \frac{Q_2^{\ddagger\prime}}{Q_1^{\ddagger\prime}} = \begin{array}{ll} 1.0041 & \text{at } 0^{\circ}C \\ 1.0037 & \text{at } 20^{\circ}C \\ 1.0031 & \text{at } 50^{\circ}C \end{array}$$

The mass ratio is as determined in part I for either atomic or mass fragments.

III. The upper limit for k_1/k_2 is given by

$$\frac{k_1}{k_2} = \frac{Q(Te^{130}O_3^{=})}{Q(Te^{122}O_3^{=})} \cdot \left[\frac{M_2^{\ddagger}}{M_1^{\ddagger}}\right]^{1/2}$$

The results of the three methods of calculation are summarized in Table VI. All these simple models give a regular decrease in the value of k_1/k_2 with increase in temperature.

Table VI

Summary of the Calculated Ratios of Rate Constants for the Reduction of K_2TeO_3

T°C	k_1/k_2					
	Low		Intermediate		High	
	Mass	Atom	Mass	Atom	Mass	Atom
0	1.002	1.004	1.00615	1.00765	1.0160	1.0175
10	1.002	1.004	1.00590	1.00740	1.0152	1.0167
20	1.002	1.004	1.00568	1.00718	1.0144	1.0159
30	1.002	1.004	1.00547	1.00697	1.0137	1.0152
40	1.002	1.004	1.00528	1.00678	1.0130	1.0145
50	1.002	1.004	1.00511	1.00661	1.0124	1.0139
60	1.002	1.004	1.00494	1.00644	1.0119	1.0134
70	1.002	1.004	1.00479	1.00629	1.0114	1.0129
80	1.002	1.004	1.00465	1.00615	1.0109	1.0124
90	1.002	1.004	1.00452	1.00602	1.0104	1.0119
100	1.002	1.004	1.00440	1.00590	1.0100	1.0115
200	1.002	1.004	1.00355	1.00505	1.0072	1.0087
300	1.002	1.004	1.00308	1.00458	1.0056	1.0071
400	1.002	1.004	1.00279	1.00429	1.0046	1.0061
500	1.002	1.004	1.00261	1.00410	1.0040	1.0055
600	1.002	1.004	1.00248	1.00397	1.0036	1.0051
700	1.002	1.004	1.00239	1.00388	1.0033	1.0048
800	1.002	1.004	1.00231	1.00381	1.0031	1.0045
900	1.002	1.004	1.00227	1.00376	1.0029	1.0044
1000	1.002	1.004	1.00223	1.00372	1.0027	1.0042

EXPERIMENTAL

In investigating the isotopes of tellurium, tellurium samples were examined to see if the isotope ratio could be altered by natural and laboratory processes. Tellurium was extracted from natural telluride samples taken from various geographical locations. A controlled chemical reduction of K_2TeO_3 to elemental tellurium was carried out in the laboratory and attempts made to measure the kinetic isotope effect. K_2TeO_3 was also partially reduced to elemental tellurium by micro-organisms and the isotope composition of the products and reactant compared.

The collected elemental tellurium samples were prepared for mass spectrometric analysis by converting them to tellurium hexafluoride (TeF_6). This method was chosen because of the simplicity of the TeF_6 spectrum (there is only one stable fluorine isotope), the stability of the gas, and because of its ease of preparation. H_2Te could also be used, but the gas is unstable and its mass spectrum is quite complicated by overlapping of the ion species, eg., Te^{130} and $Te^{128}H_2^+$ both at mass 130. Computations on such a spectrum are tedious and subject to considerable error.

A. Extraction of Tellurium from Natural Samples

In 1832 it was discovered by P. Berthier that tellurium could be precipitated from raw materials with sulphur dioxide and hydrochloric acid (76). However, the extraction of pure elemental tellurium was hampered by the presence of selenium which is closely related to tellurium being of the same chemical group. Keller (58) in 1897 showed that selenium and tellurium could be separated with sulphur dioxide in differing acidities of hydrochloric acid, and Gooch and Peirce in 1898 (42) were able to separate tellurium from selenium on the basis of the different volatilities of their tetrabromides, but this was somewhat inefficient.

To further add to the difficulty, certain heavy metals are partially precipitated by sulphur dioxide (58), and combinations of bismuth, antimony, and selenium with tellurium make separations even more complicated because of mutual interferences (88). Hillebrand and co-workers in 1953 (51) gave the different hydrochloric acid concentrations for precipitation of each of selenium and tellurium with sulphurous acid. However, they dried both elements in air at 110^{o}C; whereas, in the same year Duval showed that tel-

lurium oxidizes at temperatures above 40°C (30). Then in 1960, a method was described by Reed (88) by which pure elemental tellurium could be separated from all other elements. This method was employed in this investigation.

About 0.5 grams of sample are powdered and dissolved in 10 ml. of nitric acid and evaporated to dryness. The residue is dissolved in 100 ml. of concentrated hydrochloric acid with 25 ml. sulphurous acid. This step precipitates any selenium present, which is then filtered out.

To the filtrate, 2 grams of tartaric acid are added to prevent any antimony from hydrolyzing. Water is then added until the hydrochloric acid concentration is 3M. To speed up the reaction, 10 ml. of hydrazine hydrochloride solution is added and the tellurium is then precipitated with 25 ml. of sulphurous acid. After boiling for 1 or 2 minutes, the tellurium is separated from the supernatant solution by centrifuging. This is then washed and re-centrifuged several times to remove soluble ions.

The method works as follows: the nitric acid acts as an oxidizing agent producing H_2TeO_3 . The sulphurous

acid then reacts according to the equation

$$H_2TeO_3 + 2H_2SO_3 \xrightarrow{3M\ HCl} Te + 2H_2SO_4 + H_2O$$

(The selenium was precipitated in like manner in the concentrated hydrochloric acid solution.)

According to the literature, only gold and silver would interfere in the selenium-tellurium determination if present, but the gold not being dissolved in nitric acid can be filtered out, and any silver is easily separated as chloride (58).

The efficiency of this method was tested. The precipitated tellurium was filtered through a fritted crucible, washed with 0.2N hydrochloric acid and finally water. It was dried by placing the crucible and tellurium in a desiccator at 20 mm. pressure or less at room temperature over anhydrous calcium sulphate for two hours. Of 1346.5 mg. of sample, 1323.3 mg. or 98.28% was recovered.

B. Chemical reduction of K_2TeO_3

In order to study kinetic isotope effects, the desireable conditions for the experiment are:

1. a gaseous reaction or reaction in solution,

2. a method of halting the reaction at any point, and

3. the ability to recover the reduced product.

A solution or gaseous reaction is preferable since larger isotope effects are found under these conditions. Very little isotope fractionation is expected in a solid phase reaction where the process proceeds layer by layer. The second condition is necessary if the kinetic effect is to be measured. The reaction must be stopped and the isotope ratios determined in the unreduced reactant and the reduced product. Therefore, a chemical reduction of K_2TeO_3 in solution was chosen for study.

Halting the reaction is possible in either of two ways. A method of complete reduction can be employed and the reaction quickly halted by neutralization at the required time; or, only a percentage of the reducing agent required for complete reduction could be used. Halting by neutralization has disadvantages in that much time and many trial runs are required to determine the exact time to be allowed for the desired reduction to take place.

Furthermore, in the case of tellurium, using the hydrochloric acid-sulphur dioxide method for instance, the

reaction takes several days for complete reduction unless hydrazine-hydrochloride is used, in which case the reduction takes place too rapidly to control. Therefore, 5% - 10% reductions were affected by adding only 5% - 10% of the stoichiometrically required reducing agent.

Using the reduction equation

$$\underset{253.81}{K_2TeO_3} + \underset{164.03}{2H_2SO_3} \longrightarrow \underset{174}{K_2SO_4} + \underset{98.02}{H_2SO_4} + \underset{127.6}{Te} + \underset{18.02}{H_2O}$$

0.65 grams of H_2SO_3 are required for the complete reduction of one gram of K_2TeO_3. For a 10% reduction, 10% of 0.65 grams or 65 mg. are required per gram of K_2TeO_3. Six grams of K_2TeO_3 were reduced 10% at room temperature.

The precipitated tellurium was separated from the supernatant solution by centrifuging, was washed, recentrifuged to remove soluble ions, and then dried at 35°C.

C. Reduction of K_2TeO_3 by Scopulariopsis brevicaulis

That micro-organisms are capable of reducing a complex tellurium compound to elemental tellurium has been known for several years. As early as 1914, W. E. King and L. Davis observed that nearly all of the more common micro-organisms reacted with potassium tellurite

to form "black compounds" depending on reduction of the tellurite (59). T. L. Ch'in in 1938 discovered that living colonies of pathogenic fungi could be identified by the "black color" produced upon injection of potassium tellurite (18). A year later, Bird and Challenger (13) discovered that upon ingestion of potassium tellurite, Scopulariopsis brevicaulis (Penicillium brevicaule) reduced the tellurite to black elemental tellurium and evolved di-methyl telluride. Other micro-organisms were later discovered to reduce potassium tellurite to elemental tellurium such as Corynebacterium diphtheria by Morton and Anderson (79) in 1941, Mycobacterium tuberculosis by L. Sula in 1947 (102), and living tissues (bacteria, yeast, human leucocytes) by M. Wachstein in 1949 (125). Others can also be found in later literature.

To examine the isotopic variations by such a reduction, it was decided that Scopulariopsis brevicaulis should be used because it is non-pathogenic. Also, a culture of the organisms was readily obtainable from Dr. Carmichael of The Provincial Laboratory of Public Health, University of Alberta. Furthermore, growth of the culture is quite simple and may be carried out at room temperature.

1. Reduction of K_2TeO_3 by culture on liquid medium

The culture was grown on a liquid medium (Trypticase Soy Broth)* in an aerating flask. 500 ml. of TSB was innoculated with S. brevicaulis. The air was sterilized by passing it through H_2SO_4, sterile cotton wool, then a 1:1000 solution of mercuric chloride, and again through sterile cotton wool (17). After passing through the culture flask, it was aspired through an alcoholic iodine solution to form di-methyl telluride di-iodide, $(CH_3)_2TeI_2$ (16) from any di-methyl telluride $(CH_3)_2Te$ evolved from the culture.

The culture was allowed to grow until a good growth covered the medium surface (12 days). It was then innoculated with 1.5 grams of potassium tellurite in solution, and samples were taken every 12 hours until enough of the tellurite had been reduced to yield sufficient tellurium for analysis, which took 72 hours. At this point, 10 cc. samples were taken every 6 hours and the tellurium extracted from the broth as outlined later. Finally, after 100 hours, the yield of reduced tellurium was too small for analysis and the experiment was halted. The tellurium was then extracted from the yet unreduced tellurite, the broth, and from the di-methyl telluride di-iodide compound.

*This broth was prepared by mixing 30 grams Trypticase Soy Broth powder from Baltimore Biological Company with 1 litre of water. Hitherto this will be referred to as TSB.

2. Extraction of elemental tellurium reduced from K_2TeO_3 in the biological investigation

In order to obtain only the tellurium reduced by the bacteria for analysis, it had to be separated from the rest of the broth which still contained unreduced potassium tellurite in solution and which would also be reduced by the extraction procedure. Thus, the 10 cc. sample was washed with water and filtered to separate the tellurium reduced by the bacteria from the unreduced tellurite solution. (Elemental tellurium is insoluble in water.) The filter paper was then dissolved in nitric acid and the method of extraction carried out as outlined on page 72. The filtrate was treated with concentrated hydrochloric acid and sulphur dioxide and let stand for three hours. After this, the hydrochloric acid concentration was brought to 3M, 10 ml. of hydrazine hydrochloride was added, and sulphur dioxide was bubbled through which precipitated any tellurium present. Thus, at any sampling time the bacteriologically-reduced tellurium and tellurium representative of the unreduced tellurite were available for analysis.

The tellurium was separated from the di-methyl telluride di-iodide by a method outlined by Vernon (122). Tellurium and methyl iodide react according to the equation

$$Te + 2CH_3I \underset{100^{\circ}C}{\overset{80^{\circ}C}{\rightleftharpoons}} (CH_3)_2TeI_2$$

Thus, the di-methyl telluride di-iodide was distilled in a sulphuric acid bath at 100°C evolving methyl iodide leaving a residue of elemental tellurium which was recovered.

D. Preparation of TeF_6

As stated, TeF_6 gas was chosen as the form into which the tellurium samples were converted for mass spectrometric analysis. Fluorination of elemental tellurium can result in the production of both TeF_4 and TeF_6. According to J. H. Junkins et al (56), TeF_6 is formed at a temperature of 200°C in the presence of excess F_2; whereas, TeF_4 is formed at a temperature of 180°C with excess Te. In the method used, fluorine was present in a large excess and this resulted in a quantitative conversion of tellurium to TeF_6 at 200°C.

The fluorine line built for this purpose is shown in figure 5. The fluorine source was a commercial cylinder of fluorine obtained from Matheson Company of New Jersey. Many precautions are required since fluorine is most reactive and will react with everything except inert gases and already-fluorinated compounds. The reaction of fluorine with some metals such as copper and monel is retarded after an initial fluoride coating is formed so these metals can be safely used for construction of a fluorine line. Therefore, the tellurium was fluorinated and the TeF_6 trapped in a monel line.

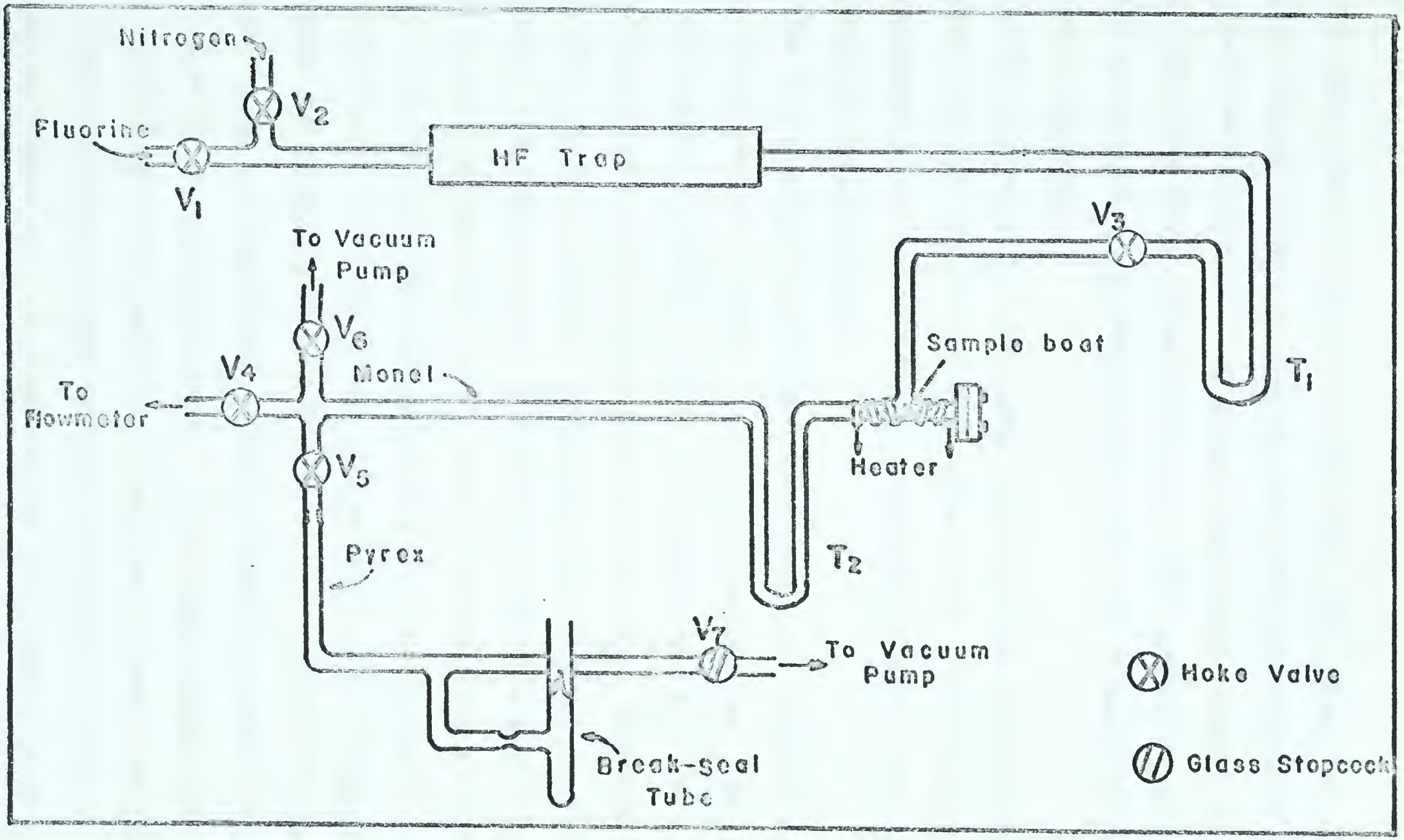

FIG. 5 FLUORINE LINE

Dry TeF_6 is fairly non-reactive so that after being purified several times to remove any unreacted fluorine, the TeF_6 could be collected into glass break-seal tubes. All glass stopcocks were greased with Kel-f#90 grease since violent reactions could occur with ordinary greases upon contact with fluorine.

Safety precautions included locating both the fluorine cylinder and the entire fluorine line under a fume hood, and the wearing of a rubber coat, polyethylene gloves, and face mask during fluorinations.

The fluorination procedure is as follows. The tellurium sample is placed in a monel boat and placed in the furnace which is heated to 200°C. With V_4 closed, V_5, V_6, and V_7 open, the line is evacuated back as far as V_3. After pumping on the sample to dry it thoroughly and testing the line for vacuum tightness, T_1 is cooled with liquid oxygen, valves V_5 and V_6 are closed and V_2, V_3, and V_4 are opened to admit a small flow of nitrogen through the line controlled by use of a flowmeter. Trap T_2 is now cooled with liquid oxygen.

With the needle valve of the fluorine cylinder closed, the main valve is opened and closed, trapping a small volume of fluorine between these valves. V_1 is then opened and the needle valve opened allowing the fluorine to pass through the line. The fluorine-nitrogen mixture is passed through a NaF trap to remove HF. T_1 freezes out any remaining HF and

water vapour present, and the TeF_6 formed is trapped in T_2. The flow of nitrogen is maintained for a further 30 minutes to ensure scavanging of elemental fluorine from the system.

After scavenging, V_3 and V_4 are closed and the liquid oxygen dewar removed from T_2. This vapourizes the frozen TeF_6 and releases any F_2 which might have been trapped by the TeF_6 molecules. The TeF_6 is again frozen down in T_2 and V_6 is opened to evacuate the line. This is repeated several times to ensure that no F_2 is present before admitting the TeF_6 to the glass line.

With V_6 and V_7 closed, V_5 is opened and the liquid oxygen dewar moved from T_2 to the break-seal tube. After the sample is frozen down, V_5 is closed and the liquid oxygen is replaced by a liquid-solid alcohol bath. V_7 is then opened allowing a final evacuation of the break-seal tube to remove any traces of silicon fluorides formed. V_7 is then closed and the break-seal tube removed.

E. Mass Spectrometric Analysis

In order to determine the Te^{130}/Te^{122} ratio, the TeF_6 gas was analyzed in a mass spectrometer using a 12-inch radius 90° magnetic analyzer to separate ion currents of different masses. The TeF_6 molecules were ionized by an electron beam travelling normally to the inlet flow direction. The ions formed were then linearly accelerated by a 3500-volt

potential difference and subsequently separated in the magnetic field. The ion currents are introduced in turn into the collector slit by magnetic scanning. Each ion current is amplified and displayed as a peak on a continuous recording chart (see Fig. 6). Since fluorine has only one stable isotope, F^{19}, the spectra yield directly the abundances of the tellurium isotopes.

In single collection with the tracing of peaks, a realizable precision is 0.1 percent. This limitation results because the peaks are traced at different times and so fluctuations in the mass spectrometer source limit the precision. The precision can be improved by the simultaneous collection of two ion beams containing the isotopes of interest and making a direct ratio measurement of the two ion currents. Fluctuations in the ion production effect both ion currents in the same way and so the ratio remains unaltered. By introducing a standard and an unknown sample alternately into the mass spectrometer by a magnetic valve system (McKinney et al, Wanless and Thode (75)) a precision of 0.01 percent can be obtained in comparing isotope ratios of different samples.

In the ionization process, TeF_6 was split into many singly and doubly charged ion species as listed in Table VII. The TeF_5^+ ion species are the most abundant and so ion currents of masses 217 ($Te^{122}F_5^+$) and 225 ($Te^{130}F_5^+$) were simul-

FIGURE 6 Te F_5^+ SPECTRUM WITH NARROW SLIT

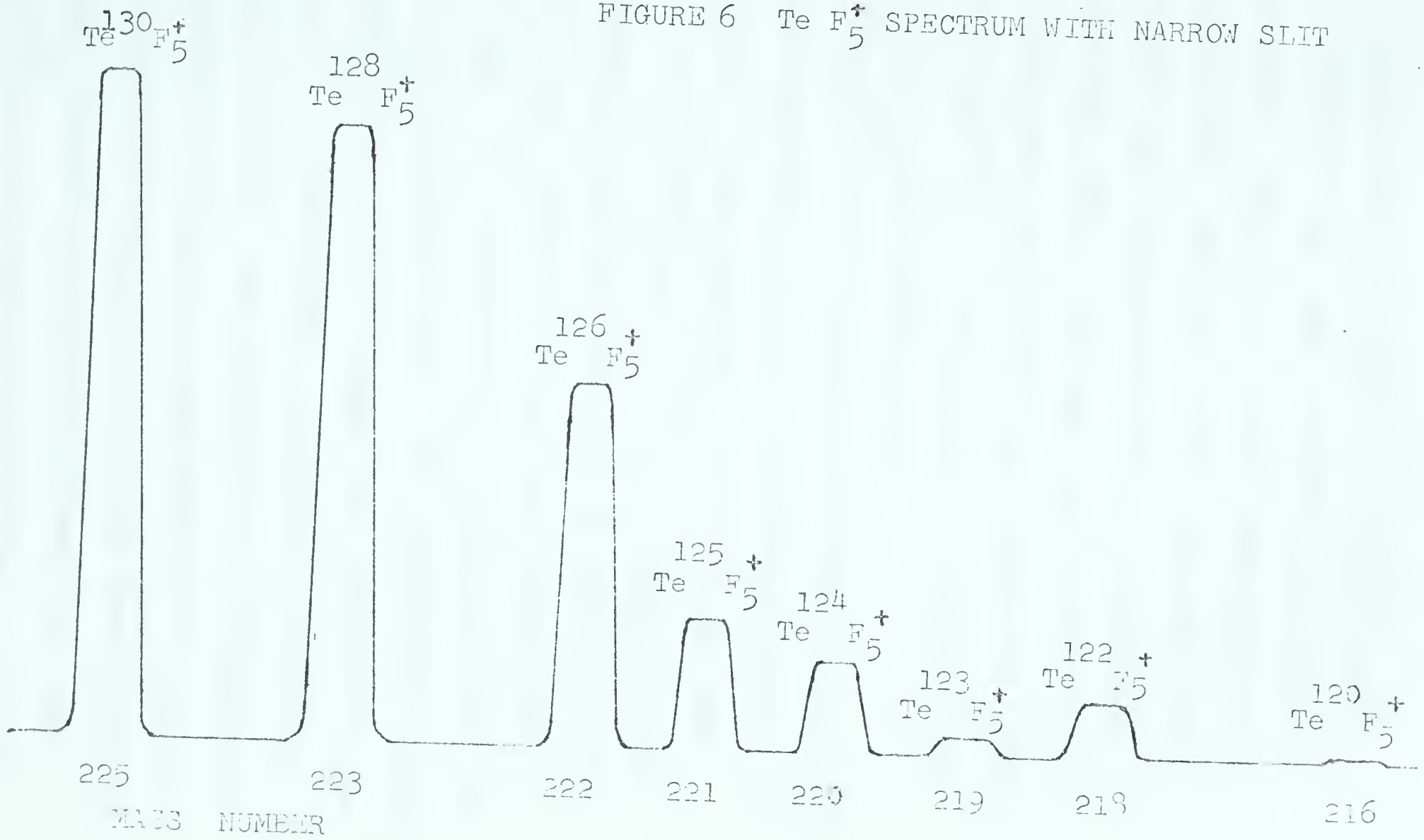

taneously collected with two slits in the collector. A narrow slit (0.024") was used to collect the mass 217 ion current while a wide slit (0.040") was used for the mass 225 ion current. With the former, the resolution of the instrument was 1/350 while with the wider slit, the resolution was 1/200. The lower resolution is permissable in the latter case since the closest ion current is of mass 223 ($Te^{128}F_5^+$). The spectrum in Figure 6 was traced using the narrow collector slit.

The Te^{130}/Te^{122} ratio is obtained directly by means of a five-figure integrating digital voltmeter-ratiometer and a digital printer in the measuring circuit of the mass spectrometer. The $Te^{122}F_5^+$ and $Te^{130}F_5^+$ ion beams are collected simultaneously and are amplified by vibrating reed electrometers. The currents are converted to voltages by means of 10^{11} and 10^{10} ohm grid leak resistors for the 122 and 130 mass currents respectively. The integrating digital voltmeter integrates an input voltage over a selected time and converts it to a proportional frequency. In passing through a counter section, this frequency is referred to a time base frequency so that the number printed is really a ratio of the converted frequency to the time base frequency. If an additional voltage-to-frequency converter is used, a second voltage can be converted into a frequency and used

in place of the time base frequency in the IDVM. The IDVM then is a ratiometer and displays the ratio of the two voltages.

The Te^{130}/Te^{122} ratios of a standard sample and an unknown sample can be calculated directly from the printed output providing the major ion currents of the two samples are matched. Because of memory effects, it was necessary to allow at least five minutes after switching of the magnetic valves before recording the ratio in order to get reproduceable results. Approximately six sets each of ten printed ratios for each sample were obtained.

TABLE VII

Ion	% Abundance
TeF_5^+	58.3
TeF_4^+	2.8
TeF_3^+	5.5
TeF_2^+	2.8
TeF^+	0.4
Te^+	6.5
TeF_4^{++}	4.2
TeF_3^{++}	7.9
TeF_2^{++}	4.6
TeF^{++}	3.6
Te^{++}	3.3

RESULTS AND DISCUSSION

The results of the theoretical calculations as summarized in Tables IV and VI indicate that the Te^{130}/Te^{122} ratio may be altered by over 3% in hypothetical reactions.

The experimental observations are consistent with some of the theoretical predictions. The measured Te^{130}/Te^{122} ratios for the samples analyzed were referred to the isotopic composition of a standard sample of telluride from Copper Cliff, Ontario. The isotopic deviation from the standard is expressed in δ_{130} units where

$$\delta_{130} = \left[\frac{(Te^{130}/Te^{122})_{sample}}{(Te^{130}/Te^{122})_{standard}} - 1 \right] \times 1000$$

Generally speaking, a standard deviation of 0.02 percent could be realized in the measurements. The results are summarized in TableVIII and depicted graphically in Fig. 7.

A. Chemical reduction of potassium tellurite

Analysis showed that the tellurium precipitated in a 10 percent reduction of tellurite was 0.71 percent depleted in the heavier isotope in comparison with the initial tellurite. Using equation (19) developed in the theory, this value can be extrapolated with the assumption of first order kinetics to give the ratio of the rate constants k_{122}/k_{130} for the competitive reactions

Table VIII Te^{130}/Te^{122} FRACTIONATION STUDY

Sample No.	Description	δ^{130}
1.	Commercial potassium tellurite B. D. H. Lot #54135	0.0 ± 0.2
2.	Elemental tellurium product of 10 percent chemical reduction of tellurite of sample 1	-7.1 ± 0.3
3.	Elemental tellurium, 41 to 53 percent reduction fraction of microbiological reduction of tellurite of sample 1	-2.1 ± 0.2
4.	Cripple Creek, Colorado (Sylvanite)	0.0 ± 0.2
5.	Copper Cliff, Ontario	0.0 ± 0.3
6.	Okanagan, B. C., PreCambrian Mines, See reference 137. (Tetradymite)	-4.0 ± 0.5

FIGURE 7 Te^{122}/Te^{130} FRACTIONATION STUDY

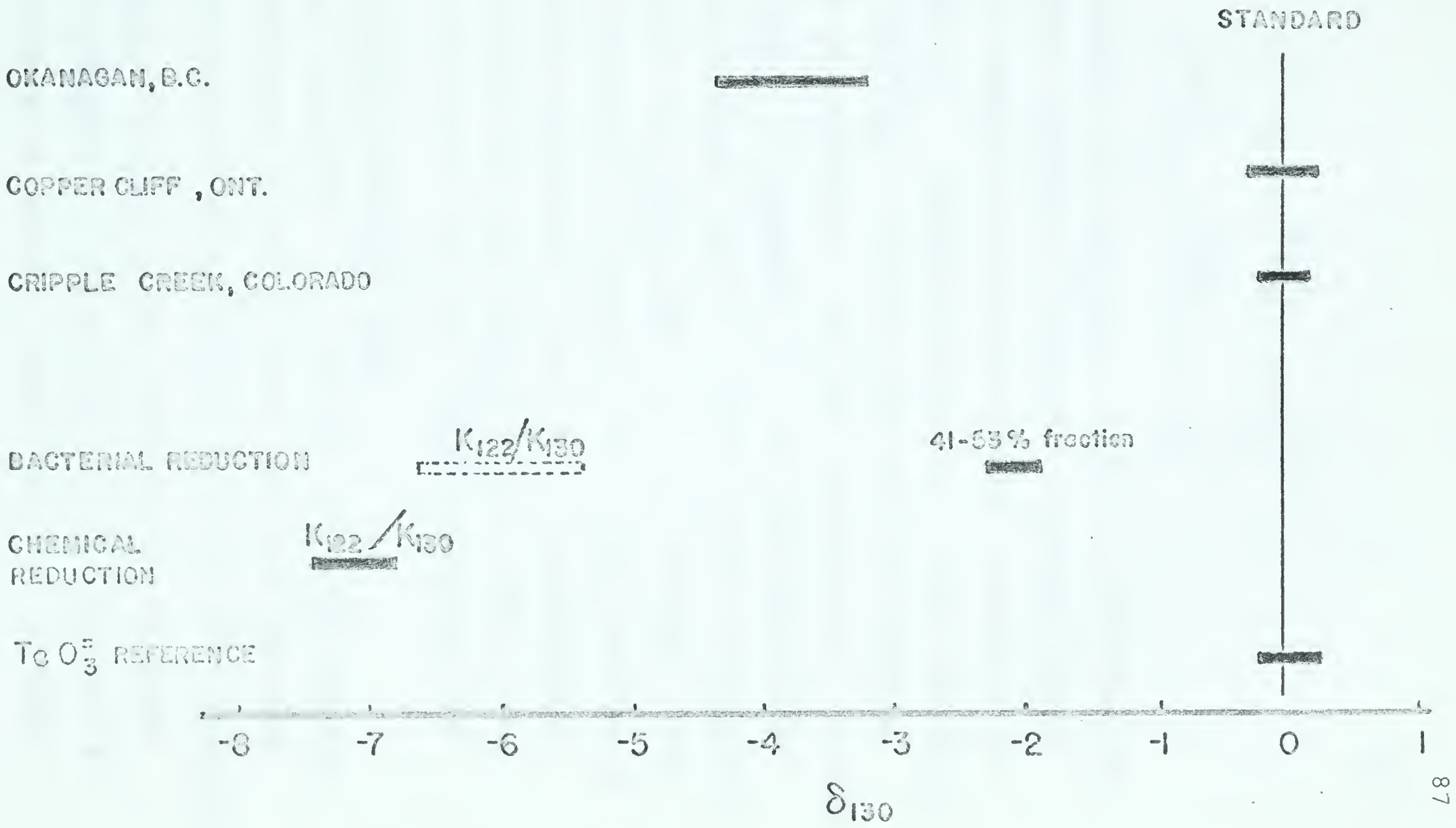

$$Te^{122}O_3^{=} \xrightarrow{k_{122}} Te_o^{122}$$

$$Te^{130}O_3^{=} \xrightarrow{k_{130}} Te_o^{130}$$

This extrapolation gives $k_{122}/k_{130} = 1.0071 \pm 0.0003$ meaning that the lighter isotopic ion ruptures 0.7 percent faster. This is to be compared with the theoretically predicted results of Table VI. Looking at Table VI, "most reasonable" values of 1.00568 and 1.00718 for mass and atom fragments respectively are predicted. $TeO_3^{=}$ has a pyramidal XY_3 structure as shown in Figure 12, Appendix II. The bond being broken is equally as strong as the other bonds so that by Wolfsberg's reasoning (136), the reduced mass term will be closer to the reduced mass of the Te - O diatomic bond. Thus the value of 1.0071 ± 0.0003 compares very closely to the predicted result of 1.00718 for the atom-fragment model. This is also consistent with results found for selenite reduction (89).

B. Microbiological reduction study

For measurement, the elemental tellurium fraction precipitated between 41 and 53 percent reduction was used. This value can also be extrapolated to give the ratio k_{122}/k_{130}. The extrapolation is however more difficult and is shown graphically in Figure 8. The quantity "r" in equation (19) is for the integrated isotopic composition of the product.

FIGURE 8 VARIATION OF ISOTOPIC COMPOSITION OF PRODUCT WITH PERCENT REACTION

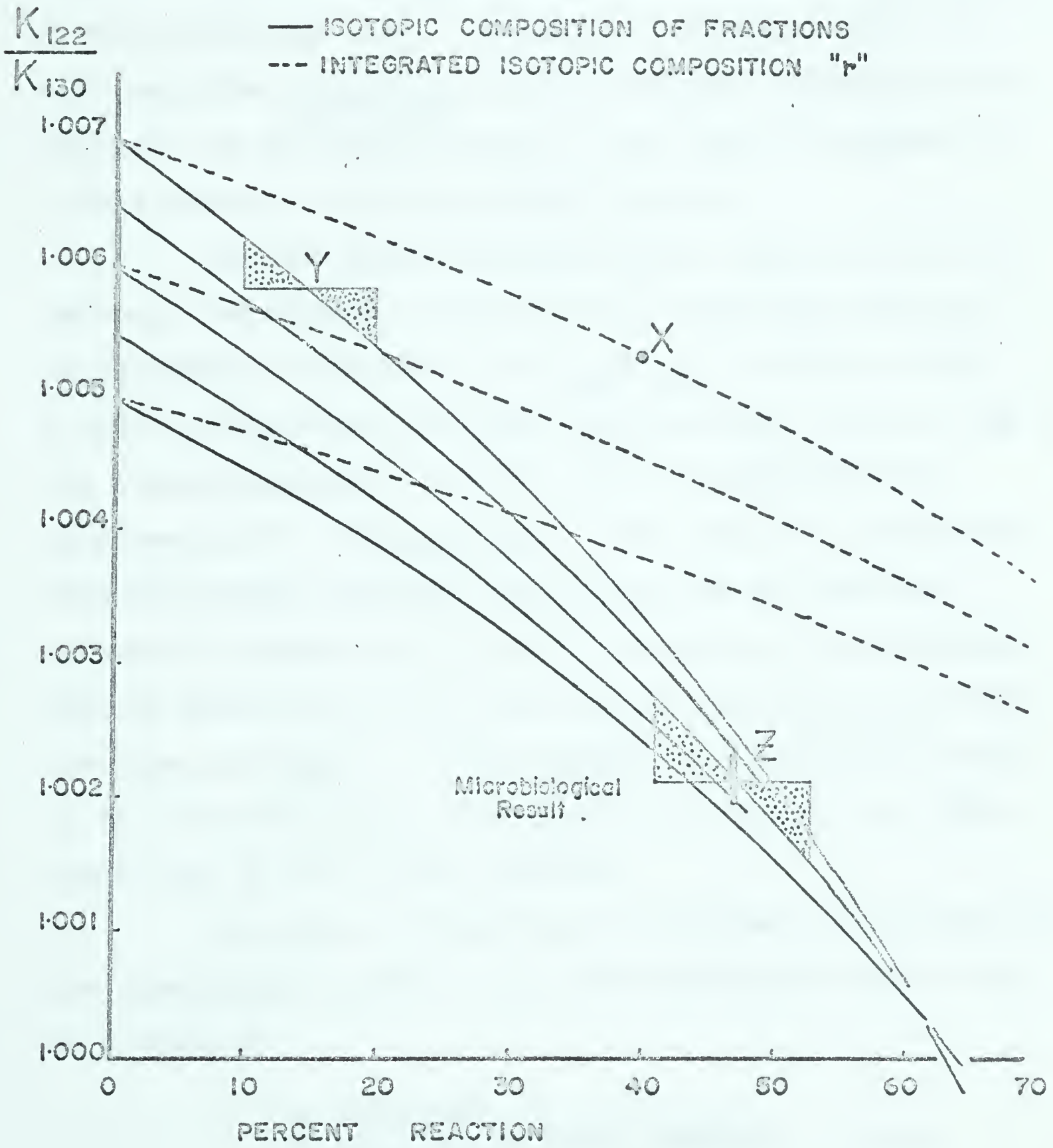

Three plots of "r" as a function of percentage reaction are shown in Figure 8 as dashed lines for values of k_{122}/k_{130} = 1.005, 1.006, and 1.007. The point X indicates that if a reaction whose k_{122}/k_{130} = 1.007 has gone 40 percent to completion, the Te^{122}/Te^{130} ratio of that total 40 percent is 1.0053 times that of the initial reactant.

For the microbiological study, however, a plot of isotopic composition of fractions vs. percentage reaction is necessary. Five plots for k_{122}/k_{130} = 1.0050, 1.0055, 1.0060, 1.0065, and 1.0070 are shown by solid lines in Fig. 8. The information given by such a plot is represented by construction Y. If k_{122}/k_{130} = 1.007, and it is desired to know the average isotopic composition for the fraction between 10 percent and 20 percent reduction, the horizontal line is drawn at Y so that the shaded areas above and below the line are equal. In this example, the Te^{122}/Te^{130} ratio of the 10 to 20 percent fraction of the product is 1.0058 times that of the initial reactant.

The above construction is performed in reverse for the experimental result. At Z, the horizontal line is the mean value of

$$\frac{(Te^{122}/Te^{130})_{\text{reduced fraction}}}{(Te^{122}/Te^{130})_{\text{initial reactant}}} = 1.0021$$

for the fraction between 41 and 53 percent reaction. It is seen that the line for $k_{122}/k_{130} = 1.0060$ very closely equalizes the shaded areas. The measurement error of ± 0.02 percent is represented by the vertical line at Z and its extremities touch the curves corresponding to $k_{122}/k_{130} = 1.0055$ and 1.0065. Therefore, for the bacterial reduction, $k_{122}/k_{130} = 1.0060 \pm 0.0005$. This compares very favourably with the result of the chemical reduction study and suggests that in the bacterial reduction, the effect noted arises essentially in tellurium-oxygen bond breakage.

k_{122}/k_{130} can be determined more accurately by measurements made of fractions produced near the beginning of the reaction. Such samples are available, but measurements are being withheld until the mass spectrometer is adapted to handle smaller samples.

C. Natural isotopic abundance studies

Two of the natural samples and the commercial tellurite have the same Te^{122}/Te^{130} ratio within the measurement errors. Similarly in the survey of natural selenium isotopes (60) a large number of samples had a similar Se^{76}/Se^{82} ratio. In both cases, the constancy of isotopic composition can be related to high temperature processes where the isotope fractionation is very small. (The isotope fractionation generally decreases with temperature as exemplified in the calculations

of Tables IV and VI.) In the selenium study (60), large alterations to the Se^{76}/Se^{82} ratio occurred only in soil and plant samples where the temperature of the processes would be very low. In the tellurium study, however, the sample of tetradymite from the west shore of the Okanagan Lake was 0.4 percent depleted in Te^{130}. This result is surprising. A measurement of yield rules out any possibility that the sample was isotopically altered in the chemical extraction. This sample behaved the same as the others in hexafluoride preparation and in mass spectrometric analysis. It would seem that the result is real but it should be interpreted as one measurement of one sample. No attempt can be made to explain this result until more natural samples are examined.

In conclusion, therefore, this preliminary survey shows that the Te^{122}/Te^{130} ratio can be altered chemically and microbiologically in agreement with theoretical predictions. Further, it would seem that a more extensive study of natural samples might be beneficial in elucidating natural processes.

BIBLIOGRAPHY

1. Aldrich, L. T., and Nier, A. O., Phys. Rev., 74, 876, 159, (1948)

2. Aston, F. W., Phil. Mag. 38, 707, (1919); 39, 449, (1920)

3. Aston, F. W., Phil. Mag. 49, 1191, (1925)

4. Aston, F. W., Proc. Roy. Soc. (London), A132, 487, (1931)

5. Bach F, Bonhoeffer, K. F., and Fajans, E., Zeits. für Physik chemie, A168, 313, (1934)

6. Baertschi, P., Nature 168, 288, (1951)

7. Bainbridge, K. T., Phys. Rev. 39, 1021, (1932)

8. Bartlett, James H. Jr., Phys. Rev. 45, 847, (1934)

9. Bigeleisen, J., J. Chem. Phys. 17, 675 (1940)

10. Bigeleisen, J., and Mayer, M.G., J. Chem. Phys., 15, 261, (1947)

11. Bigeleisen, J., J. Chem. Phys., 17, 675, (1949)

12. Bigeleisen, H., and Friedman, L., J. Chem. Phys., 17, 998, (1949)

13. Bird, Marjorie L., and Challenger, Frederick, J. Chem. Soc. p163, (1939)

14. Bose, H., and Ray, B. B., Indian J. Phys., 15, 233, (1941)

15. Butlin, K. R., Research 6, 184, (1953)

16. Carr, F., and Pearson, T. G., J. Chem. Soc., p 282, (1938)

17. Challenger, F., Higginbottom, C., and Ellis, L., J. Chem. Soc., page 95 (1933)

18. Ch'in, T. L., Proc. Soc. Expt'l. Med., 38, 700, (1938)

19. Clarke, F. W., and Washington, H. S., Proc. Nat. Acad., 8, 108, (1952)

20. Clayton, R. N., J. Chem. Phys., 30, 1246, (1955)

21. Cohen, E., and Krüner, J. F., Zeit. Phys. Chem., 82, 587, (1913)

22. Craig, H., Geochim, et Cosmochim. Acta., 3, 53, (1953)

23. Craig, H., and Boato, G., Am. Rev. Phys. Chem., 6, 403, (1955)

24. Davy, H., Phil. Trans., 100, 161, (1810)

25. Dempster, A. J., Phys. Rev., 11, 316, (1918)

26. Dempster, A. J., Phys. Rev., 50, 186, (1936)

27. Dodwell, L. G., Proc. Ind. Acad. Sci., 55, (1945)

28. Duckworth, H. E., Kegley, C. L., Olson, J. M., and Stanford, G. S., Phys. Rev. 83, 1114, (1951)

29. DuFresne, Ann., Geochim et Cosmochim Acta, 20, 141, (1960)

30. Duval, Clement, "Inorganic Thermo-gravimetric Analysis", pp. 302, 384, Elsevier, New York, (1953)

31. Eidinoff, M. L., Trans. N. Y. Acad. Sci., 16, 76, (1953)

32. Epstein, S., Buchsbaum, R., Lowenstem, H., and Urey, H. C., Bull. Geol. Soc. Amer., 62, 417, (1953)

33. Epstein, S., "Mass Spectroscopy in Physical Research", National Bur. Std. U. S. Circ. 522, page 133, (1953)

34. Epstein, S., "Oxygen Isotope Measurements in Glacial Ice", Nat. Acad. Sci. - Nat. Res. Council Bull. 845, p. 1521, (1960)

35. Evans, M. G., and Polanyi, M., Trans. Far. Soc., 31, 875, (1935)

36. Eyring, H., J. Chem. Phys., 3, 107, (1935)

37. Farkas, L., and Farkas, A., Naturwiss, 22, 218, (1934)

38. Freely, H. W., and Kulp, J. L., Bull. Amer. Assoc. Petrol. Geol., 41, 1802, (1957)

39. Friedman, I., Geochim. et Cosmochim Acta, 4, 89, (1953)

40. Gaunt, J., Trans. Far. Soc., 50, 546, (1954)

40a. Glasstone, S., Laidler, K. J., and Eyring, H., "The Theory of Rate Processes", McGraw Hill, N. Y., (1941)

41. Glockler, G., and Tung, J. Y., J. Chem. Phys., 13, 338, (1945)

42. Gooch, F. A., and Peirce, A. W., Am. Jour. Sci., 1, 181, (1896)

43. Halsted, Richard E., Phys. Rev. 88, 666, (1952)

44. Harrison, A., and Thode, H. G., Trans. Far. Soc., 54, 84, (1958)

45. Heath, D. F., and Linnett, J. W., Trans. Far. Soc., 44, 878, (1948)

46. Heath, D. F., and Linnett, J. W., Trans. Far. Soc., 45, 264, (1949)

47. Heslop, R. B., and Robinson, P. L., "Inorganic Chemistry", Elsevier Publishing Company, New York, p 352, (1963)

48. Herzberg, G., "Spectra of Diatomic Molecules", D. Van Nostrand, Princeton, New Jersey, (1950)

49. Herzberg, G., "Infrared and Raman Spectra", D. Van Nostrand Co. Inc., Princeton, New Jersey, (1956)

50. Hill, R. A., Edwards, T. H., Rossman, K., Harahari Rao, K., Nielsen, H. H., J. Mol. Spectry., 14(3), 221, (1964)

51. Hillebrand, W. F., Lundell, G. E. R., Bright, H. A., Hoffman, J. I., "Applied Inorganic Analysis", pp. 228, 334, Wiley, New York, (1953)

52. Hirschfelder, J. O., and Wigner, J., J. Chem. Phys., 1, 616, (1939)

53. Hoering, T. C., Science, 122, 1233, (1955)

54. Hollander, J. M., Perlman, I., and Seaborg, G. T., Revs. Modern Phys., 25, 469, (1953)

55. Johnson, C. W., and Krouse, R. H., Unpublished work, University of Alberta, Edmonton, Alberta, (1964)

56. Junkins, J. H. Bernhardt, H. A., and Barber, E. J., J. Am. Chem. Soc., 74, 5749, (1952)

57. Kaplan, I. R., and Rittenberg, S. C., J. gen. Microbiol, 34, 195, (1964)

58. Keller, Edward, J. Am. Chem. Soc., 19, 771, (1897)

59. King, W. E., and Davis, L., Am. Jour. of Pub. Health, 4, 917, (1914)

60. Krouse, R. H., and Thode, H. G., Can. Jour. Chem., 40, 367, (1958)

61. Kruse, P. W., McGlauchin, L. D., and McQuisten, R. B., "Elements of Infrared Technology", John Wiley and Sons, Inc., New York, (1962)

62. Landergren, V. S., Z. Naturf., 8b, 537, (1953)

63. Lindsay, J. G., Bourns, A. N., and Thode, H. G., Can. J. Chem., 29, 192, (1951)

64. Lindsay, J. G., Bourns, A. N., and Thode, H. G., Can. J. Chem., 30, 163, (1952)

65. Lindsay, J. G., McElheran, D. E., and Thode, H. G., Journ. Chem. Phys., 17, 589, (1949)

66. Linnett, J. W., and Simpson, C. J. S. M., Trans. Far. Soc., 55, 857, (1959)

67. Lippincott, E. R., and Dayhoff, M. O., Spectrochim Acta, 16, 807, (1960)

68. Macnamara, J., and Thode, H. G., Phys. Rev., 78, 307, (1950)

69. Macnamara, J., and Thode, H. G., Research 4, 582, (1951)

70. Macnamara, J., Fleming, W., Szabo, A., and Thode, H. G., Can. J. Chem., 30, 73, (1952)

71. Mars, K. E., Jour. Geol., 59, 131, (1951)

72. Mayer, J. E., and Mayer, M. G., "Statistical Mechanics", p. 207 ff., J. Wiley and Sons, Inc., N. Y., (1940)

73. McCrea, J. M., J. Chem. Phys., 18, 849, (1950)

74. McElheran, P. E., M. Sc. Thesis, McMaster University, Hamilton, Ontario, (1951)

75. McKinney, C. R., McCrea, J. M., Epstein, S., Allen, H. H., and Urey, H. C., Rev. Sci. Inst., 21, 724, (1950)

76. Mellor, J. W., "A Comprehensive Treatise on Inorganic and Theoretical Chemistry", p. 5, Longman's Green and Co., Toronto, (1931)

77. Migeotte, R., Bull. Soc. Roy. Sci..Liege, 11, 44, (1942)

78. Miller, L. P., Contrib. Boyce Thompson Inst., 15, 437, (1949)

79. Morton, Harry E., and Anderson, Thomas F., Proc. Soc. Expt'l Biol. Med., 46, 272, (1941)

80. Munther, V., and Dansgard, W., Medd. Dansk. Geol. Foren, 12, 159, (1951)

81. Nakai, N., and Jensen, M. L., Geochim et Cosmochim Acta, 28, 1893, (1964)

82. Nakomoto, K., "Infrared Spectra of Inorganic and Co-ordination Compounds", John Wiley and Sons, Inc., New York, (1963)

83. Nier, A. O., and Gulbransen, E. J., J. Am. Chem. Soc., 61, 697, (1939)

84. Nier, A. O., and Murphy, B. F., Phys. Rev., 59, 771, (1941)

85. Pistorius, C. W. F. T., J. Chem. Phys., 27, 965, (1957)

86. Rankama, K., Bull. Geol. Soc. Amer., 59, 389, (1948)

87. Redlich, O., Z. Physik. Chem., B28, 371, (1935)

88. Reed, James. F., Analytical Chem., 32, 662, (1960)

89. Rees, C. E. Unpublished Ph. D. Thesis, McMaster University, Hamilton, Ontario, (1964)

90. Richards, T. W., and Lembert, M. C., J. Am. Chem. Soc., 36, 1329, (1914)

91. Rittenberg, D., Bleakney, W., and Urey, H. C., J. Chem. Phys., 2, 98, (1934)

92. Ropp, G. A., Nucleonics, 10, #10, 22, (1952)

93. Rossmann, Kurt, and Straley, Joseph W., J. Chem. Phys., 24, 1276, (1956)

94. Semat, Henry, "Introduction to Atomic and Nuclear Physics", Rinehart and Co. Inc., New York, (1960)

95. Siebert, H.,Z. anorg. u. allgem. chem., 275, 225, (1955)

96. Sienko, M. J., and Plane, R. A., "Chemistry", McGraw-Hill Book Co. Inc., New York, (1957)

97. Silverman, S. R., and Epstein, S., Bull. Amer. Ass. Petrol. Geol., 42, 998, (1958)

98. Sindeeva, N. D., "Mineralogy and Types of Deposits of Selenium and Tellurium", Interscience Publishers, New York, p. 255, (1964)

99. Smith, S., and Linnett, J. W., Trans. Far. Soc., 52, 891, (1956)

100. Soddy, F., Chem. Soc. Ann., Rep. 1, 285, (1910)

101. Stevenson, D. P., Jour. Chem. Phys., 8, 285, (1940)

102. Sula, L., Am. Rev. Tuberc., 56, 241, (1947)

103. Thanalakshmi, Miss R., Current Science, 31, 374, (1962)

104. Thode, H. G. Macnamara, J., and Collins, C. B., Can. J. Research, 27B, 361, (1947)

105. Thode, H. G., Kleerekoper, H., and McElheran, D. E., Research, 4, 581, (1951)

106. Thode, H. G., Ann. Rev. Phys., Chem., 4, 95, (1953)

107. Thode, H. G., Wanless, R. K., and Wallauch, R., Geochim et Cosmochim Acta, 5, 286, (1954)

108. Thode, H. G., Bulletin of Canadian Petroleum Geology, 12, 246, (1963)

109. Thomson, J. J., "Rays of Positive Electricity and their Applications to Chemical Analysis", Longman's Green and Company, London, (1913)

110. Trofimov, A., Doklady Akad. Nauk., SSR85, 169, (1952)

111. Trudge, A. P., and Thode, H. G., "Thermodynamic Properties of Isotopic Compounds of Sulphur", Can. Jour. Res., 28B, 567, (1950)

112. Urey, H. C., Brickwedde, F. G., and Murphy, G. M., Phys. Rev., 39, 164, 864, (1932)

113. Urey, H. C., and Washburn, E. W., Proc. Nat. Acad. Sci., 18, 496, (1932)

114. Urey, H. C., and Rittenberg, D. J., Jour. Chem. Phys., 1, 137, (1933)

115. Urey, H. C., and Rittenberg, D. J., J. Am. Chem. Soc., 56, 1885, (1934)

116. Urey, H. C., and Greiff, L., J. Am. Chem. Soc., 57, 321, (1935)

117. Urey, H. C., and Teal, G. K., Rev. Mod. Phys., 1, 34, (1935)

118. Urey, H. C., J. Chem. Soc., p562, (1947)

119. Urey, H. C., Science, 108, 489, (1948)

120. Urey, H. C., Epstein, S., McKinney, C., and McCrea, J. M., Bull. Geol. Soc. Amer., 59, 1359, (1948)

121. Venkateswarlu, K., Somasundaram, V., and Krishna, M. G., Z. Physik, Chem., 212, 145, (1960)

122. Vernon, Richard Henry, J. Chem. Soc., p. 86, (1920)

123. Vinogradov, A. P., "The Geochemistry of Rare and Dispersed Chemical Elements in the Soil", trans. from Russian-Consultants' Bureau, N.Y., (1959)

124. Voge, H. H., and Libby, W. F., J. Am. Chem. Soc., 59, 2474, (1937)

125. Wachstein, M., Proc. Soc. Exptl. Biol. Med., 72, 175, (1949)

126. Wanless, R. K., and Thode, H. G., J. Sci. Inst., 30, 395, (1953)

127. Weber, L. A., Wahl, M. H., and Urey, H. C., J. Chem. Phys., 3, 129, (1935)

128. Wells, A. F., and Bailey, M., J. Chem. Soc., p.1282, (1949)

129. Wentink, Tunis Jr., J. Chem. Phys., 30, 105, (1959)

130. West, S. S., Geophysics, 10, 406, (1945)

131. White, J. R., and Cameron, A. F., Phys. Rev., 74, 991, (1948)

132. Williams, D., and Yuster, P., Phys. Rev., 69, 556, (1946)

133. Wickman, F. E., and von Ubish, H., Geochim et Cosmochim Acta, 1, 119, (1951)

134. Wickman, F. E., Geochim et Cosmochim Acta, 2, 243, (1952)

135. Wickman, F. E., Nature, 169, 1051, (1951)

136. Wolfsberg, M., J. Chem. Phys., 33, 21, (1960)

137. Summary report, Geological Survey of Canada, Part b, "White Elephant Mines - PreCambrian Mines", (1931)

APPENDIX I

CALCULATIONS OF ISOTOPIC VIBRATIONAL FREQUENCY SHIFTS FOR TELLURIUM - CONTAINING MOLECULES

Values for the normal vibrational frequencies of many tellurium-containing molecules are available from infra-red spectra and can be found in various publications. However, since no consideration is given for differing isotopic masses therein, it is assumed that these experimental values apply to the most abundant tellurium isotope, Te^{130}. The frequencies of the Te^{122} containing molecules were then calculated from these known frequencies using normal force equations which describe molecules of different symmetries.

A. Diatomic Molecules

In considering diatomic molecules, the anharmonic oscillator is chosen as a model. The potential energy function is then given in the form

$$U = f(r - r_e)^2 - g(r - r_e)^3 + \ldots \qquad (I.1)$$

where r_e is the equilibrium internuclear distance and $(r - r_e)$ is the displacement from this equilibrium position.

Schroedinger's equation for such a model then becomes

$$\nabla^2\psi + \frac{8\pi^2\mu}{h^2}(E - U)\psi = 0 \qquad \text{(I.2)}$$

If the anharmonicity if small, ($g \ll f$), the energy values of this equation will be the eigenvalues given by

$$E_{vib} = hc\left[\omega_e(v+\tfrac{1}{2}) - \omega_e x_e(v+\tfrac{1}{2})^2 + \omega_e y_e(v+\tfrac{1}{2})^3 \ldots\right] \qquad \text{(I.3)}$$

where v is the vibrational quantum number, ω_e is the classical vibrational frequency in cm^{-1}, and μ is the reduced mass of the two atoms, $(\frac{m_1 m_2}{m_1+m_2})$.

Classically, for a harmonic oscillator

$$\nu_{osc} = \frac{1}{2\pi}\sqrt{\frac{K}{\mu}} \quad sec^{-1}$$

where ν_{osc} is the vibrational frequency and the restoring force is $-K(r - r_e)$ during a displacement of $(r - r_e)$.

The potential energy curves for isotopic molecules are identical to a high degree since they depend only on the motions of the electrons and the coulomb repulsion of the nuclei (48). This means that the force constant K can

be assumed independent of isotopic substitution. Therefore the ratio of the classical frequencies between two isotopic molecules would be given as

$$\frac{\nu_1}{\nu_2} = \sqrt{\frac{\mu_2}{\mu_1}}$$

Or in terms of the most abundant isotope,

$$\frac{\nu_{\text{isotope}}}{\nu} = \sqrt{\frac{\mu}{\mu_{\text{isotope}}}} = \rho$$

From the relationship that $\nu = c\omega$,

$$\frac{\omega_e^{\,i}}{\omega} = \rho \qquad \text{(I.4)}$$

Thus from equations I.3 and I.4 the energy levels of the isotopic molecule are given by

$$(E_v)_i = hc \left[\rho\omega_e(v+\tfrac{1}{2}) - \rho^2\omega_e x_e(v+\tfrac{1}{2})^2 + \ldots \right] \qquad \text{(I.5)}$$

The only vibrational energy transitions possible are those dictated by the selection rule, i.e., $\Delta v = \pm 1$. Thus the vibrational energy change in a transition from $v = 0$ to $v = 1$ is given by equation I.3 as

$$\Delta E_v = hc \quad [\omega_e - 2\omega_e x_e + \ . \ . \ .] \qquad (I.6)$$

$$= hc\omega$$

From I.4, the energy change for a v = 1 to v = 0 transition for the isotopic molecule is given in terms of the transition for the abundant molecule as

$$(\Delta E_v)_i = hc \ [\ \rho\omega_e - 2\rho^2\omega_e x_e + \ . \ . \ . \ ] \qquad (I.7)$$

$$= hc\omega_i$$

From equation (I.7), the expression for the vibrational frequency of the isotopic molecule in terms of the frequency of the more abundant molecule as

$$\omega_i = \rho\omega_e - 2\rho^2\omega_e x_e + \ . \ . \ . \qquad (I.8)$$

Experimental values for ω_e and $\omega_e x_e$ for the Te^{130}-containing molecules are obtained from observed data (48), (67). Then from I.4,

$$\omega_e{}^{122} = \sqrt{\frac{\mu^{130}}{\mu^{122}}} \ . \ \omega_e{}^{130} = \rho\omega_e{}^{130}$$

and

$$(\omega_e x_e)^{122} = (\rho)^2 \ (\omega_e x_e)^{130} \qquad .$$

Table IX gives the calculations for the vibrational frequencies of Te^{122}-containing molecules from the available data. These were computed with the IBM 7040 computer program found on page A37, Appendix II.

B. Polyatomic Molecules

In these molecules, a simple model cannot be chosen for the vibrational frequencies. Detailed information must be obtained about the structure of the molecule in order to describe the force fields and set up equations for the vibrational frequencies. The force equations which seemed to best describe the observed spectra were chosen. The force constants were solved in terms of the most abundant Te^{130} isotope and experimentally observed frequencies. Then the other isotopic masses were substituted to find the corresponding isotopic frequencies.

In several cases even the best description of the molecule did not give results in perfect agreement with the observed vibrational frequencies. Therefore, linear correction factors are used when needed to align the calculated frequencies to those observed.

TABLE IX

Calculation of Vibrational Frequency Shifts for Te^{130} and Te^{122}-containing molecules

Molecule	ω_e^{130} cms^{-1}	$(\omega_e x_e)^{130}$ cms^{-1}	$\frac{\mu^{130}}{\mu^{122}}$	$\left[\frac{\mu^{130}}{\mu^{122}}\right]^{\frac{1}{2}}$	ω_e^{122} cms^{-1}	$\omega_e x_e^{122}$ cms^{-1}	ω^{130} cms^{-1}	ω^{122} cms^{-1}
$Ge^{74}Te$	323.4	1.00	1.024	1.0118	327.2	1.024	321.40	325.18
$Pb^{208}Te$	211.8	0.12	1.040	1.0200	216.0	0.125	211.56	215.79
$Sn^{120}Te$	259.5	0.50	1.032	1.0156	263.6	0.516	258.50	262.52
TeO^{16}	796.0	3.50	1.007	1.0036	798.9	3.525	789.00	791.81
$Si^{28}Te$	480.4	1.16	1.012	1.0058	483.2	1.173	478.08	480.84
$Te^{130}Te^{130}$	251.5	0.55	1.033	1.0163	255.6	0.568	250.40	254.46
HTe	2250.0	41.30	1.001	1.0003	2250.6	41.32	2167.40	2167.40

TeF_6

Tellurium hexafluoride is of octahedral structure of O_h symmetry. The octahedral molecules, XY_6, of symmetry O_h each show six fundamental vibration frequences. Of these six modes, ω_1 is non-degenerate, ω_2 is double degenerate, and ω_3, ω_4, ω_5, and ω_6 are triply degenerate. The form of these are shown in Fig. 9 in which the vibrational frequencies are labelled ω_1 . . . ω_6. ω_1, ω_2, and ω_3 are associated with essentially valency vibrations and ω_4, ω_5 and ω_6 with essentially deformation vibrations. ω_1, ω_2, and ω_5 appear in the Raman spectrum, ω_3 and ω_4 appear in the infra-red spectrum, ω_6 does not appear in either because the transtion is forbidden for both Raman and infra-red spectrum. This means that only the first five fundamental vibrational frequencies can be directly determined spectroscopically. ω_6 has to be obtained either from combination tones or from specific-heat data and it is, therefore, less accurate. With TeF_6, ω_4 was not directly observed but was also derived from overtones. Heath and Linnett (46) feel that any value between 340 and 370 cm^{-1} would account satisfactorily for the overtones observed and that the value cannot be fixed more closely. However, more recent publications (40) and (66) assign a value of 327 cm^{-1} for this vibration.

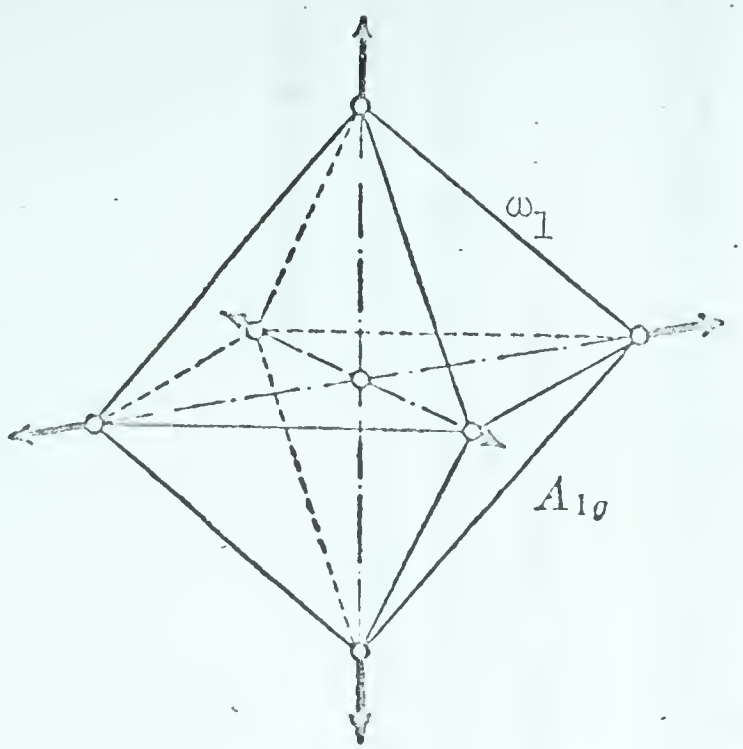

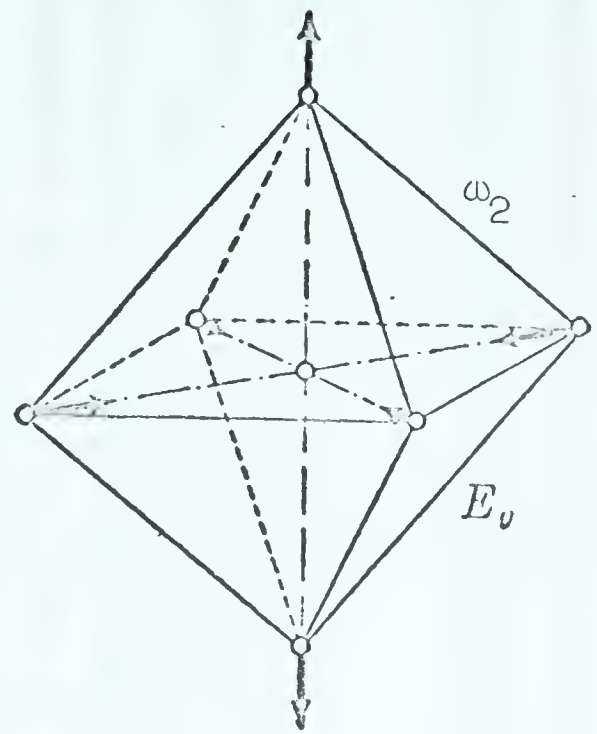

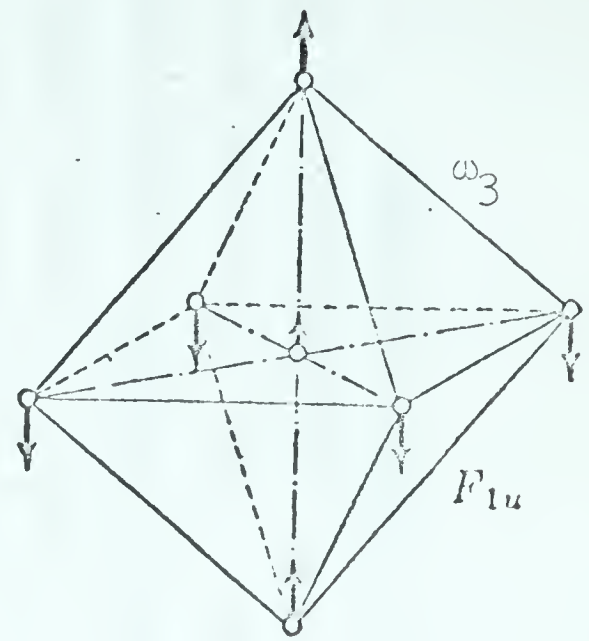

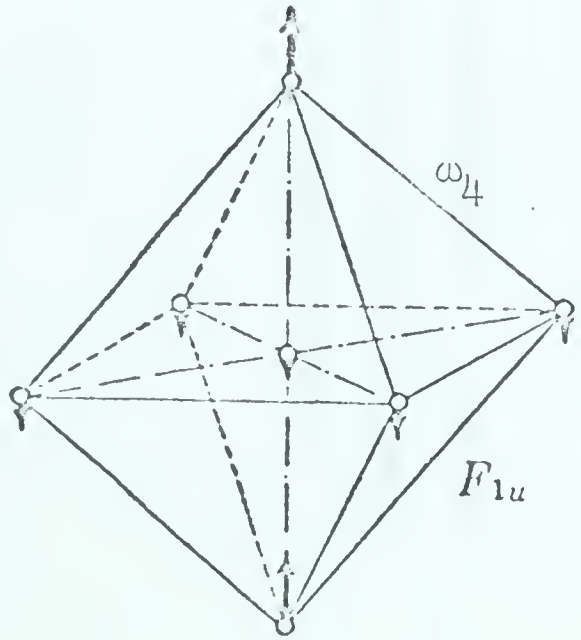

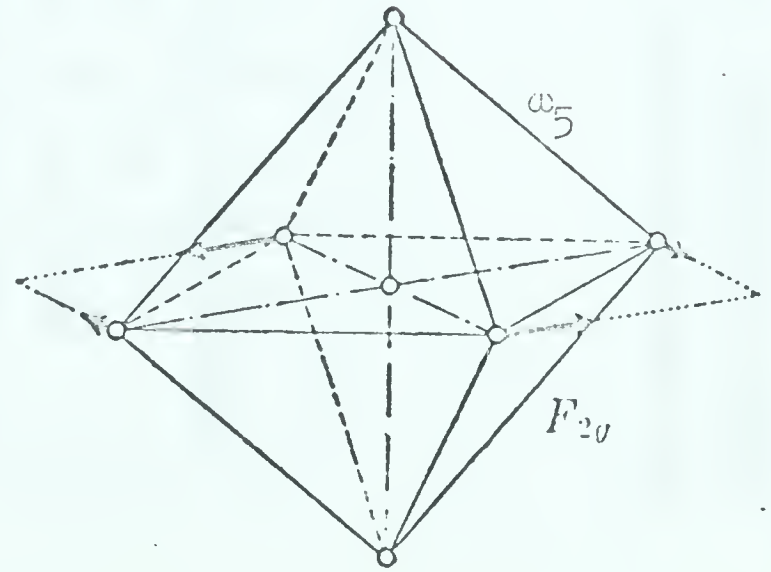

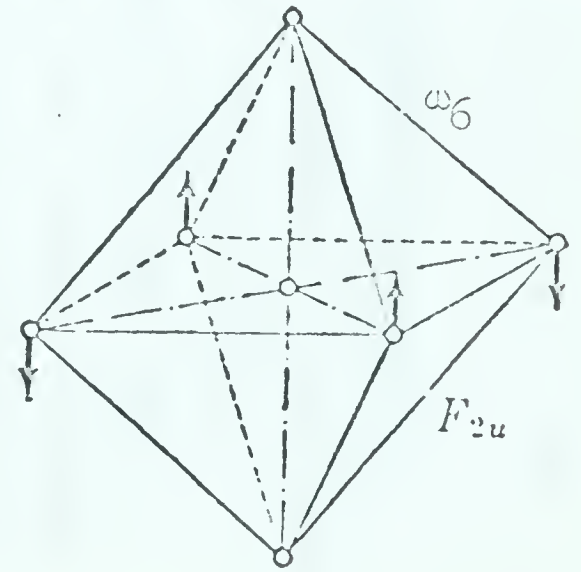

Fig. 9 NORMAL VIBRATIONS OF AN OCTAHEDRAL XY_6 MOLECULE

Heath and Linnett (46) have examined the application of two different force fields to octahedral XY_6 molecules, and in particular TeF_6. They found the "Orbital Valency Force Field" equations, which are based on the view that valency bonds are related to the form of the atomic orbitals, to give superior results to the "Simple Valency Force Field" equations. The following table shows a comparative agreement between observed and calculated frequencies using the OVFF and SVFF approach respectively.

Vibrational Frequencies of TeF_6 in cm^{-1}

TeF_6	ω_1	ω_2	ω_3	ω_4	ω_5	ω_6
Observed (46)	701	674	751	327	313	165
Calculated OVFF	698	669	775	351	313	388
Calculated SVFF	704	674	780	277	320	224

It is noted that the normal vibration, ω_4, is in fairly good agreement with the calculated value; whereas the ω_6 value is not satisfactorily considered in the OVFF approach.

Heath and Linnett (46) give the following equations for TeF_6 from the OVFF approach:

$$\lambda_1 = (k_1 + 8A)/m_F \qquad (I.9)$$

$$\lambda_2 = (k_1 - \frac{8}{3}\frac{B}{R} + \frac{8A}{3})\ m_F \qquad (I.10)$$

$$\lambda_3 + \lambda_4 = f_{11}(1/m_F + 2/m_{Te}) + f_{22}(4/m_{Te} + 1/m_F) - 4\ \ 2(f_{12}/m_{Te}) \qquad (I.11)$$

$$\lambda_3\lambda_4 = (f_{11}f_{22} - f_{12}^2)\ (1/m_F^2 + 6/m_Fm_{Te}) \qquad (I.12)$$

where,

$$f_{11} = (k_1 - \frac{2B}{R} + 4A)$$

$$f_{12} = (2\ \ 2\ A - 2\ B/R)$$

$$f_{22} = (k_B + \frac{3B}{R} + 2A)$$

$$\lambda_5 = (k_B + \frac{2B}{R} + 4A)/m_F \qquad (I.13)$$

$$\lambda_6 = (k_B + 2A)/m_F \qquad (I.14)$$

where,

$\lambda_i = 4\pi^2 c^2 \omega_i^2$ ω_i = frequency in cm^{-1}

m_F = mass of fluorine atom (amu)

m_{Te} = mass of tellurium atom (amu)

k_1 = the bond stretching constant of the Te-F bond

k_B = the angle bending constant of the F-Te-F bond

-B and 2A are the first and second differentials of the potential energy function representing repulsion between non-bonded atoms.

The constants have been calculated by Heath and Linnett to be:

$k_1 = 4.85 \times 10^5$ dyne/cm

$k_B = 0.78 \times 10^5$ dyne/cm

$A = 0.075 \times 10^5$ dyne/cm

$\frac{B}{R} = 0.0115 \times 10^5$ dyne/cm

The values used for the fluorine and tellurium masses are those given by Semat (94).

It is immediately seen from the equations that λ_1, λ_2, λ_5, and λ_6 are independent of the mass of tellurium and, therefore, remain the same for isotopic substitution of tellurium. For this reason, the poor agreement of the calculated value of ω_6 with the observed value can be overlooked in calculating isotopic shifts. Using equations I.11 and I.12, $\lambda_3 + \lambda_4$ and $\lambda_3\lambda_4$ are obtained. Then, λ_3 and λ_4 and subsequently ω_3 and ω_4 can be obtained by using the equation:

$$\lambda^2 - (\lambda_3 + \lambda_4)\,\lambda + \lambda_3\lambda_4 = 0 \qquad \text{(I.15)}$$

whose roots are given by

$$2\lambda = \lambda_3 + \lambda_4 \pm \sqrt{(\lambda_3 + \lambda_4)^2 - 4\lambda_3\lambda_4} \qquad \text{(I.16)}$$

An IBM 7040 computer program was set up to calculate ω_3 and ω_4 for all isotopic masses of tellurium using the foregoing considerations. (See pages A63, 65, Appendix II).

The values of ω_3 and ω_4 were found to be the following:

Isotope	ω_3 cm^{-1}	ω_4 cm^{-1}
$Te^{120}F_6$	775.42	356.47
$Te^{122}F_6$	773.78	355.79
$Te^{123}F_6$	772.98	355.46
$Te^{124}F_6$	772.19	355.13
$Te^{125}F_6$	771.42	354.80
$Te^{126}F_6$	770.66	354.48
$Te^{128}F_6$	769.17	353.85
$Te^{130}F_6$	767.72	353.22

The computed values for $Te^{130}F_6$ are now compared with the observed values as follows:

$Te^{130}F_6$	ω_3 cm^{-1}	ω_4 cm^{-1}
Observed	752	327
Computed	767.72	353.22

Correction factors $\frac{752}{767.72}$ and $\frac{327}{353.22}$ are used to align the calculated vibrational frequencies for the isotopic mass with the observed vibrational frequencies for $Te^{130}F_6$.

Then in terms of the corrected frequencies, we have:

	ω_1 cm^{-1}	ω_3 cm^{-1}	ω_3 cm^{-1}	ω_4 cm^{-1}	ω_5 cm^{-1}	ω_6 cm^{-1}
$Te^{120}F_6$	701	674	758.52	330.00	313	164
$Te^{122}F_6$	701	674	756.92	329.38	313	164
$Te^{123}F_6$	701	674	756.14	329.07	313	164
$Te^{124}F_6$	701	674	755.37	328.77	313	164
$Te^{125}F_6$	701	674	754.61	328.47	313	164
$Te^{126}F_6$	701	674	753.87	328.17	313	164
$Te^{128}F_6$	701	674	752.41	327.58	313	164
$Te^{130}F_6$	701	674	751.00	327.00	313	164

$TeBr_4$

$TeBr_4$ belongs to the group XY_4 having a tetrahedral structure. There are four normal modes of vibration; one totally symmetric (non-degenerate) mode (ω_1) of symmetry type A_1, one doubly degenerate mode (ω_2) of type E, and two triply degenerate modes (ω_3 and ω_4) of type F_2. These normal vibrations are shown in Fig.10.

FIG. 10

NORMAL VIBRATIONS of a TETRAHEDAL XY_4 MOLECULE

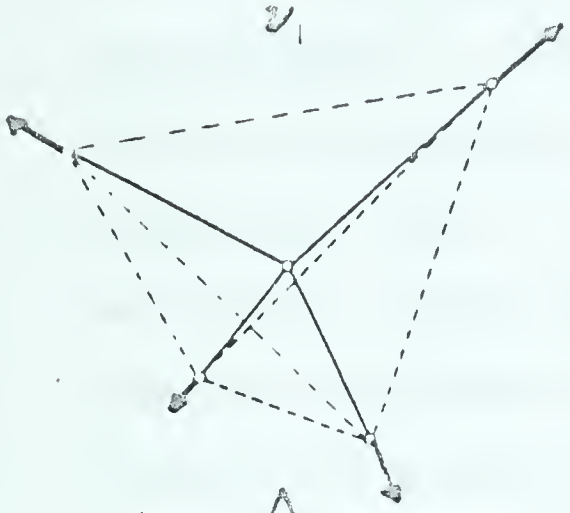

A_1

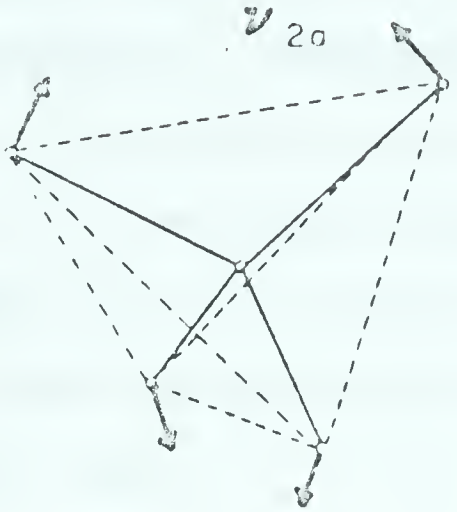

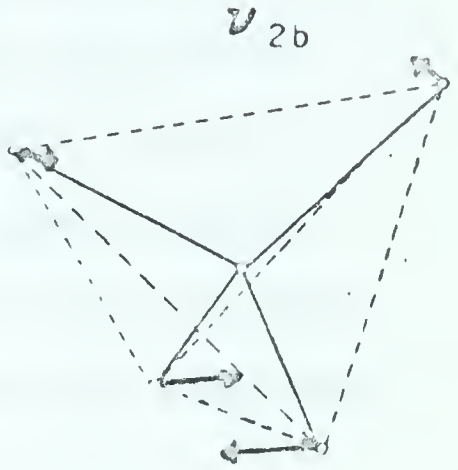

E

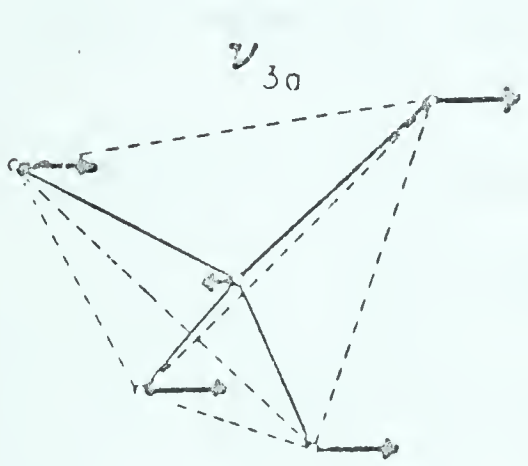

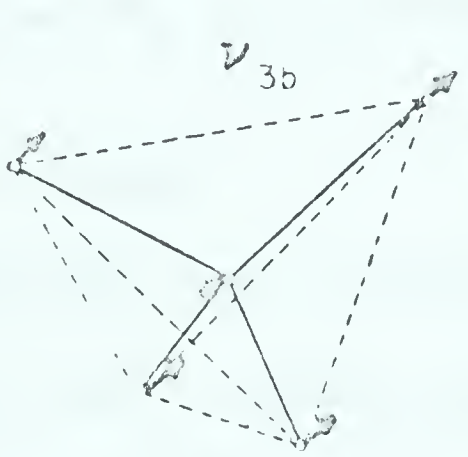

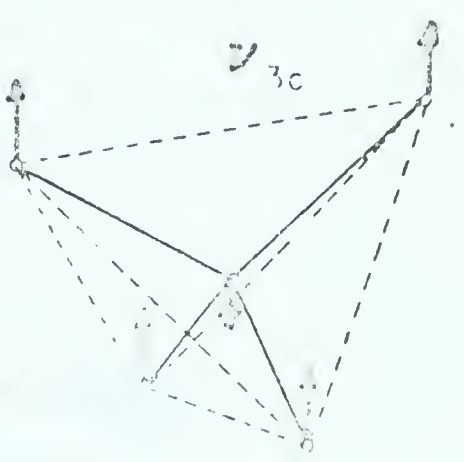

F_2

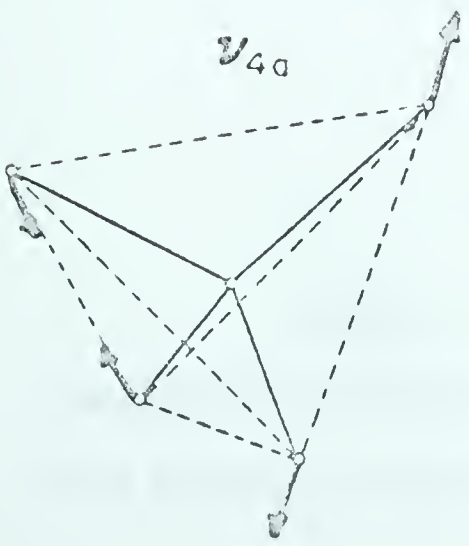

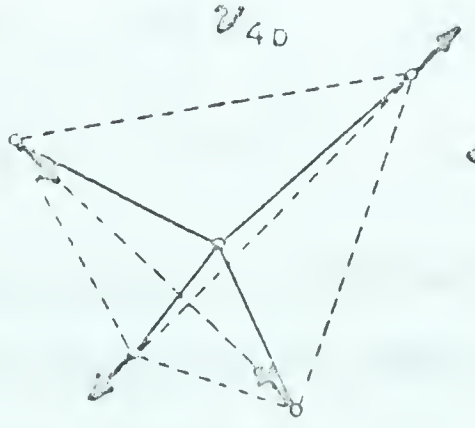

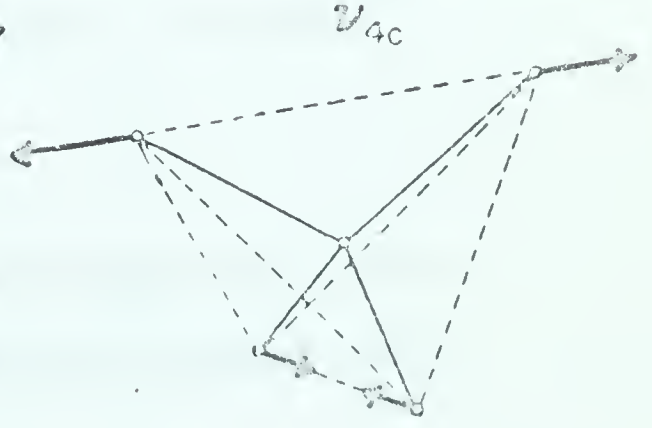

F_2

Various workers have set down force equations for this molecule. Venkateswarlu, Somasundaram, and Krishna (121) give a method of evaluation, but to quote C.W.F.T. Pistorius, (85), " . . .they seem to have made a numerical error, because they list real values while the correct results according to their method undoubtedly are imaginary." I found the same to be true.

The best results were found to be those of the OVFF approach of Heath and Linnett (45). They give the force equations for some XY_4 tetrahalides as:

$$\lambda_1 = (k + 8A)/M_F$$

$$\lambda_2 = (3k/(r^o)^2 + 2A + B/R^o)M_F$$

$$\lambda_3 + \lambda_4 = (k + 8A/3 - 4B/3R^o)(1/M_F + 4/3M_{Te}) + (2k/(r^o)^2 + 4A/3 + 10B/3R^o)(1/M_F + 8/3M_{Te}) - (8A/3 - 4B/3R^o)(8/3M_{Te})$$

$$\lambda_3\lambda_4 = (R + 8A/3 - 4B/3R^o)(2k/(r^o)^2 + 4A/3 + 10B/3R^o) - 1/2(8A/3 - 4B/3R^o)^2 \; 1/M_F^2 + 4/M_{Te}.M_F$$

Miss R. Thanalakshmi (103) calculated the force constants of the OVFF equations of Heath and Linnett (45) and gives the following values:

$$k = 1.4500 \times 10^5 \text{ dyne/cm.}$$

$$k/(r^o)^2 = 0.0192 \times 10^5 \text{ dyne/cm.}$$

$$B/R^o = 0.0040 \times 10^5 \text{ dyne/cm.}$$

$$A = 0.0300 \times 10^5 \text{ dyne/cm.}$$

It is noted that $\lambda_1 + \lambda_2$ are independent of the mass of tellurium and therefore remain the same for isotopic substitution of tellurium. The method of determining the roots and thus the frequencies ω_3 and ω_4 is exactly the same as was done for TeF_6. See equations I.15 and I.16.

Again an IBM 7040 computer program was set up (Pages A63 and 65) and results are given as follows:

Isotope	ω_3 cm^{-1}	ω_4 cm^{-1}
$Te^{120}Br_4$	244.92	61.49
$Te^{122}Br_4$	243.96	61.36
$Te^{123}Br_4$	243.50	61.30
$Te^{124}Br_4$	243.04	61.23
$Te^{125}Br_4$	242.58	61.17
$Te^{126}Br_4$	242.14	61.11
$Te^{128}Br_4$	241.26	60.99
$Te^{130}Br_4$	240.41	60.86

Again a discrepancy is found between the computed and observed frequencies for $Te^{130}Br_4$

$Te^{130}Br_4$	ω_3 cm^{-1}	ω_4 cm^{-1}
observed	209	64
calculated	240.41	60.86

Upon correction, the final normal frequencies are then:

	ω_1 cm^{-1}	ω_2 cm^{-1}	ω_3 cm^{-1}	ω_4 cm^{-1}
$Te^{120}Br_4$	190	51	212.92	64.66
$Te^{122}Br_4$	190	51	212.09	64.52
$Te^{123}Br_4$	190	51	211.68	64.46
$Te^{124}Br_4$	190	51	211.29	64.39
$Te^{125}Br_4$	190	51	210.89	64.32
$Te^{126}Br_4$	190	51	210.50	64.26
$Te^{128}Br_4$	190	51	209.74	64.13
$Te^{130}Br_4$	190	51	209.00	64.00

SCTe

This molecule is of the triatomic linear type having a symmetric stretching mode ω_1, a bending mode ω_2, and an asymmetric stretching mode ω_3. Of these, the

asymmetric stretching mode (ω_2) is doubly degenerate, and ω_1 and ω_3 non-degenerate (49). The forms of the normal vibrations would look like the following:

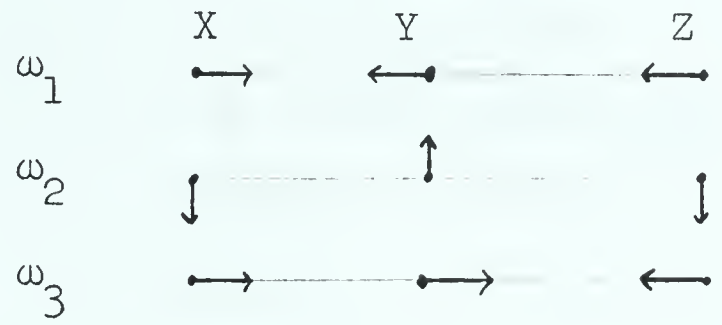

Wentink (120) gives the following force equations for this molecule:

$$\lambda_1 + \lambda_3 = K_1(1/M_S + 1/M_C) + K_2(1/M_C + 1/M_{Te}) - 2K_3/M_C$$

$$\lambda_1\lambda_3 = \frac{M_S + M_C + M_{Te}}{M_S M_C M_{Te}} \quad (K_1K_2 - K_3^2)$$

$$\lambda_2 = (1/r_1^2 r_2^2) \cdot (r_1^2/M_{Te} + r_2^2/M_S + r_{12}^2/M_C)K_\alpha$$

where

K_1 = stretching constant for the S-C bond

K_2 = stretching constant for the C-Te bond

K_3 = stretching interaction constant

K_α = bending constant

r_1 = S-C internuclear distance

r_2 = C-Te internuclear distance

r_{12} = S-Te internuclear distance

He gives the values for these constants as follows:

$$K_1 = 7.04 \times 10^5 \text{ dyne/cm.}$$
$$K_2 = 4.58 \times 10^5 \text{ dyne/cm.}$$
$$K_3 = 0.30 \times 10^5 \text{ dyne/cm.}$$
$$K_\alpha = 0.52 \times 10^{11} \text{ dyne/cm-rad}$$
$$r_1 = 1.557 \text{ Å}$$
$$r_2 = 1.904 \text{ Å}$$
$$r_{12} = 3.461 \text{ Å}$$

As noted, each λ is dependent on the mass of tellurium and therefore, each is affected by isotopic substitution. Knowing $\lambda_1 + \lambda_3$ and $\lambda_1\lambda_3$ one uses equations I.15 and I.16 as before for obtaining λ_1 and λ_3 and subsequently ω_1 and ω_3. λ_2 is calculated directly and from this ω_2 is obtained.

Using the computer program (pages A63, 64) the values of ω_1, ω_2, and ω_3 were found to be as follows:

	ω_1 cm^{-1}	ω_2 cm^{-1}	ω_3 cm^{-1}
$SCTe^{120}$	1347.64	340.05	426.35
$SCTe^{122}$	1347.54	340.00	425.45
$SCTe^{123}$	1347.48	339.98	425.00
$SCTe^{124}$	1347.43	339.95	424.57
$SCTe^{125}$	1347.38	339.93	424.14
$SCTe^{126}$	1347.33	339.91	423.72
$SCTe^{128}$	1347.23	339.86	422.89
$SCTe^{130}$	1347.14	337.00	422.08

Again a discrepancy is found between the calculated and observed frequencies for $SCTe^{130}$.

$SCTe^{130}$	ω_1 cm^{-1}	ω_2 cm^{-1}	ω_3 cm^{-1}
Observed	1347.00	337.00	423.00
Calculated	1347.14	337.00	422.08

When this has been corrected for, the final normal frequencies are then:

	ω_1 cm^{-1}	ω_2 cm^{-1}	ω_3 cm^{-1}
$SCTe^{120}$	1347.51	340.50	427.28
$SCTe^{124}$	1347.40	340.00	426.37
$SCTe^{123}$	1347.35	339.98	425.93
$SCTe^{124}$	1347.30	339.95	425.49
$SCTe^{125}$	1347.24	339.93	425.06
$SCTe^{126}$	1347.19	339.91	424.64
$SCTe^{128}$	1347.10	339.86	423.81
$SCTe^{130}$	1347.00	337.00	423.00

H_2Te

This molecule is of non-linear XY_2 structure having the form of normal vibrations shown below. Each vibration is non-degenerate.

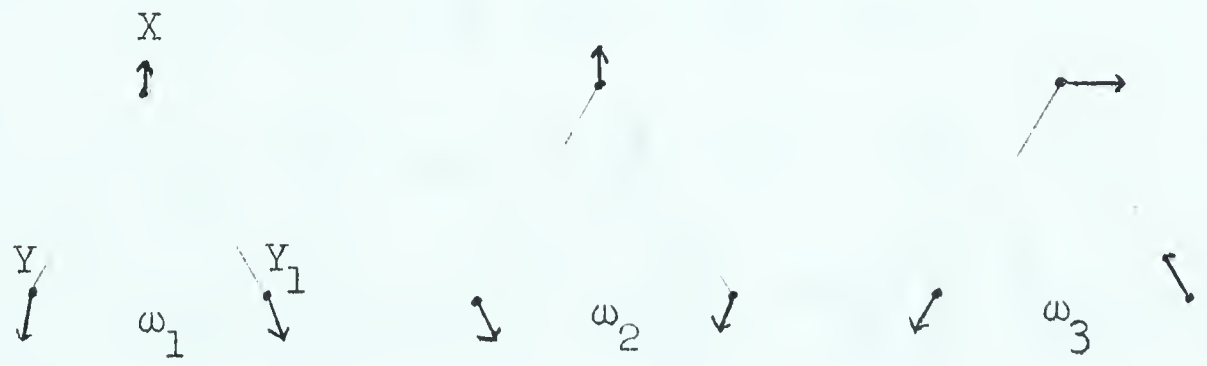

Due to the chemical instability of this gas (93) high resolution spectroscopy has been limited and the vibrational frequencies given are peak values for bands of unresolved spectral lines. Some overlapping of bands is also reported.

Triatomic non-linear molecules have been studied by Glockler and Tung (41) with the assumption of general force fields which produce three equations with four force constants for isosceles non-linear triatomic molecules as follows:

$$\lambda_1 + \lambda_2 = L_{11} + L_{12} + L_{33}$$

$$\lambda_1\lambda_2 = L_{33}\,(L_{11} + L_{12}) - 2L_{13}L_{31} \qquad \text{(I.17)}$$

$$\lambda_3 = L_{11} - L_{12}$$

where

$$-L_{11} = \frac{C_1}{\mu} + \frac{C_3}{M}\sin\alpha - \frac{C_4}{M}\cos\alpha$$

$$L_{12} = \frac{C_1}{M}\cos\alpha - \frac{C_3}{M}\sin\alpha + \frac{C_4}{\mu}$$

$$-L_{13} = \frac{C_1}{M}\sin\alpha - 2C_3\left[\frac{1}{\mu} - \frac{\cos\alpha}{M}\right] + \frac{C_4}{M}\sin\alpha$$

$$-L_{31} = \frac{C_2}{M}\sin\alpha - C_3\left[\frac{1}{\mu} + \frac{\cos\alpha}{M}\right]$$

$$L_{33} = 2C_2\left[\frac{1}{\mu} - \frac{\cos\alpha}{M}\right] - \frac{2C_3}{M}\sin\alpha$$

where

M = mass of central atom

m = mass of terminal atoms

$$\frac{1}{\mu} = \frac{1}{M} + \frac{1}{m}$$

α is the apex angle as shown

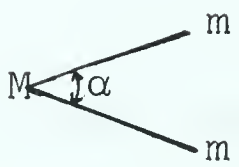

The observed angle α for the H-Te bond is close to 90° (101) (Rossmann and Straley in 1956 gave it as $89^{\circ}30'$ (93)). The two observed symmetric frequencies are 2047 cm^{-1} and 2133 cm^{-1} and the anti-symmetric frequency observed is 860.79 cm^{-1} (50, 102). Since α is so close to 90°, the equations are simplified to

$$-L_{11} = \frac{-C_1}{\mu} + \frac{C_3}{M}$$

$$L_{12} = \frac{-C_3}{M} + \frac{C_4}{\mu}$$

$$-L_{13} = \frac{C_1}{M} - \frac{2C_3}{\mu} + \frac{C_4}{M}$$

$$-L_{31} = \frac{C_2}{M} - \frac{C_3}{\mu}$$

$$L_{33} = \frac{2C_2}{\mu} - \frac{2C_3}{M}$$

giving

$$\lambda_1 + \lambda_2 = \frac{1}{\mu}\ [2C_2 + C_4 + C_1] - \frac{4C_3}{M}$$

$$\lambda_1\lambda_2 = [2C_2(C_1 + C_4) - 4C_3{}^3][\frac{1}{\mu^2} - \frac{1}{M^2}] \quad \ldots \quad (I.18)$$

$$\lambda_3 = (C_1 - C_4)\ (\frac{1}{\mu})$$

It is seen from I.18 that the isotopic frequencies for ω_3 are related by

$$\frac{\lambda_3'}{\lambda_3} = \frac{\mu}{\mu'}, \qquad \text{or} \qquad \frac{\omega_3'}{\omega_3} = \sqrt{\frac{\mu}{\mu'}}$$

and are thus independent of the force constants.

Also,

$$\frac{\lambda_1'\lambda_2'}{\lambda_1\lambda_2} = \frac{\left[\frac{1}{\mu'^2} - \frac{1}{M'^2}\right]}{\left[\frac{1}{\mu^2} - \frac{1}{M^2}\right]}$$

which is also independent of the force constants. Thus only the calculation of $\lambda_1 + \lambda_2$ depends on the values of the force constants and being of much smaller magnitude than the product $\lambda_1\lambda_2$, any error in the values chosen for the force constants is very nearly negligible as affecting isotopic vibrational frequency computations.

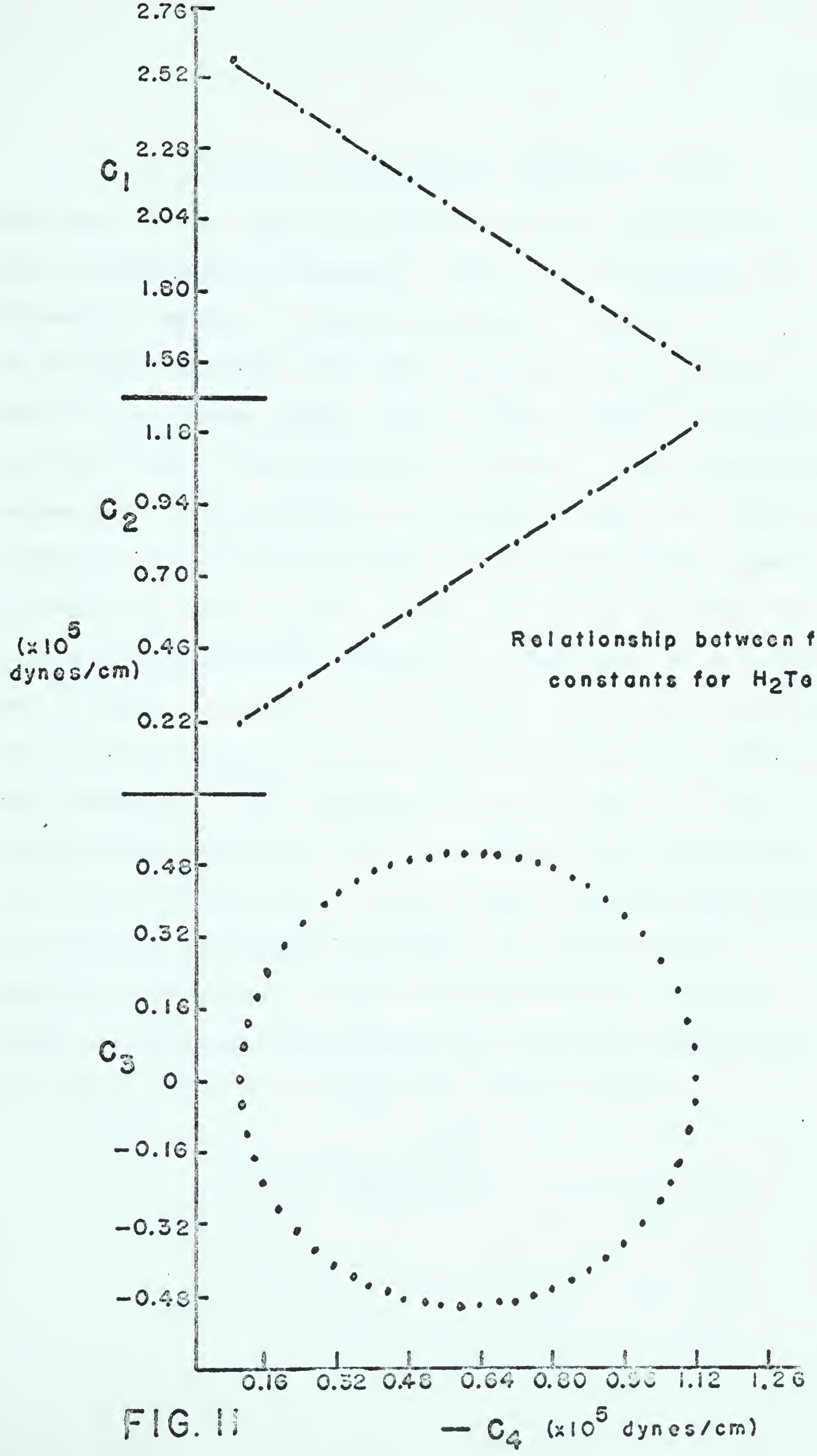

Relationship between force constants for H_2Te

FIG. 11

It is seen by the set of equations (I.18) that only three equations are available for determining four unknown force constants. Thus it is impossible to determine the force constants uniquely. However, if C_4 is assumed known and the other constants calculated in terms of C_4, there exists only a limited range of values of C_4 which give a 'non-imaginary' solution. The relationship between the four constants is plotted in Fig. 11. Thus the constants have a limited range of possible values, namely, $C_4 = 0.61 \pm 0.50$, $C_3 = 0 \pm 0.50$, $C_2 = 0.72 \pm 0.50$, and $C_1 = 2.05 \pm 0.50$ (x 10^5 dyne/cm.). Therefore, if a unique set of force constants is to be found, one of the constants must be determined by some other means. ω_3 is the stretching frequency of the hydrogen-tellurium bond. In the polyatomic molecule its value is affected by interaction with the other forces, but one can get an approximate value for the H-Te stretching constant C_1 by considering a diatomic H-Te molecule where the interaction forces are absent. Lippincott and Dayhoff (67) give the value of ω_3 for TeH as 2250 cm^{-1}. Using the relation that

$$\omega_e = \frac{1}{2\pi c}\sqrt{\frac{k}{\mu}}$$

where c = velocity of light

μ = reduced mass

k = bond constant

k is deduced to be 2.66×10^5 dyne/cm. for the diatomic H-Te bond. This would thus delimit the values of the constants to those values appearing to the left in Fig. 10 where C_1 has the maximum value of 2.55×10^5 dyne/cm.

Smith and Linnett (99) have calculated the constants for the other members of the group VIA elements using similar considerations along with the relation:

$$[\log C_1 = -6 \log r + a]$$

from excited state spectroscopic data to deduce C_1 and therefore deduce C_2, C_3 and C_4. They give the following set of force constants: ($\times 10^5$ dynes/cm)

	C_1	C_2	C_3	C_4
H_2O	8.36	0.75	0.20	-0.10
H_2S	4.4±0.2	0.55±0.05	0.2±0.2	-0.15±0.5
H_2Se	3.4±0.1	0.38±0.06	0.15±0.03	-0.15±0.15

It is noted that the value of the constants decreases with increasing order in the periodic table. Thus, this further delimits the values of the constants to $C_3 < 0.18$ which in turn limits $C_2 < 0.25$, $C_1 > 2.52$, $C_4 > -0.14$. It is noted also that C_3 is positive. In terms of this value we can then quite accurately assign the following values to the H_2Te force constants.

$$C_1 = 2.54 \pm 0.01 \times 10^5 \text{ dyne/cm}$$
$$C_2 = 0.23 \pm 0.01 \times 10^5 \text{ dyne/cm}$$
$$C_3 = 0.13 \pm 0.05 \times 10^5 \text{ dyne/cm}$$
$$C_4 = -0.12 \pm 0.01 \times 10^5 \text{ dyne/cm}$$

Having thus determined the force constants, the isotopic frequencies are calculated and corrected to line up with the observed frequencies for H_2Te^{130}. These are as follows below:

	ω_1 cm^{-1}	ω_2 cm^{-1}	ω_3 cm^{-1}
H_2Te^{120}	2047.49	861.13	2133.68
H_2Te^{122}	2047.39	861.39	2133.54
H_2Te^{123}	2047.33	861.02	2133.47
H_2Te^{124}	2047.28	860.99	2133.40
H_2Te^{125}	2047.24	860.95	2133.33
H_2Te^{126}	2047.19	860.92	2133.26
H_2Te^{128}	2047.09	860.85	2133.13
H_2Te^{130}	2047.00	860.79	2133.00

Tellurite ion ($TeO_3^=$)

The fundamental vibrational frequencies have been reported by Siebert (95) to be as follows (cm^{-1})

ω_1	ω_2	ω_3	ω_4
758	364	703	326

The tellurite ion has pyramidal XY_3 structure (see fig. 12) and a force constant analysis must take into account the apex angle of the pyramid. No experimental report of the apex angle for this ion has been reported in the literature. Therefore, the expression from Page 163 of Herzberg (49)

$$\cos^2\beta = \frac{1}{4\,\frac{\nu_3^2\nu_4^2}{\nu_1^2\nu_2^2} + \frac{3M_Y - M_X}{3M_Y - M_X}}$$

where $\sin\beta = \frac{2}{\sqrt{3}} \sin\frac{\alpha}{2}$

and α = apex angle

ν_i = i^{th} vibrational frequency

M_Y = mass of oxygen

M_X = mass of tellurium

was used to calculate the angle. It is noted from the expression that the angle is dependent on the tellurium mass. Therefore, α was calculated for each isotope but the computations showed a range in alpha from 101.16° in $Te^{130}O_3^=$ to 101.15° in Te^{122} so one could use a value of 101.15° and be well within the limits of experimental error. As to the accuracy of such a calculation, the observed angle for $SeO_3^=$ has been determined to be 100.6° (128) whereas the calculated value for $^{80}SeO_3^=$ was 99.7°. Assuming the mean observed angle to apply to $^{80}SeO_3^=$, this represents an error of less than 0.8%.

The Wilson F-G Matrix method has been used to determine the force constants. Following Nakomoto (82) the F and G matrix elements are:

F matrix elements:

For A_1 vibrations

$$F_{11} = f_r + 2f_{rr}$$
$$F_{12} = r(2f_{r\alpha} + f_{r\alpha'})$$
$$F_{22} = r^2(f_\alpha + 2f_{\alpha\alpha})$$

For E vibrations

$$F_{11} = f_r - f_{rr}$$
$$F_{12} = r(-f_{r\alpha} + f_{r\alpha'})$$
$$F_{22} = r^2(f_\alpha - f_{\alpha\alpha})$$

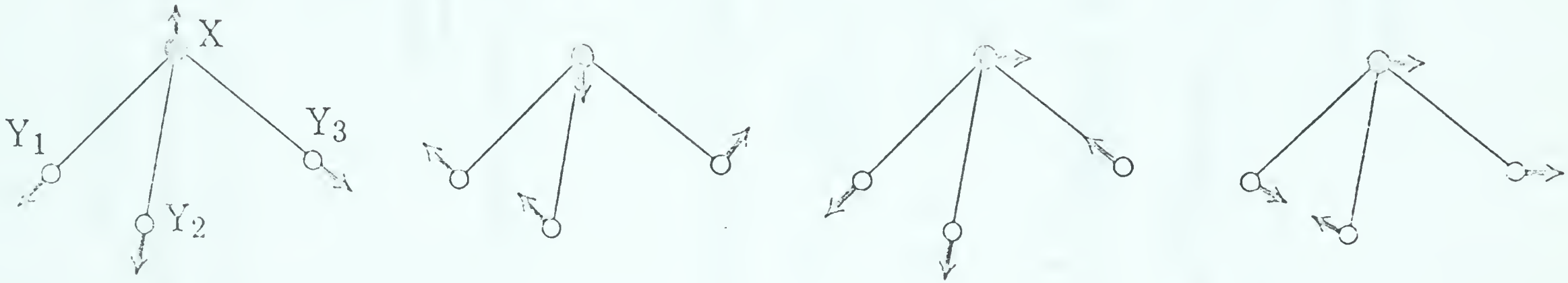

$\nu_1(A_1)$ $\nu_2(A_1)$ $\nu_{3a}(E)$ $\nu_{4a}(E)$

$\nu_s(XY)$ $\delta_s(YXY)$ $\nu_d(XY)$ $\delta_d(YXY)$

Fig. 12 NORMAL VIBRATIONS OF A PYRAMIDAL XY_3 MOLECULE
Taken from Nakamoto (82)

G Matrix elements:

For A_1 vibrations

$$G_{11} = \mu_y + (1 + 2\cos\alpha)\,\mu_x$$

$$G_{12} = -\frac{2}{r}\,\frac{(1+2\cos\alpha)(1-\cos\alpha)}{\sin\alpha}\,\mu_x$$

$$G_{22} = \frac{2}{r^2}\left[\frac{1+2\cos\alpha}{1+\cos\alpha}\right]\left[\mu_y + 2\mu_x(1-\cos\alpha)\right]$$

For E_1 vibrations

$$G_{11} = \mu_y + \mu_x(1 - \cos\alpha)$$

$$G_{12} = -\frac{1}{r}\,\frac{(1-\cos\alpha)^2}{\sin\alpha}\,\mu_x$$

$$G_{22} = \frac{1}{r^2(1+\cos\alpha)}\left[(2+\cos\alpha)\mu_y + (1-\cos\alpha)^2\mu_x\right]$$

where

r = Te-O bond distance

$$\mu_y = \frac{1}{M_{Oxygen}}$$

$$\mu_x = \frac{1}{M_{Te}}$$

The A_1 vibrations consist of the two non-degenerate vibrations ω_1 and ω_2 and the E vibrations consist of the doubly degenerate ω_3 and ω_4 vibrations.

The secular equation for both A_1 and E vibrations is

$$\lambda^2 - \lambda(F_{11}G_{11}+2F_{12}G_{12}+F_{22}G_{22})+(F_{11}F_{22}-F_{12}^2)(G_{11}G_{22}-G_{12}^2) = 0$$

There are six force constants but only four distinguishable frequencies so in performing the analysis it has been assumed that $f_{r\alpha}$ and $f_{r\alpha'}$ may be neglected leaving f_r, f_{rr}, f_α, and $f_{\alpha\alpha}$ to be determined. It is to be noted also, that because F_{ij} is always multiplied by G_{ij}, the "r's" cancel, so for this particular molecular structure, the Te-O bond distance need not be known if the apex angle is known. Using the frequency data and the IBM 7040 program (page A58) the following set of force constants was selected:

$$f_r = 4.377 \times 10^5 \text{ dyne/cm.}$$
$$f_\alpha = 0.493 \times 10^5 \text{ dyne/cm.}$$
$$f_{rr} = 0.321 \times 10^5 \text{ dyne/cm.}$$
$$f_{\alpha\alpha} = 0.078 \times 10^5 \text{ dyne/cm.}$$

These were then used to calculate the isotopic frequencies given below:

	ω_1 cm^{-1}	ω_2 cm^{-1}	ω_3 cm^{-1}	ω_4 cm^{-1}
Te^{120}	760.56	366.97	706.89	326.79
Te^{122}	760.01	366.35	706.07	326.62
Te^{123}	759.74	366.04	705.66	326.54
Te^{124}	759.48	365.74	705.26	326.46
Te^{125}	759.22	365.44	704.87	326.38
Te^{126}	759.97	365.14	704.49	326.30
Te^{128}	758.40	364.56	703.73	326.15
Te^{130}	758.00	364.00	703.10	326.00

APPENDIX II

IBM 7040 computer programs for calculation of isotopic vibrational frequencies and partition function ratios.

A. Calculation of isotopic vibrational frequencies and partition function ratios for diatomic species

In this program, ω_{heavy} and ω_{light} are computed for diatomic species for which values of ω_e and $\omega_e x_e$ are available. The partition function ratio for temperatures 0° - 100° in steps of 10° and from 100° - 1000°C. in steps of 100° is then computed according to equation 15 on page 48.

The following symbols were employed for data which must be supplied:

X130,X122 = masses of the two Y-atom isotopes for which isotopic data is desired (atomic weight units)

WE130(I) = known value of ω_e for the I^{th} diatomic molecule applying to the most abundant Y isotope, in this case Te^{130}.

WEX130(I) = known value of $\omega_e x_e$ for the I^{th} molecule and most abundant isotope.

X1(I) = mass of the I^{th} X atom in XY diatomic molecules, eg., Ge^{74} (awu).

In this work, the ratio of Te^{130}/Te^{122} was needed. Te^{130} is the most abundant isotope so computation of ω_e and $\omega_e x_e$ for the heavy isotope was unnecessary. Should the heavy isotope not be the most abundant, then statements must be included computing ω_e and $\omega_e x_e$ for the heavy isotope.

```
$IBSYS
$JOB            735003  PARTITION FUNCTIONS DIATOMIC
$TIME           003
$IBJOB TF       NODECK
$IBFTC DIATOM  NOLIST
      DIMENSION WE130(7), WEX130(7), RM130(7), RM122(7), X1(7), P(7),
     1SQRP(7), WE122(7), WEX122(7), W130(7), W122(7), T(20), UU(20),
     2U130(7,20), U122(7,20), A(7,20), B(7,20), PR(7,20)
      X130=129.94853
      X122=121.94193
      WE130(1)=323.4
      WE130(2)=211.8
      WE130(3)=259.5
      WE130(4)=796.0
      WE130(5)=480.4
      WE130(6)=251.5
      WE130(7)=2250.0
      WEX130(1)=1.00
      WEX130(2)=0.12
      WEX130(3)=0.50
      WEX130(4)=3.50
      WEX130(5)=1.16
      WEX130(6)=0.55
      WEX130(7)=41.3
      X1(1)=73.9426
      X1(2)=208.04754
      X1(3)=119.94059
      X1(4)=16.
      X1(5)=27.985825
      X1(6)=129.94853
      X1(7)=1.008
      DO 20 I=1,7
      RM130(I)=X1(I)*X130/(X1(I)+X130)
      RM122(I)=X1(I)*X122/(X1(I)+X122)
      SQRP(I)=RM130(I)/RM122(I)
      P(I)=SQRP(I)**0.5
      WE122(I)=P(I)*WE130(I)
      WEX122(I)=SQRP(I)*WEX130(I)
      W130(I)=WE130(I)-2.*WEX130(I)
20    W122(I)=WE122(I)-2.*WEX122(I)
      DO 28 I=2,11
      T(1)=0.
28    T(I)=T(I-1)+10.
      DO 29 I=12,20
29    T(I)=T(I-1)+100.
      E=2.71828
      V=1.438828
```

```
      DO 21 I=1,7
      DO 21 J=1,20
      UU(J)=V/(T(J)+273.)
      U130(I,J)=UU(J)*W130(I)
      U122(I,J)=UU(J)*W122(I)
      A(I,J)=-U130(I,J)/2.
      B(I,J)=-U122(I,J)/2.
   21 PR(I,J)=(U130(I,J)*(E**A(I,J))*(1.-(E**(2.*B(I,J)))))
     1/(U122(I,J)*(E**B(I,J))*(1.-(E**(2.*A(I,J)))))
      WRITE (6,4)
      WRITE (6,3) (SQRP(I), I=1,7)
      WRITE (6,5)
      WRITE (6,3) (P(I),I=1,7)
      WRITE (6,6)
      WRITE (6,3) (WF122(I),I=1,7)
      WRITE (6,7)
      WRITE (6,3) (WEX122(I), I=1,7)
      WRITE (6,8)
      WRITE (6,3) (W130(I), I=1,7)
      WRITE (6,9)
      WRITE (6,3) (W122(I), I=1,7)
      WRITE (6,11)
      DO 10 J=1,20
   10 WRITE (6,12) (PR(I,J), I=1,7)
    3 FORMAT (2X,F15.8)
    4 FORMAT (18H THIS IS U130/U122)
    5 FORMAT (10H THIS IS P)
    6 FORMAT (14H THIS IS WF122)
    7 FORMAT (16H THIS IS WFXE122)
    8 FORMAT (13H THIS IS W130)
    9 FORMAT (13H THIS IS W122)
   11 FORMAT (40H THESE ARE THE PARTITION FUNCTION RATIOS)
   12 FORMAT (7(2X,F15.8))
      CALL EXIT
      END
$ENTRY          DIATOM
```

B. Computation of isotopic vibrational frequencies for XY_6 molecules

This program was set up to compute isotopic vibrational frequencies according to the OVFF equations of Heath and Linnett (46). The masses of the (I) isotopes (awu) for which vibrational data is desired are used in the program as data cards. The following symbols apply to data which must be supplied:

AK = force constant k_1 (dynes/cm)

BK = force constant k_β

A = force constant A

C = force constant B/R

YM = mass of the Y atom (awu)

```
$IBSYS
$JOB              735003  VIBRATIONAL WAVELENGTHS XY6
$IBJOB TEF6       NODECK
$IBFTC OCTA       NOLIST
      DIMENSION XM(8),H(8),P(8),Q1(8),Q2(8),
     1W1(8),W2(8),CW1(8),CW2(8)
      AK=4.85E+05
      BK=0.78E+05
      A=0.075E+05
      C=0.0115E+05
      YM=19.004444
      F11=(AK-2.*C+4.*A)
      F12=(2.8284*A-1.4142*C)
      F22=(BK+3.*C+2.*A)
      READ (5,1) N
      DO 22 I=1,N
      READ (5,2) XM(I)
      H(I)=(F11)*(1./YM+2./XM(I))+F22*(4./XM(I)+1./YM)
     1-5.6568*F12/XM(I)
      P(I)=(F11*F22-F12**2)*(1./YM**2+6./(YM*XM(I)))
      Q1(I)=.5*(H(I)+SQRT (H(I)**2-4.*P(I)))
      Q2(I)=.5*(H(I)-SQRT (H(I)**2-4.*P(I)))
      W1(I)=SQRT (Q1(I)/.058894)
   22 W2(I)=SQRT (Q2(I)/.058894)
      DO 30 I=1,N
      CW1(I)=751.*W1(I)/W1(8)
   30 CW2(I)=327.*W2(I)/W2(8)
      WRITE (6,3)
      WRITE (6,11) (H(I),I=1,N)
      WRITE (6,4)
      WRITE (6,11) (P(I),I=1,N)
      WRITE (6,5)
      WRITE (6,11) (Q1(I),I=1,N)
      WRITE (6,6)
      WRITE (6,11) (Q2(I),I=1,N)
      WRITE (6,7)
      WRITE (6,11) (W1(I),I=1,N)
      WRITE (6,8)
      WRITE (6,11) (W2(I),I=1,N)
      WRITE (6,9)
      WRITE (6,11) (CW1(I),I=1,N)
      WRITE (6,10)
      WRITE (6,11) (CW2(I),I=1,N)
    1 FORMAT (I4)
    2 FORMAT (2X,F10.5)
    3 FORMAT (30H THESE ARE THE WAVELENGTH SUMS)
    4 FORMAT (34H THESE ARE THE WAVELENGTH PRODUCTS)
    5 FORMAT (24H THESE ARE THE SUM ROOTS)
    6 FORMAT (31H THESE ARE THE DIFFERENCE ROOTS)
```

```
     7 FORMAT (31H THIS IS ONE SET OF WAVELENGTHS)
     8 FORMAT (37H THIS IS THE OTHER SET OF WAVELENGTHS)
     9 FORMAT (28H THESE ARE THE CORRECTED W1S)
    10 FORMAT (28H THESE ARE THE CORRECTED W2S)
    11 FORMAT (2X,E14.8)
       CALL EXIT
        END
$ENTRY          OCTA
    8
    119.94288
    121.94193
    122.94368
    123.94278
    124.94460
    125.94420
    127.94649
    129.94853
```

C. Computation of isotopic vibrational frequencies for XY_4 molecules

This program is a solution of the OVFF equations of Heath and Linnett (45). In the program, the mass of the (I) X isotopes (awu) for which frequency data is desired are put in as data cards to be read and,

B = K

A = A

Z = $2k/(r_o)^2$

YM = mass of the Y atom (awu)

```
$IBSYS
$JOB            735003    VIBRATIONAL WAVELENGTHS TETRAHEDRAL
$IBJOB TEBR4    NODECK
$IBFTC TETRA    NOLIST
      DIMENSION XM(8),H(8),P(8),Q1(8),Q2(8),
     1W1(8),W2(8),CW1(8),CW2(8)
      B=145.0E3
      A=3.0E3
      Z=0.0384E+05
      W=400.0
      YM=79.916
      READ (5,1) N
      DO 22 I=1,N
      READ (5,2) XM(I)
      H(I)=(B+2.6666667*A-1.3333333*W)*(1./YM+1.3333333/XM(I))
     S+(1./YM+2.6666667/XM(I))*(Z+1.3333333*A+3.333333*W)
     S-(2.6666667*A-1.3333333*W)*(2.6666667/XM(I))
      P(I)=(1./(YM**2)+4./(XM(I)*YM))*((B+2.6666667*A-1.3333333*W)
     S*(Z+1.3333333*A+3.3333333*W)-.5*(2.6666667*A-1.3333333*W)**2)
      Q1(I)=.5*(H(I)+SQRT (H(I)**2-4.*P(I)))
      Q2(I)=.5*(H(I)-SQRT (H(I)**2-4.*P(I)))
      W1(I)=SQRT (Q1(I)/.058894)
   22 W2(I)=SQRT (Q2(I)/.058894)
      DO 30 I=1,N
      CW1(I)=209.*W1(I)/W1(8)
   30 CW2(I)=64.*W2(I)/W2(8)
      WRITE (6,3)
      WRITE (6,11) (H(I),I=1,N)
      WRITE (6,4)
      WRITE (6,11) (P(I),I=1,N)
      WRITE (6,5)
      WRITE (6,11) (Q1(I),I=1,N)
      WRITE (6,6)
      WRITE (6,11) (Q2(I),I=1,N)
      WRITE (6,7)
      WRITE (6,11) (W1(I),I=1,N)
      WRITE (6,8)
      WRITE (6,11) (W2(I),I=1,N)
      WRITE (6,9)
      WRITE (6,11) (CW1(I),I=1,N)
      WRITE (6,10)
      WRITE (6,11) (CW2(I),I=1,N)
    1 FORMAT (I4)
    2 FORMAT (2X,F10.5)
    3 FORMAT (30H THESE ARE THE WAVELENGTH SUMS)
    4 FORMAT (34H THESE ARE THE WAVELENGTH PRODUCTS)
    5 FORMAT (24H THESE ARE THE SUM ROOTS)
    6 FORMAT (31H THESE ARE THE DIFFERENCE ROOTS)
```

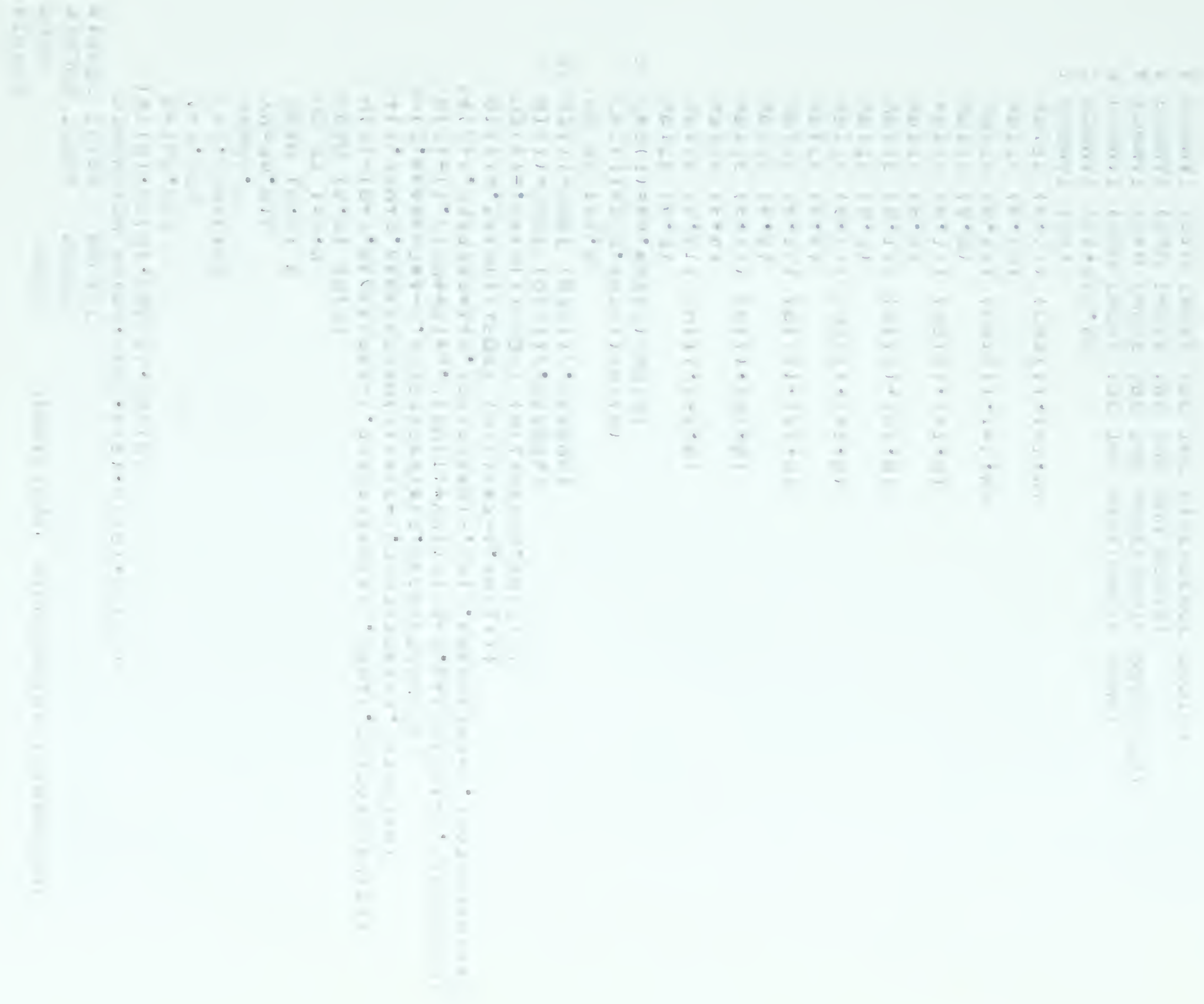

```
     7 FORMAT (31H THIS IS ONE SET OF WAVELENGTHS)
     8 FORMAT (37H THIS IS THE OTHER SET OF WAVELENGTHS)
     9 FORMAT (28H THESE ARE THE CORRECTED W1S)
    10 FORMAT (28H THESE ARE THE CORRECTED W2S)
    11 FORMAT (2X,F14.8)
       CALL EXIT
       END
$ENTRY          TETRA
    8
    119.94288
    121.94193
    122.94368
    123.94278
    124.94460
    125.94420
    127.94649
    129.94853
```

D. Computation of vibrational frequencies for linear XYZ molecules

This program computes the isotopic vibrational frequencies using the force field equations and force constants of Wentink (138). The (I) X-isotopic masses for which vibrational frequencies are desired are put into the program and read as data cards. The symbols used are the following:

A = k_1 (dynes/cm)

B = k_2

C = k_3

D = k_α

E = r_1 (cm)

F = r_2

G = r_{12}

YM = mass of the Y atom (awu)

The program computes k_α for the most abundant isotope (in this case the eighth). If a known value of k_α is desired to be used, instead of using D = A2/DM, put D = (value of k_α) and remove statements for A2, R, and DM.

```
$IBSYS
$JOB            735003  VIBRATIONAL WAVELENGTHS TRIATOMIC LINEAR
$IBJOB TRI      NODECK
$IBFTC SCTE     NOLIST
      DIMENSION XM(8),H(8),P(8),Q1(8),Q2(8),Q3(8),
     1W1(8),W2(8),W3(8),CW1(8),CW2(8),CW3(8)
      A=704.0E3
      B=458.0E3
      C=30.0E3
      R=337.
      A2=0.058894*(R**2)
      E=1557.0E-11
      F=1904.0E-11
      G=3461.0E-11
      ZM=31.98
      YM=12.
      READ (5,1) N
      DO 32 I=1,N
      READ (5,2) XM(I)
      DM=((F**2/XM(8))+(F**2/ZM)+(G**2/YM))/((E**2)*(F**2))
      D=A2/DM
      H(I)=A*(1./ZM+1./YM)+B*(1./YM+1./XM(I))-2.*C/YM
      P(I)=(ZM+YM+XM(I))*((A*B)-C**2)/(ZM*YM*XM(I))
      Q2(I)=((F**2/XM(I))+(F**2/ZM)+(G**2/YM))*D/((E**2)*(F**2))
      Q1(I)=.5*(H(I)+SQRT(H(I)**2-4.*P(I)))
      Q3(I)=.5*(H(I)-SQRT (H(I)**2-4.*P(I)))
      W1(I)=SQRT (Q1(I)/0.058894)
      W2(I)=SQRT (Q2(I)/0.058894)
   32 W3(I)=SQRT (Q3(I)/0.058894)
      DO 33 I=1,N
      CW1(I)=1347.*W1(I)/W1(8)
      CW2(I)=337.*W2(I)/W2(8)
   33 CW3(I)=423.*W3(I)/W3(8)
      WRITE (6,3)
      WRITE (6,14) (H(I),I=1,N)
      WRITE (6,4)
      WRITE (6,14) (P(I),I=1,N)
      WRITE (6,5)
      WRITE (6,14) (Q2(I),I=1,N)
      WRITE (6,6)
      WRITE (6,14) (Q1(I),I=1,N)
      WRITE (6,7)
      WRITE (6,14) (Q3(I),I=1,N)
      WRITE (6,8)
      WRITE (6,14) (W1(I),I=1,N)
```

```
      WRITE (6,9)
      WRITE (6,14) (W2(I),I=1,N)
      WRITE (6,10)
      WRITE (6,14) (W3(I),I=1,N)
      WRITE (6,11)
      WRITE (6,14) (CW1(I),I=1,N)
      WRITE (6,12)
      WRITE (6,14) (CW2(I),I=1,N)
      WRITE (6,13)
      WRITE (6,14) (CW3(I),I=1,N)
      WRITE (6,15)
      WRITE (6,14) D
    1 FORMAT (I4)
    2 FORMAT (2X,F10.5)
    3 FORMAT (30H THESE ARE THE WAVELENGTH SUMS)
    4 FORMAT (34H THESE ARE THE WAVELENGTH PRODUCTS)
    5 FORMAT (11H THIS IS Q2)
    6 FORMAT (24H THESE ARE THE SUM ROOTS)
    7 FORMAT (31H THESE ARE THE DIFFERENCE ROOTS)
    8 FORMAT (11H THIS IS W1)
    9 FORMAT (11H THIS IS W2)
   10 FORMAT (11H THIS IS W3)
   11 FORMAT (28H THESE ARE THE CORRECTED W1S)
   12 FORMAT (28H THESE ARE THE CORRECTED W2S)
   13 FORMAT (28H THESE ARE THE CORRECTED W3S)
   14 FORMAT (2X,E15.8)
   15 FORMAT (16H THIS IS K-ALPHA)
      CALL EXIT
      END
$ENTRY          SCTE
    8
    119.94288
    121.94193
    122.94368
    123.94278
    124.94460
    125.94420
    127.94649
    129.94853
```

E. Computation of force constants for non-linear XY_2 molecules

The force equations used are those given by Glockler and Tung (41). Only three equations are available to determine four force constants. Therefore, programs were set up to determine (1) the possible range of values of the constant C_4 (other values give imaginary results), and (2) the values of the other three constants for values of the permissible range of C_4.

Program (1) gives the lower limit to the permissible range of C_4, and program (2) gives the upper limit.

In these programs,

TM = mass of the most abundant isotope to which the observed fundamental frequencies apply (grams).

U = the reduced mass of the X-Y atom

ie., $1/u = 1/M_x + 1/M_y$

A1 = $\lambda_1 + \lambda_2$

A2 = $\lambda_1\lambda_2$

A3 = λ_3

C4 = force constant C_4 (dynes/cm)

The observed fundamental vibrational frequencies are put in as data cards to be read in order ω_1, ω_2, ω_3 (cm^{-1}).

```
$IBSYS
$JOB              735003        FORCE CONSTANTS TRIATOMIC (1)
$IBJOB H2TE     NODECK
$IBFTC FORCON   NOLIST
       DIMENSION WW(3)
       TM=130.*(1./(6.025*(10.**3)))
       U=1./((6.025*(10.**3))*((1./130.)+1.))
       READ (5,1)N
       DO 22 I=1,N
    22 READ (5,2) WW(I)
       A1=355.306*(WW(1)**2+WW(2)**2)
       A2=355.306**2*(WW(1)**2*WW(2)**2)
       A3=355.306*(WW(3)**2)
       B=A1-A3
       D=A2/(1./(U**2)-1./(TM**2))
       E=D/2.
       P=(2.*(U**2)*A3)/TM
       R=(4.*U)/TM
       S=((U**2)*A3*B)/2.
       T=((2.*P*R)/8.)-(U*A3)+(U*B)
       V=((R**2)/8.)-2.
       X=((P**2)/8.)-S
       C4=((-T-((T**2)-(4.*X*V))**0.5)/(2.*V))
         WRITE (6,9)
         WRITE (6,7) C4
       1 FORMAT (I4)
       2 FORMAT (2X,F10.5)
       7 FORMAT (2X,E15.8)
       9 FORMAT (11H THIS IS C4)
         CALL EXIT
         END
$ENTRY          FORCON
    3
    2047.
    860.79
    2133.
```

```
```

```
$IBSYS
$JOB              735 03        FORCE CONSTANTS TRIATOMIC (2)
$IBJOB H2TE     NODECK
$IBFTC FORCON   NOLIST
       DIMENSION WW(3)
       TM=130.*(1./(6.025*(10.**3)))
       U=1./((6.025*(10.**3))*((1./130.)+1.))
       READ (5,1)N
       DO 22 I=1,N
    22 READ (5,2) WW(I)
       A1=355.306*(WW(1)**2+WW(2)**2)
       A2=355.306**2*(WW(1)**2*WW(2)**2)
       A3=355.306*(WW(3)**2)
       B=A1-A3
       D=A2/(1./(U**2)-1./(TM**2))
       E=D/2.
       P=(2.*(U**2)*A3)/TM
       R=(4.*U)/TM
       S=((U**2)*A3*B)/2.
       T=((2.*P*R)/8.)-(U*A3)+(U*B)
       V=((R**2)/8.)-2.
       X=((P**2)/8.)-S
       C4=((-T+((T**2)-(4.*X*V))**0.5)/(2.*V))+(0.01*10.**5)
         WRITE (6,9)
         WRITE (6,7) C4
       1 FORMAT (I4)
       2 FORMAT (2X,F10.5)
       7 FORMAT (2X,E15.8)
       9 FORMAT (11H THIS IS C4)
         CALL EXIT
         END
$ENTRY          FORCON
    3
    2047.
    860.79
    2133.
```

```
      END
      CALL EXIT
    5 FORMAT (1H1,I2,1X,I2,1X,I2)
    4 FORMAT (3X,E13.6)
    3 FORMAT (3X,E13.6,E13.6)
    2 FORMAT (I7)
      WRITE (6,2) IV
      WRITE (6,3) T,V
      WRITE (6,4) X
      WRITE (6,5) IH,IM,IS
      STOP
      END
```

Programs (3) and (4) then give the values of the constants C_1, C_2, and C_3 for the permissible range of C_4, C_4 going in steps of 0.01×10^5 from maximum value to minimum value. Two programs are necessary, since for each value of C_4, C_3 has values

$$\frac{H \pm \sqrt{H^2 - 8G}}{4}$$

where H and G are defined as in the program.

Defining the symbols,

TM = mass of the most abundant isotope to which the observed fundamental frequencies apply (grams)

U, A1, A2, A3, C4 as previously defined

C1 = force constant C_1 (dynes/cm)

C32 = force constant C_3

C22 = force constant C_2

The observed fundamental frequencies are again read in as data cards in order.

```
$IBSYS
$JOB            735003        FORCE CONSTANTS TRIATOMIC (3)
$TIME           005
$IBJOB H2TF     NODECK
$IBFTC FORCON   NOLIST
      DIMENSION WW(3)
      TM=130.*(1./(6.025*(10.**3)))
      U=1./((6.025*(10.**3))*((1./130.)+1.))
      READ (5,1)N
      DO 22 I=1,N
   22 READ (5,2) WW(I)
      A1=355.306*(WW(1)**2+WW(2)**2)
      A2=355.306**2*(WW(1)**2*WW(2)**2)
      A3=355.306*(WW(3)**2)
      B=A1-A3
      D=A2/(1./(U**2)-1./(TM**2))
      E=D/2.
      P=(2.*(U**2)*A3)/TM
      R=(4.*U)/TM
      S=((U**2)*A3*B)/2.
      T=((2.*P*R)/8.)-(U*A3)+(U*B)
      V=((P**2)/8.)-2.
      X=((P**2)/8.)-S
      C4=-0.05*10.**5
   10 C1=U*A3+C4
      F=B/2.-C4/U
      G=F-((U**2)*A3*F)-2.*U*F*C4
      H=(2.*(U**2)*A3/TM+4.*U*C4/TM)
      C32=(H-((H**2)-8.*G)**0.5)/4.
      C22=U*(F+(2.*C32/TM))
      WRITE (6,9)
      WRITE (6,7) C4
      WRITE (6,4)
      WRITE (6,7) C32
      WRITE (6,6)
      WRITE (6,7) C22
      WRITE (6,8)
      WRITE (6,7) C1
      C4=C4-(0.01*10.**5)
      IF(C4.GE.-1.15*10.**5) GO TO 10
    1 FORMAT (I4)
    2 FORMAT (2X,F10.5)
    4 FORMAT (11H THIS IS C3)
    6 FORMAT (11H THIS IS C2)
    7 FORMAT (2X,E15.8)
    8 FORMAT (11H THIS IS C1)
    9 FORMAT (11H THIS IS C4)
      CALL EXIT
      END
$ENTRY          FORCON
   3
   2047.
   860.79
   2133.
```

```
$IBSYS
$JOB            735003        FORCE CONSTANTS TRIATOMIC (4)
$TIME           005
$IBJOB H2TE     NODECK
$IBFTC FORCON   NOLIST
      DIMENSION WW(3)
      TM=130.*(1./(6.025*(10.**3)))
      U=1./((6.025*(10.**3))*((1./130.)+1.))
      READ (5,1)N
      DO 22 I=1,N
   22 READ (5,2) WW(I)
      A1=355.306*(WW(1)**2+WW(2)**2)
      A2=355.306**2*(WW(1)**2*WW(2)**2)
      A3=355.306*(WW(3)**2)
      B=A1-A3
      D=A2/(1./(U**2)-1./(TM**2))
      E=D/2.
      P=(2.*(U**2)*A3)/TM
      R=(4.*U)/TM
      S=((U**2)*A3*B)/2.
      T=((2.*P*R)/8.)-(U*A3)+(U*B)
      V=((P**2)/8.)-2.
      X=((P**2)/8.)-S
      C4=-0.05*10.**5
   10 C1=U*A3+C4
      F=B/2.-C4/U
      G=E-((U**2)*A3*F)-2.*U*F*C4
      H=(2.*(U**2)*A3/TM+4.*U*C4/TM)
      C32=(H+((H**2)-8.*G)**0.5)/4.
      C22=U*(F+(2.*C32/TM))
      WRITE (6,9)
      WRITE (6,7) C4
      WRITE (6,4)
      WRITE (6,7) C32
      WRITE (6,6)
      WRITE (6,7) C22
      WRITE (6,8)
      WRITE (6,7) C1
      C4=C4-(0.01*10.**5)
      IF(C4.GE.-1.15*10.**5) GO TO 10
    1 FORMAT (I4)
    2 FORMAT (2X,F10.5)
    4 FORMAT (11H THIS IS C3)
    6 FORMAT (11H THIS IS C2)
    7 FORMAT (2X,F15.8)
    8 FORMAT (11H THIS IS C1)
    9 FORMAT (11H THIS IS C4)
      CALL EXIT
      END
$ENTRY          FORCON
   3
   2047.
   860.79
   2133.
```

F. Computation of isotopic vibrational frequencies and partition function ratios for non-linear XY_2 molecules

Knowing the value of the four force constants C_1 ..... C_4, this program computes the isotopic vibrational frequencies and partition function ratios for non-linear XY_2 molecules according to the equations given by Glockler and Tung (41).

The partition function ratios are given for temperatures 0° - 100°C in steps of 10° and from 100° - 1000°C in steps of 100°. The isotopic masses (awu) are read in as data cards, and symbols for which data must be supplied are:

W(I) = ω(I) observed (cm^{-1})

CI = force constants C_1 ... C_4 (dyne/cm)

YM = mass of the Y atom (awu)

DEGI = degree of degeneracy of the I^{th} vibration

U(L etc) = hc·CWW(I,J)/kT(L) where CWW(I,J) is the corrected I^{th} frequency of the J^{th} isotope for which the partition function ratio is desired

The partition function ratio is computed according to equation 16, page 49 and will be the ratio for those masses included in the U(L) statements, eg. CWW(I,1) will give the ratio of the 7^{th} isotope to the first (see page A58)

```
$IBSYS
$JOB            735003  WAVELENGTHS-PARTITION FUNCTIONS XY2 NON-LINEAR
$IBJOB H2TE     NODECK
$IBFTC PARRAT   NOLIST
       DIMENSION T(20), W(3), XM(10), UX(10), A(3,10), AL(3,10),
      1WW(3,10), CWW(3,10), U(140), PR(20), ZM(10)
       T(1)=0.
       DO 28 I=2,11
   28  T(I)=T(I-1)+10.
       DO 29 I=12,20
   29  T(I)=T(I-1)+100.
       W(1)=2047.
       W(2)=860.79
       W(3)=2133.
       READ (5,1) N
       DO 30 I=1,N
   30  READ (5,2) ZM(I)
       YM=1.008
       C1=2.5425591*10.**5
       C2=0.23362281*10.**5
       C3=0.13090571*10.**5
       C4=-0.12*10.**5
       DO 31 I=1,N
       XM(I)=ZM(I)/(6.025*10.**3)
       UX(I)=((6.025*10.**3)/YM)+(1./XM(I))
       A(1,I)=(UX(I)*((2.*C2)+C4+C1))-(4.*C3/XM(I))
       A(2,I)=(2.*C2*(C1+C4)-(4.*(C3**2)))*((UX(I)**2)-(1./XM(I)**2))
       A(3,I)=(C1-C4)*UX(I)
       AL(1,I)=(A(1,I)+((A(1,I)**2)-4.*A(2,I))**0.5)/2.
       AL(2,I)=(A(1,I)-((A(1,I)**2)-4.*A(2,I))**0.5)/2.
   31  AL(3,I)=A(3,I)
       DO 36 K=1,3
       DO 36 L=1,N
       DO 35 I=1,3
       DO 35 J=1,N
   35  WW(I,J)=(AL(I,J)/(4.*((22./7.)**2)*9.))**0.5
   36  CWW(K,L)=(W(K)/WW(K,1))*WW(K,L)
       WRITE (6,19)
       WRITE (6,16) (WW(1,J),J=1,N)
       WRITE (6,20)
       WRITE (6,16) (WW(2,J),J=1,N)
       WRITE (6,21)
       WRITE (6,16) (WW(3,J),J=1,N)
       WRITE (6,23)
       WRITE (6,16) (CWW(1,J),J=1,N)
       WRITE (6,24)
       WRITE (6,16) (CWW(2,J),J=1,N)
       WRITE (6,25)
       WRITE (6,16) (CWW(3,J),J=1,N)
```

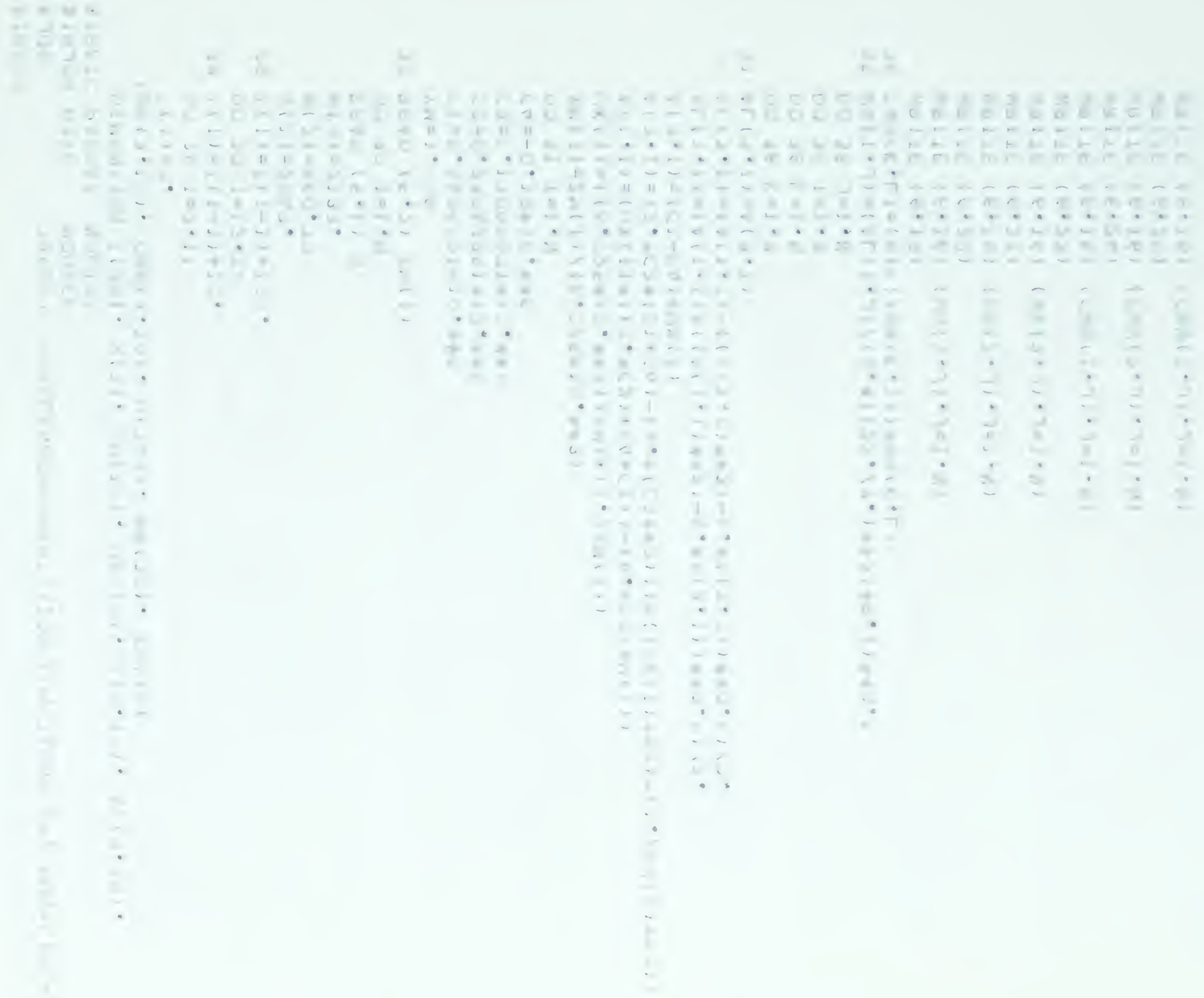

```
      V=1.438828
      DO 37 L=1,20
      UU=V/(T(L)+273.)
      U(L)=UU*CWW(1,7)
      U(L+20)=UU*CWW(1,1)
      U(L+40)=UU*CWW(2,7)
      U(L+60)=UU*CWW(2,1)
      U(L+80)=UU*CWW(3,7)
   37 U(L+100)=UU*CWW(3,1)
      E=2.71828
      DEG1=1
      DEG2=1
      DEG3=1
      DO 38 I=1,20
      H=-U(I)/2.
      B=-U(I+20)/2.
      C=-U(I+60)/2.
      D=-U(I+40)/2.
      F=-U(I+100)/2.
      G=-U(I+80)/2.
      P=-U(I+140)/2.
      Q=-U(I+120)/2.
   38 PR(I)=((U(I+20)*(E**B)*(1.-(E**(-U(I)))))
     1/(U(I)*(E**H)*(1.-(E**(-U(I+20)))))**DEG1
     2*((U(I+60)*(E**C)*(1.-(E**(-U(I+40))))))
     3/(U(I+40)*(E**D)*(1.-(E**(-U(I+60)))))**DEG2
     4*((U(I+100)*(E**F)*(1.-(E**(-U(I+80))))))
     5/(U(I+80)*(E**G)*(1.-(E**(-U(I+100)))))**DEG3
       WRITE (6,27)
       WRITE (6,16) (PR(I),I=1,20)
    1 FORMAT (I4)
    2 FORMAT (2X,F10.5)
   16 FORMAT (2X,F15.8)
   19 FORMAT (22H THESE ARE THE OMEGA1S)
   20 FORMAT (22H THESE ARE THE OMEGA2S)
   21 FORMAT (22H THESE ARE THE OMEGA3S)
   23 FORMAT (32H THESE ARE THE CORRECTED OMEGA1S)
   24 FORMAT (32H THESE ARE THE CORRECTED OMEGA2S)
   25 FORMAT (32H THESE ARE THE CORRECTED OMEGA3S)
   27 FORMAT (31H THESE ARE THE PARTITION RATIOS)
      CALL EXIT
      END
$ENTRY          PARRAT
   8
   129.94853
   127.94649
   125.94420
   124.94460
   123.94278
   122.94368
   121.94193
   119.94288
```

G. Computation of force constants, apex angle, isotopic vibrational frequencies, and partition function ratios for pyramidal XY_3 molecules

This program uses the Wilson F-G matrix method for finding the force constants. The apex angle is determined using Herzberg's formula (see page A30). Once these are known, isotopic vibrational frequencies and thus the partition function ratios can be computed. These are computed for the range of temperatures defined in parts A and F.

In the program, the following must be supplied:

YM = mass of the Y atom (awu)

W(I) = observed fundamental vibration frequencies in cm^{-1} in order

DEGI = degree of degeneracy of the I^{th} vibration

Isotopic masses are read in as data cards, so for example, if the partition function ratio of the molecule containing the first isotope to the molecule containing the seventh isotope is desired, the values, CWW(1,7), CWW(1,1), CWW(2,7), CWW(2,1), CWW(3,7), CWW(3,1), etc. are used to define successive U's. If the ratio of the fourth isotope to the fifth is desired, one would use CWW(1,5), CWW(1,4), CWW(2,5), CWW(2,4), CWW(3,5), CWW(3,4), etc. in that order designating the U's from U(1) ..... U(140).

```
$IBSYS
$JOB            735003 FORCE CONSTANTS - PARTITION FUNCTIONS, PYRAMIDAL-XY3
$TIME           005,300
$IBJOB TF04     NODECK
$IBFTC FORCON   NOLIST
      DIMENSION W(4), XM(10), UX(10), AB(4), BETA(10),
     1ALPHA(10), ANGLE(10), G11A(10), G12A(10), G22A(10),
     2G11E(10), G12E(10), G22E(10), AA(10), BA(10), AE(10),
     3BE(10), AL(4,10), WW(4,10), T(20), U(160), PR(20),
     4CWW(4,10), RR(20), SR(20), COA(20), COM(20), HRA(20), HRM(20)
      DO 28 I=2,11
      T(1)=0.
   28 T(I)=T(I-1)+10.
      DO 29 I=12,20
   29 T(I)=T(I-1)+100.
      YM=16.
      UY=(6.025*10.**3)/16.
      W(1)=758.
      W(2)=364.
      W(3)=703.
      W(4)=326.
      READ (5,1) N
      DO 30 I=1,N
   30 READ (5,2) XM(I)
      DO 31 I=1,N
   31 UX(I)=(6.025*10.**3)/XM(I)
      DO 32 I=1,4
   32 AB(I)=4.*((22./7.)**2)*9.*(W(I)**2)
      CA=AB(1)+AB(2)
      DA=AB(1)-AB(2)
      CE=AB(3)+AB(4)
      DE=AB(3)-AB(4)
      DO 33 I=1,N
      R=1.
      BETA(I)=ARCOS(1./(4.*(W(3)**2)*(W(4)**2)/((W(1)**2)*(W(2)**2)))
     1+((3.*YM)-XM(I))/((3.*YM)*XM(I)))**0.5
      ALPHA(I)=2.*(ARSIN(((3.**0.5)/2.)*SIN(BETA(I))))
      ANGLE(I)=ALPHA(I)*57.2958
      G11A(I)=UY+((1.+2.*COS(ALPHA(I)))*UX(I))
      G12A(I)=-(2.*(1.+2.*COS(ALPHA(I)))*(1.-COS(ALPHA(I)))*UX(I))
     1/(R*SIN(ALPHA(I)))
      G22A(I)=(2.*(1.+2.*COS(ALPHA(I)))*(UY+2.*UX(I)
     1*(1.-COS(ALPHA(I)))))/((R**2)*(1.+COS(ALPHA(I))))
      G11E(I)=UY+(UX(I)*(1.-COS(ALPHA(I))))
      G12E(I)=-(((1.-COS(ALPHA(I)))**2)*UX(I))/(R*SIN(ALPHA(I)))
      G22E(I)=((2.+COS(ALPHA(I)))*UY+((1.-COS(ALPHA(I)))**2)*UX(I))/
     1((R**2)*(1.+COS(ALPHA(I))))
```

```
      EA=(4.*CA*(G12A(1)**2)/G11A(1))-(4.*CA*G22A(1))
      HA=(4.*(G22A(1)**2))-(4.*G22A(1)*(G12A(1)**2))/G11A(1)
      PA=(CA**2)-(DA**2)
      EE=(4.*CE*(G12E(1)**2)/G11E(1))-(4.*CE*G22E(1))
      HE=(4.*(G22E(1)**2))-(4.*G22E(1)*(G12E(1)**2))/G11E(1)
      PE=(CE**2)-(DE**2)
      F22A=(-EA-((EA**2)-4.*HA*PA)**0.5)/(2.*HA)
      F22E=(-EE-((EE**2)-4.*HE*PE)**0.5)/(2.*HE)
      F11A=(CA-F22A*G22A(1))/G11A(1)
      F11E=(CF-F22E*G22E(1))/G11E(1)
      FRR=(F11A-F11E)/3.
      FR=(F11A+2.*F11E)/3.
      FALPHA=(F22A+2.*F22E)/(3.*(R**2))
      FALPAL=(F22A-F22E)/(3.*(R**2))
      AA(I)=(F11A*G11A(I))+(F22A*G22A(I))
      BA(I)=(F11A*F22A)*(G11A(I)*G22A(I)-G12A(I)**2)
      AE(I)=(F11E*G11E(I))+(F22E*G22E(I))
   33 BE(I)=(F11E*F22E)*(G11E(I)*G22E(I)-G12E(I)**2)
      DO 34 J=1,N
      AL(1,J)=(AA(J)+((AA(J)**2)-4.*BA(J))**0.5)/2.
      AL(2,J)=(AA(J)-((AA(J)**2)-4.*BA(J))**0.5)/2.
      AL(3,J)=(AE(J)+((AE(J)**2)-4.*BE(J))**0.5)/2.
   34 AL(4,J)=(AE(J)-((AE(J)**2)-4.*BE(J))**0.5)/2.
      DO 36 K=1,4
      DO 36 L=1,N
      DO 35 I=1,4
      DO 35 J=1,N
   35 WW(I,J)=(AL(I,J)/(4.*((22./7.)**2)*9.))**0.5
   36 CWW(K,L)=(W(K)/WW(K,1))*WW(K,L)
      V=1.438828
      DO 37 L=1,20
      UU=V/(T(L)+273.)
      U(L)=UU*CWW(1,7)
      U(L+20)=UU*CWW(1,1)
      U(L+40)=UU*CWW(2,7)
      U(L+60)=UU*CWW(2,1)
      U(L+80)=UU*CWW(3,7)
      U(L+100)=UU*CWW(3,1)
      U(L+120)=UU*CWW(4,7)
   37 U(L+140)=UU*CWW(4,1)
      E=2.71828
      DO 38 I=1,20
      A=-U(I)/2.
      B=-U(I+20)/2.
      C=-U(I+60)/2.
      D=-U(I+40)/2.
      F=-U(I+100)/2.
      G=-U(I+80)/2.
      P=-U(I+140)/2.
      Q=-U(I+120)/2.
```

```
      DEG1=1
      DEG2=1
      DEG3=2
      DEG4=2
      PR(I)=((U(I+20)*(E**B)*(1.-(E**(-U(I)))))
     1/(U(I)*(E**A)*(1.-(E**(-U(I+20))))))**DEG1
     2*((U(I+60)*(E**C)*(1.-(E**(-U(I+40))))))
     3/(U(I+40)*(E**D)*(1.-(E**(-U(I+60))))))**DEG2
     4*((U(I+100)*(E**F)*(1.-(E**(-U(I+80))))))
     5/(U(I+80)*(E**G)*(1.-(E**(-U(I+100))))))**DEG3
     6*((U(I+140)*(E**P)*(1.-(E**(-U(I+120))))))
     7/(U(I+120)*(E**Q)*(1.-(E**(-U(I+140))))))**DEG4
      WRITE (6,3)
      WRITE (6,16) (G11A(I),I=1,N)
      WRITE (6,4)
      WRITE (6,16) (G12A(I),I=1,N)
      WRITE (6,5)
      WRITE (6,16) (G22A(I),I=1,N)
      WRITE (6,6)
      WRITE (6,16) CA
      WRITE (6,7)
      WRITE (6,16) DA
      WRITE (6,8)
      WRITE (6,16) F22A
      WRITE (6,9)
      WRITE (6,16) F11A
      WRITE (6,10)
      WRITE (6,16) F22E
      WRITE (6,11)
      WRITE (6,16) F11E
      WRITE (6,12)
      WRITE (6,16) FRR
      WRITE (6,13)
      WRITE (6,16) FR
      WRITE (6,14)
      WRITE (6,16) FALPHA
      WRITE (6,15)
      WRITE (6,16) FALPAL
      WRITE (6,17)
      WRITE (6,16) (ALPHA(I),I=1,N)
      WRITE (6,18)
      WRITE (6,16) (ANGLE(I),I=1,N)
      WRITE (6,19)
      WRITE (6,16) (WW(1,J),J=1,N)
      WRITE (6,20)
      WRITE (6,16) (WW(2,J),J=1,N)
      WRITE (6,21)
      WRITE (6,16) (WW(3,J),J=1,N)
      WRITE (6,22)
      WRITE (6,16) (WW(4,J),J=1,N)
```

```
      WRITE (6,23)
      WRITE (6,16) (CWW(1,J),J=1,N)
      WRITE (6,24)
      WRITE (6,16) (CWW(2,J),J=1,N)
      WRITE (6,25)
      WRITE (6,16) (CWW(3,J),J=1,N)
      WRITE (6,26)
      WRITE (6,16) (CWW(4,J),J=1,N)
      WRITE (6,27)
      WRITE (6,16) (PR(I),I=1,20)
    1 FORMAT (I4)
    2 FORMAT (2X,F10.5)
    3 FORMAT (13H THIS IS G11A)
    4 FORMAT (13H THIS IS G12A)
    5 FORMAT (13H THIS IS G22A)
    6 FORMAT (11H THIS IS CA)
    7 FORMAT (11H THIS IS DA)
    8 FORMAT (13H THIS IS F22A)
    9 FORMAT (13H THIS IS F11A)
   10 FORMAT (13H THIS IS F22E)
   11 FORMAT (13H THIS IS F11E)
   12 FORMAT (12H THIS IS FRR)
   13 FORMAT (11H THIS IS FR)
   14 FORMAT (15H THIS IS FALPHA)
   15 FORMAT (16H THIS IS FALPALP)
   16 FORMAT (2X,E14.8)
   17 FORMAT (14H THIS IS ALPHA)
   18 FORMAT (25H THIS IS ALPHA IN DEGREES)
   19 FORMAT (22H THESE ARE THE OMEGA1S)
   20 FORMAT (22H THESE ARE THE OMEGA2S)
   21 FORMAT (22H THESE ARE THE OMEGA3S)
   22 FORMAT (22H THESE ARE THE OMEGA4S)
   23 FORMAT (32H THESE ARE THE CORRECTED OMEGA1S)
   24 FORMAT (32H THESE ARE THE CORRECTED OMEGA2S)
   25 FORMAT (32H THESE ARE THE CORRECTED OMEGA3S)
   26 FORMAT (32H THESE ARE THE CORRECTED OMEGA4S)
   27 FORMAT (31H THESE ARE THE PARTITION RATIOS)
      CALL EXIT
      END
$ENTRY          FORCON
   8
   129.94853
   127.94649
   125.94420
   124.94460
   123.94278
   122.94368
   121.94193
   119.94288
```

H. Computation of partition function ratios for general molecules

This program computes the partition function ratio for any molecule for which isotopic vibrational data is known, using equation 16, page 49. The isotopic vibrational frequencies (cm^{-1}) are read in as data cards. If Q_2/Q_1 is wanted where subscript 1 refers to the light molecule, and 2 refers to the heavy, the data cards are ordered as follows: ω_1 (light), ω_1 (heavy), ω_2 (light), ω_2 (heavy), etc.

The degeneracy of the frequency is indicated by DEGI corresponding to ω(I). For example, the degeneracy of ω_2 for SCTe is 2, thus DEG2 = 2 etc. Should there be more or less than three frequencies per isotopic molecule in the partition function ratio, the statements of PR(I) must be altered accordingly. The program for TeF_6 (page A65) is an example where two of the normal frequencies are altered by isotopic substitution; whereas, the program for $TeO_3^{=}$ is an example where four of the normal frequencies are altered by isotopic substitution.

```
$IBSYS
$JOB              735003    PARTITION FUNCTION RATIOS
$IBJOB SCTE     NODECK
$IBFTC PARRAT   NOLIST
      DIMENSION T(20), W(6), PR(20), U(120)
      A=1.438828
      T(1)=0.
      DO 24 I=2,11
   24 T(I)=T(I-1)+10.
      DO 25 I=12,20
   25 T(I)=T(I-1)+100.
      READ (5,1) N
      DO 26 I=1,N
   26 READ (5,2) W(I)
      K=0
      DO 28 J=1,N
      DO 27 I=1,20
      K=K+1
   27 U(K)=(A/(T(I)+273.))*W(J)
   28 CONTINUE
      E=2.71828
      DEG1=1
      DEG2=2
      DEG3=1
      DO 29 I=1,20
      H=-U(I)/2.
      B=-U(I+20)/2.
      C=-U(I+60)/2.
      D=-U(I+40)/2.
      F=-U(I+100)/2.
      G=-U(I+80)/2.
      P=-U(I+140)/2.
      Q=-U(I+120)/2.
   29 PR(I)=((U(I+20)*(E**B)*(1.-(E**(-U(I)))))
     1/(U(I)*(E**H)*(1.-(E**(-U(I+20)))))**DEG1
     2*((U(I+60)*(E**C)*(1.-(E**(-U(I+40))))))
     3/(U(I+40)*(E**D)*(1.-(E**(-U(I+60)))))**DEG2
     4*((U(I+100)*(E**F)*(1.-(E**(-U(I+80))))))
     5/(U(I+80)*(E**G)*(1.-(F**(-U(I+100)))))**DEG3
      DO 36 I=1,20
   36 WRITE (6,8) PR(I)
    1 FORMAT(I4)
    2 FORMAT(2X,F7.2)
    8 FORMAT (2X,F15.8)
      CALL EXIT
      END
$ENTRY          PARRAT
   6
   1347.4004
   1347.0
   340.0
   337.0
   426.3703
   423.0
```

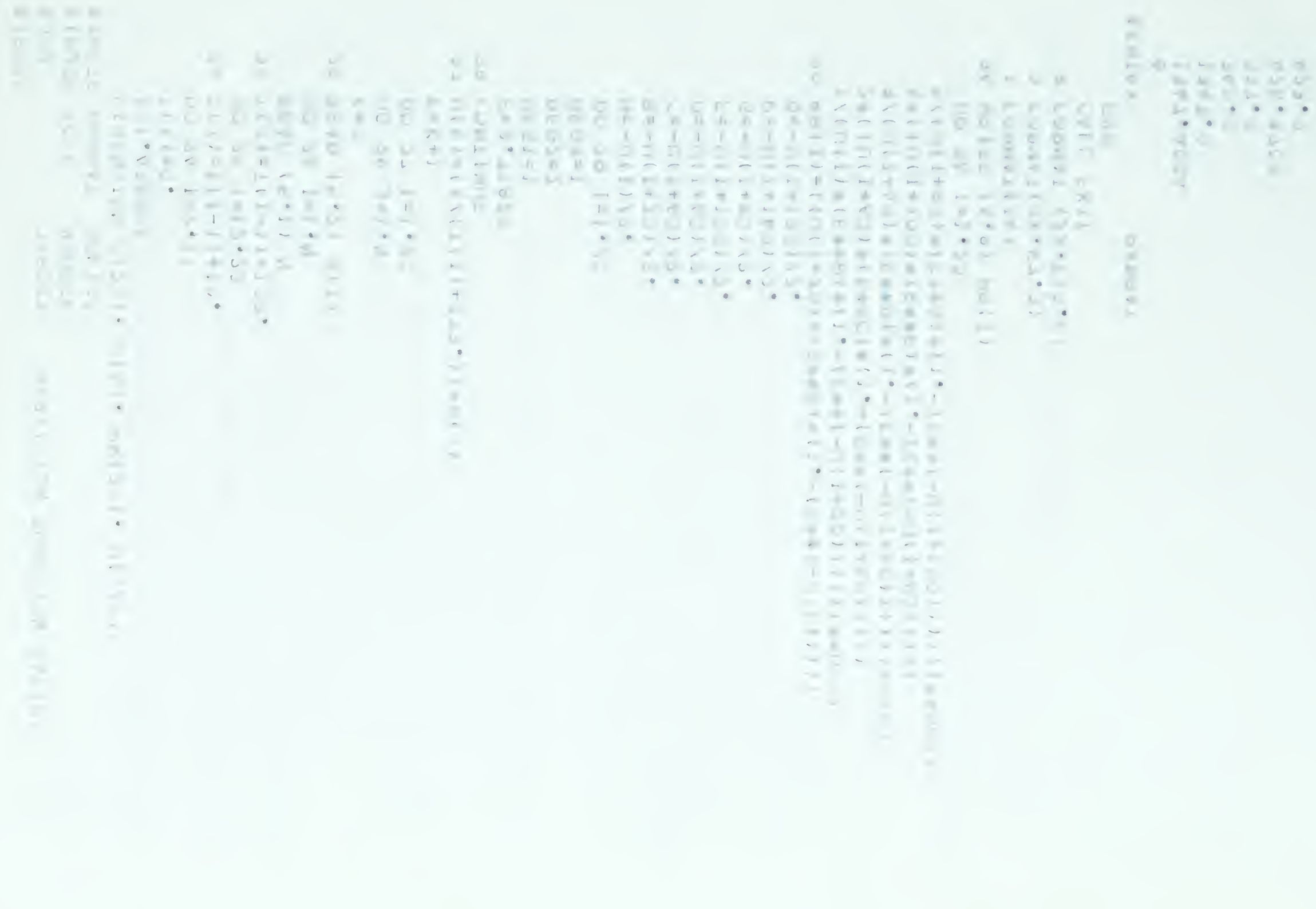

```
$IBSYS
$JOB              735003    PARTITION FUNCTION RATIOS
$IBJOB TEF6       NODECK
$IBFTC PARRAT     NOLIST
       DIMENSION T(20), W(6), PR(20), U(120)
       A=1.438828
       T(1)=0.
       DO 24 I=2,11
    24 T(I)=T(I-1)+10.
       DO 25 I=12,20
    25 T(I)=T(I-1)+100.
       READ (5,1) N
       DO 26 I=1,N
    26 READ (5,2) W(I)
       K=0
       DO 28 J=1,N
       DO 27 I=1,20
       K=K+1
    27 U(K)=(A/(T(I)+273.))*W(J)
    28 CONTINUE
       E=2.71828
       DEG1=3
       DEG2=3
       DO 29 I=1,20
       H=-U(I)/2.
       B=-U(I+20)/2.
       C=-U(I+60)/2.
       D=-U(I+40)/2.
       F=-U(I+100)/2.
       G=-U(I+80)/2.
    29 PR(I)=((U(I+20)*(F**B)*(1.-(E**(-U(I)))))
      1/(U(I)*(E**H)*(1.-(E**(-U(I+20)))))**DEG1
      2*((U(I+60)*(E**C)*(1.-(E**(-U(I+40)))))
      3/(U(I+40)*(E**D)*(1.-(E**(-U(I+60)))))**DEG2
       DO 36 I=1,20
    36 WRITE (6,8) PR(I)
     1 FORMAT(I4)
     2 FORMAT(2X,F7.2)
     8 FORMAT (2X,E15.8)
       CALL EXIT
       END
$ENTRY          PARRAT
    4
    756.92
    751.0
    329.38
    327.0
```

```
      SUBROUTINE SUBMTX (IDIM,JDIM,IER)
      DIMENSION A(IDIM,JDIM),B(IDIM,JDIM),C(IDIM,JDIM),
     1          D(IDIM,JDIM),E(IDIM,JDIM),F(IDIM,JDIM),
     2          G(IDIM,JDIM),H(IDIM,JDIM),P(IDIM,JDIM)
      COMMON A,B,C,D,E,F,G,H,P
      IF (IDIM .LT. 1 .OR. JDIM .LT. 1) GO TO 20
      DO 10 I=1,IDIM
      DO 10 J=1,JDIM
      P(I,J)=A(I,J)-B(I,J)-C(I,J)+D(I,J)-E(I,J)+F(I,J)-G(I,J)+H(I,J)
   10 CONTINUE
      IER=0
      RETURN
   20 IER=1
      RETURN
      END
      SUBROUTINE ADDMTX (IDIM,JDIM,IER)
      DIMENSION A(IDIM,JDIM),B(IDIM,JDIM),C(IDIM,JDIM),
     1          D(IDIM,JDIM),E(IDIM,JDIM),F(IDIM,JDIM),
     2          G(IDIM,JDIM),H(IDIM,JDIM),P(IDIM,JDIM)
      COMMON A,B,C,D,E,F,G,H,P
      IF (IDIM .LT. 1 .OR. JDIM .LT. 1) GO TO 20
      DO 10 I=1,IDIM
      DO 10 J=1,JDIM
      P(I,J)=A(I,J)+B(I,J)+C(I,J)+D(I,J)+E(I,J)+F(I,J)+G(I,J)+H(I,J)
   10 CONTINUE
      IER=0
      RETURN
   20 IER=1
      RETURN
      END
      SUBROUTINE MULMTX (IDIM,JDIM,IER)
      DIMENSION A(IDIM,JDIM),B(IDIM,JDIM),C(IDIM,JDIM),
     1          D(IDIM,JDIM),E(IDIM,JDIM),F(IDIM,JDIM),
     2          G(IDIM,JDIM),H(IDIM,JDIM),P(IDIM,JDIM)
      COMMON A,B,C,D,E,F,G,H,P
      IF (IDIM .LT. 1 .OR. JDIM .LT. 1) GO TO 20
      DO 10 I=1,IDIM
      DO 10 J=1,JDIM
      P(I,J)=A(I,J)*B(I,J)*C(I,J)*D(I,J)*E(I,J)*F(I,J)*G(I,J)*H(I,J)
   10 CONTINUE
      IER=0
      RETURN
   20 IER=1
      RETURN
      END
      SUBROUTINE DIVMTX (IDIM,JDIM,IER)
      DIMENSION A(IDIM,JDIM),B(IDIM,JDIM),C(IDIM,JDIM),
     1          D(IDIM,JDIM),E(IDIM,JDIM),F(IDIM,JDIM),
     2          G(IDIM,JDIM),H(IDIM,JDIM),P(IDIM,JDIM)
      COMMON A,B,C,D,E,F,G,H,P
      IF (IDIM .LT. 1 .OR. JDIM .LT. 1) GO TO 20
      DO 10 I=1,IDIM
      DO 10 J=1,JDIM
      P(I,J)=A(I,J)/B(I,J)/C(I,J)/D(I,J)/E(I,J)/F(I,J)/G(I,J)/H(I,J)
   10 CONTINUE
      IER=0
      RETURN
   20 IER=1
      RETURN
      END
C***********************************************************************
C
C  SUBROUTINE NAME:  MATRIX
C
C  PURPOSE:  MATRIX IS A SUBROUTINE WHICH PERFORMS MATRIX OPERATIONS
C            ON UP TO EIGHT MATRICES.  THE OPERATIONS ARE ADDITION,
C            SUBTRACTION, MULTIPLICATION, AND DIVISION.
C
C  USAGE:  CALL MATRIX (IDIM,JDIM,IOPT,IER)
C
C  PARAMETERS:  IDIM - NUMBER OF ROWS IN THE MATRICES
C               JDIM - NUMBER OF COLUMNS IN THE MATRICES
C               IOPT - OPTION CODE
C                      1 - ADD
C                      2 - SUBTRACT
C                      3 - MULTIPLY
C                      4 - DIVIDE
C               IER  - ERROR CODE
C                      0 - NO ERROR
C                      1 - IDIM OR JDIM LESS THAN 1
C                      2 - IOPT NOT 1, 2, 3, OR 4
C
C  REMARKS:  THE MATRICES ARE STORED IN A, B, C, D, E, F, G, H, AND
C            THE RESULT IS STORED IN P.
C
C  SUBROUTINES CALLED:  SUBMTX, ADDMTX, MULMTX, DIVMTX
C
C  FILES:  NONE
C
C  LANGUAGE:  FORTRAN
C
C  AUTHOR:  JOHN DOE, COMPUTATION CENTER, STATE UNIVERSITY
C
C***********************************************************************
      SUBROUTINE MATRIX (IDIM,JDIM,IOPT,IER)
      GO TO (10,20,30,40),IOPT
      IER=2
      RETURN
   10 CALL ADDMTX (IDIM,JDIM,IER)
      RETURN
   20 CALL SUBMTX (IDIM,JDIM,IER)
      RETURN
   30 CALL MULMTX (IDIM,JDIM,IER)
      RETURN
   40 CALL DIVMTX (IDIM,JDIM,IER)
      RETURN
      END
```

B29831